ISTANBUL TECHNICAL UNIVERSITY ★ GRADUATE SCHOOL

ADAPTIVE SIGNAL PROCESSING BASED INTELLIGENT METHOD FOR FAULT DETECTION AND CLASSIFICATION IN MICROGRIDS

Ph.D. THESIS

Resul AZİZİ

Department of Electrical Engineering

Electrical Engineering Programme

FEBRUARY 2022

ISTANBUL TECHNICAL UNIVERSITY ★ GRADUATE SCHOOL

ADAPTIVE SIGNAL PROCESSING BASED INTELLIGENT METHOD FOR FAULT DETECTION AND CLASSIFICATION IN MICROGRIDS

Ph.D. THESIS

Resul AZİZİ
(504152022)

Department of Electrical Engineering

Electrical Engineering Programme

Thesis Advisor: Prof. Dr. Şahin Serhat ŞEKER

FEBRUARY 2022

ISTANBUL TEKNİK ÜNİVERSİTESİ ★ LİSANSÜSTÜ EĞİTİM ENSTİTÜSÜ

MİKROŞEBEKELERDE ARIZA TESPİTİ VE SINIFLANDIRMASI İÇİN ADAPTİF SİNYAL İŞLEME TABANLI AKILLI YÖNTEM

DOKTORA TEZİ

Resul AZİZİ
(504152022)

Elektrik Mühendisliği Anabilim Dalı

Elektrik Mühendisliği Programı

Tez Danışmanı: Prof. Dr. Şahin Serhat ŞEKER

ŞUBAT 2022

Resul AZİZİ a Ph.D. student of ITU Graduate School student ID 504152022 successfully defended the thesis/dissertation entitled "ADAPTIVE SIGNAL PROCESSING BASED INTELLIGENT METHOD FOR FAULT DETECTION AND CLASSIFICATION IN MICROGRIDS", which he prepared after fulfilling the requirements specified in the associated legislations, before the jury whose signatures are below.

Thesis Advisor : **Prof. Dr. Serhat ŞEKER** .....
Istanbul Technical University

Jury Members : **Prof. Dr. Emine AYAZ** .....
Istanbul Technical University

Prof. Dr. M. Hakan HOCAOĞLU .....
Istanbul Commerce University

Prof. Dr. Ömer USTA .....
Istanbul Technical University

Prof. Dr. GÖKHAN GÖKMEN .....
Marmara University

Date of Submission : 5 January 2022
Date of Defense : 23 February 2022

To my beloved mother,

FOREWORD

I would like to thank my mother for their financial and moral support at all levels of academic education. I know that without her unconditional support, I would not have been able to reach this degree and level. Thanks to her support, I had the strength to get up and move on after every defeat.

My thesis advisor, Prof. Dr. Serhat ŞEKER I would like to express my gratitude to for providing me this opportunity and for his technically and mentally support in every field during my thesis.

I would lıke to thank to Scientific and Technological Research Council of Turkey (TÜBİTAK) Marmara Research Centre for its support in my Ph.D. studies.

February 2022

Resul AZİZİ
(M.Sc Electrical Engineer)

TABLE OF CONTENTS

ABBREVIATIONS

BESS : Battery Energy Storage System
CWT : Continuous Wavelet Transform
DER : Distributed Energy Resources
DFIG : Doubly Fed Induction Generator
ECOC : Error Correcting Output Coding
EMD : Empirical Mode Decomposition
ESS : Energy Storage System
EWT : Empirical Wavelet Transform
HHT : Hilbert Huang Transform
IMF : Intrinsic Mode Function
LVRT : Low Voltage Ride Through
MG : Microgrid
MPPT : Maximum Power Point Tracking
PCC : Point of Common Coupling
PMSG : Pemanent Magnet Synchronous Generator
PV : Photovoltaic
RES : Renewable Energy Sources
SCIG : Squirrel Cage Induction Machine
SNR : Signal to Noise Ratio
VMD : Variational Mode Decomposition
VSC : Voltage Source Converter

SYMBOLS

$\psi_j(t)$	: Mother Wavelet
$\phi_j(t)$	: Father Wavelet
a, b	: Scalling Parameter, Translation Parameter
a_{jk}, d_{jk}	: Approximation, Detail Ceofficients
τ	: Parameter Control Position of Gaussian Window
t	: Time
$A(j,n)$	: Amplitude Spectrum
$\phi(j,n)$	: Phase Spectrum
$A_k(t), \varphi_k(t)$	: Envelope, Phase
$e_l(t), e_u(t)$	: Lower, Upper Envelope
$r_i(t)$	: Residue
$s(t)$	: Main Signal
$*$	: Convolution
$\|f(.)\|^2$	: Norm-2
$\Phi(\omega)$	: Empirical Wavelet Function
ω_k	: Central Frequency
F^{-1}	: Inverse Fourier Transform
$\langle . \rangle$	: Inner Product
$D(t)$	: Amplitude
$\theta(t)$	: Phase
X, Y	: Denote The Instance Space And The Set Of Class Labels
D	: Training Data Set
D_t	: Learning Round
h_t	: Base Learner
$\Phi(m,t)$	: Potential Function
c	: Clock Cutoff
ϵ	: Target Error
$H(x)$	: Output Of Final Hypothesis
k_p, k_i	: Controller Proportional and Integral Gain
$\omega, \omega_s, \omega_r, \omega_m$	: Grid Frequency, Synchronous Frequency, Rotor's Voltage And Current Frequency, Rotor Electrical Speeds
Ω_m	: Mechanical Speed
$C_p(\lambda, \beta)$	: Power Coefficient
λ	: Tip Speed Ratio
Ω_t	: Rotational Speed Of Wind Turbine
β	: Pitch Angle
$C_{pmax}(\lambda, \beta)$	: Maximum Power Coefficient

LIST OF TABLES

Page

LIST OF FIGURES

ADAPTIVE SIGNAL PROCESSING BASED INTELLIGENT METHOD FOR FAULT DETECTION AND CLASSIFICATION IN MICROGRIDS

SUMMARY

The ever-increasing energy demand, the environmental issue of fossil fuels and the high investment cost for the establishment of bulk power plants lead energy plans to more flexible and scattered small-scale energy sources. The main feature of these new topologies is that they consume renewable energy sources for electricity generation. It also requires less time to plan, build and operate. Moreover, they are close to energy sources and local loads. So, there are more efficient, with minimal environmental issues. However, besides their benefits and advantages, they pose a new challenge for traditional power systems. These challenges include protection issues, stability concerns, complex control systems and so on.

Traditional power systems include mass generation followed by transmission and distribution. In this topology, it is possible to plan generation because consumption at the transmission level of the power system is more predictable and fuel resources are always available for generation units. On the other hand, the transmission system and its conditions can be controlled by state estimators and SCADA system. Therefore, production and consumption uncertainties are minimal and conventional protection is sufficient to protect these systems. Also, distribution systems have no generating units, systems are mostly radial and overcurrent protection systems are sufficient to protect them. In these passive networks, it is not necessary to have fast and reliable protection systems as in transmission systems.

The initial role of these new energy sources was to act as a backup for mass production and to eliminate the small generation and consumption mismatch during peak consumption. On the other side, huge demand growth and investment time of mass production units and environmental concerns make these distributed energy resources (DERs) (wind, solar, biomass, etc.) popular in the distribution system. However, the contribution of the early DER groups to the total production is low and the control systems are very sensitive to voltage disturbances such as faults. Thus, according to the grid codes, after any minor fault or disturbance in the system, the DERs are disconnected, synchronized manually and reconnected after the fault is cleared.

With the increasing penetration of DERs in distribution systems, they play an important and rapidly increasing role in the total production of the system. Therefore, de-energizing all these DERs in an area in the distribution system after a fault has occurred can lead to stability problems due to generation and consumption imbalance.

Accordingly, a new concept called microgrid emerged and mainly established in distribution systems. This topology is the microscale of the power system. It can operate autonomously and cover the total demand of this local distribution system. Like the SCADA power system, it has an equivalent centralized monitoring and control system. The total generation is almost sufficient for the total demand of the loads in distribution networks converted to microgrid. It can operate as a standalone

ecosystem separated from the main grid and is self-sufficient. The basic requirement of this topology for connecting to the main grid through PCC (point of common coupling) is to increase the total inertia of the system and increase the post-fault stability region. In addition, this topology can transfer energy to the main system if it produces more power than the loads consume. This can reduce the stress of mass production units. Last but not least, if the main upper grid disturbed, the microgrid can continue to supply its loads by disconnecting from the grid.

In this new concept, grid codes expect the micro grid to be able to ride through faults and disturbances thanks to low voltage ride through (LVRT) systems. In fact, as a micro-scale model of the power system, the voltage of the DERs at the time of fault occurance is controlled by the LVRT, and the DERs continue to operate without disconnection after the fault is cleared by circuit breakers or other elements). Therefore, more complex control systems are required for DERs.

However, microgrids are distribution systems and unlike traditional power systems, there is a high amount of uncertainty in generation and consumption (loads). The distribution system has changed from a passive network to an active dynamic network. In this system, topology, generation and consumption are changed faster and faster than in conventional power systems. This situation constantly changes the fault current level and direction, and the conventional overcurrent protection is completely insufficient to protect them. Also, due to the high penetration of sensitive DERs, prolonged fault current is not allowed (stability concerns). Moreover, inverter-based DERs have a very small contribution to the fault current level.

The current protection method of microgrids is adaptive protection. In this model, all operating conditions of the system are extracted and all components of the systems are continuously monitored by central or decentralized control system or even dynamic load estimation. This model cannot be applied to a central control system because it has to process large amounts of data at a high sampling rate and it is impossible to make real-time decisions.

Based on these facts, a new intelligence-based method for fault detection and classification of microgrid is proposed in this thesis. In the proposed method, three different adaptive signal processing methods are used to extract the short-time transient component of the signal instead of the fault current level. It transfers data (feature extraction) into three different data spaces. The main feature of these signal processing methods is that they do not use a predefined basis to decompose a signal. The basis is adaptive to signal and extract components depend on the noise penetration level and frequency components of the signal.

An intelligence-based method called Brwonboost is used to make decisions in these data spaces, and the total decision is taken by the majority of votes of these three intelligence-based methods in these three data spaces. The main unique feature of the proposed method compared to traditional machine learning methods is its adaptability and uses a non-convex optimization method for detection and classification. The proposed method is a set of weak classifiers and tries to learn the data space step by step and iteratively. It tries to adapt the data by classifying the data that was misclassified in previous iterations. On the other hand, the unique non-convex optimization feature of the proposed method gives it an intelligence to select or discard misclassified data. It can decide step-by-step removal of the algorithm's iteration data in the training process if there is an outlier or a violation in another class area. This feature provides evidence against overfitting and becomes as practical a method as it

is for real-world measured data. Finally, a Brownboost decision is also made by a majority vote of the weak classifiers.

An intelligence-based method called Brwonboost is used to make decisions in these data spaces, and the total decision is taken by the majority of votes of these three intelligence-based methods in these three data spaces. In this method the classifier works base on the margin. This means, instead of only finding a classifier that minimize the classification error, it selects a classifier that has maximum discrimination between data of every class. The unique feature of the proposed method compared to traditional machine learning methods is its adaptability and uses a non-convex optimization method for detection and classification. The proposed method is an ensemble of weak classifiers and tries to learn the data space step by step and iteratively. It tries to adapt to the data by classifying the data that was misclassified in previous iterations. On the other hand, the unique non-convex optimization feature of the proposed method gives it an intelligence to select or discard misclassified data. During this step-by-step process, the algorithm can detect outliers or misclassified data that intensely violated other class area and remove it. This feature makes it robust against overfitting and becomes as practical method for real-world measured data.

In total, the proposed method tries to classify the data in three different data spaces. The data area that makes maximum distinction between the data of each class is less sensitive to noise. Thus, a classifier has are fewer generalization errors to unseen new data (higher margin). Therefore, its Brownboost has more voting power in decision making.

The results are test in test benchmark microgrid. DERs are modeled with the detailed model to extract the true detail form of the signal. Various types of control model and fault ride thruogh feature of DERs are implemented.

MİKROŞEBEKELERDE ARIZA TESPİTİ VE SINIFLANDIRMASI İÇİN ADAPTİF SİNYAL İŞLEME TABANLI AKILLI YÖNTEM

ÖZET

Sürekli artan enerji talebi, fosil yakıtların çevre sorunu ve büyük santrallerin kurulması için yüksek yatırım maliyeti, enerji planlarını daha esnek ve dağınık küçük ölçekli enerji kaynaklarına yönlendirmektedir. Bu yeni topolojilerin temel özelliği, elektrik üretimi için yenilenebilir enerji kaynakları tüketmeleridir. Ayrıca planlamak, inşa etmek ve işletmek için daha az zaman gerektirir. Bundan başka enerji kaynaklarına ve yüklere yakın noktalarda inşa edilirler. Dolayısıyla, minimum çevre sorunlarıyla birlikte yüksek verimlilik elde edilir. Fakat, bununla birlikte, faydaları ve avantajlarının yanı sıra, geleneksel güç sistemleri için yeni bir zorluk teşkil etmektedirler. Bu zorluklar arasında koruma sorunları, kararlılık endişeleri, karmaşık kontrol sistemleri vb. sayılabilir.

Geleneksel güç sistemleri, üretim, iletim ve dağıtımın olacak şekilde bir sıralı yapıdan oluşur. Bu topolojide, güç sisteminin iletim seviyesinde tüketimin daha öngörülebilir olması ve üretim birimleri için yakıt kaynaklarının her zaman kullanılabilir olması nedeniyle üretimi planlamak mümkündür. Öte yandan, iletim sistemi ve koşulları durum tahmin edicileri ve SCADA sistemi ile kontrol edilebilir. Bu nedenle üretim ve tüketim belirsizlikleri minimum düzeydedir ve bu sistemleri korumak için geleneksel koruma yeterlidir. Ayrıca dağıtım sistemlerinde üretici ünite yoktur, sistemler çoğunlukla radyaldir ve aşırı akım koruma sistemleri onları korumak için yeterlidir. Bu pasif şebeklerde iletim sistemlerindeki gibi hızlı ve güvenilir koruma sistemlerine sahip olmak gerekli değildir.

Bu yeni enerji kaynaklarının başlangıçtaki rolü, seri üretim için bir yedek olarak hareket etmek ve en yüksek tüketim sırasındaki küçük üretim ve tüketim uyumsuzluğunu ortadan kaldırmaktı. Öte yandan, hızlı talep artışı ve büyük güçteki üretim birimlerinin yatırım süresi ve çevresel kaygılar, bu dağıtık üretim kaynaklarını (DÜK'ler) (rüzgâr, güneş, biokütle vb.) dağıtım sisteminde popüler hale getirmektedir. Ancak ilk zamanlardaki DÜK'lerin toplam üretime katkısı düşüktü ve kontrol sistemleri arıza gibi gerilim dalgalanmalarına karşı çok hassastı. Böylece şebeke kodlarına göre sistemdeki herhangi bir küçük arıza veya dalgalanmadan sonra DÜK 'ler devreden çıkar, manuel olarak senkronize edilir ve arıza giderildikten sonra tekrar bağlanır.

DÜK'lerin dağıtım sistemlerinde artan entegrasyonuyla, sistemin toplam üretiminde önemli ve hızla artan bir rol oynama başlamıştır. Bu nedenle, bir arıza meydana geldikten sonra o bölgedeki dağıtım sistemindeki tüm bu DÜK'lerin enerjisinin kesilmesi, üretim ve tüketim dengesizliği nedeniyle kararlılık sorunlarına yol açabilir.

Buna göre, mikro şebeke adı verilen yeni bir kavram ortaya çıktı ve genel olarak dağıtım sistemlerinde kurulmaya başladı. Bu topoloji, güç sisteminin mikro ölçeğidir. Otonom olarak çalışabilir ve bu yerel dağıtım sisteminin toplam talebini karşılayabilir. SCADA güç sistemi gibi, eşdeğer bir merkezi izleme ve kontrol sistemine sahiptir.

Toplam üretim, mikro şebekeye dönüştürülen dağıtım şebekelerindeki yüklerin toplam talebi için neredeyse yeterlidir. Ana şebekeden ayrılmış bağımsız bir ekosistem olarak çalışabilir ve kendi kendine yeterlidir. Ortak bağlantı noktası aracılığıyla ana şebekeye bağlanmaya gerek duymasının nedeni, bu sistemin toplam ataletini artırmak ve arıza sonrası karasızlık olasılığını düşürmektir. Ayrıca bu topoloji, yüklerin tükettiğinden daha fazla güç üretiyorsa enerjiyi ana sisteme aktarabilir. Bu, özellikse ana şebekenin puant tüketim esnasındaki üretim ünitelerinin üzerindeki stresi azaltabilir. Son olarak, ana üst şebeke oluşan bir arızada, mikro şebeke şebekeden ayrılarak yüklerini beslemeye devam edebilir.

Bu yeni konseptte, şebeke kodları, mikro şebekenin gerilim salınımlarından alçak gerlim sürüşü (AGS) sayesinde geçebilmesini beklemektedir. Aslında, güç sisteminin mikro ölçekli bir modeli olarak, DÜK'lerin arıza anında voltajı AGS tarafından kontrol edilir ve arıza devre kesiciler veya diğer elemanlar tarafından temizlendikten sonra DÜK'ler bağlantı kesilmeden çalışmaya devam eder. Bu nedenle, DÜK'ler için daha karmaşık kontrol sistemleri gereklidir.

Ancak mikro şebekeler dağıtım sistemleridir ve geleneksel güç sistemlerinden farklı olarak üretim ve tüketimde (yüklerde) yüksek miktarda belirsizlik vardır. Dağıtım sistemi pasif bir şebekeden aktif bir dinamik şebekeye dönüşmüştür. Bu sistemde, üretim ve tüketim, geleneksel güç sistemlerine göre daha hızlı değişir. Bu durum sürekli olarak arıza akım seviyesini ve yönünü değiştirir ve konvansiyonel aşırı akım koruma röleleri korumak için tamamen yetersizdir. Ayrıca, hassas DÜK'lerin yüksek katkısı nedeniyle, uzun süreli arıza akımına izin verilmez (kararlılık sorunlarından dolayı). İlaveten, evirici temelli DÜK'lerin arıza akımı seviyesine çok küçük bir katkısı vardır. Öte yandan, mesafe röleleri mikro şebeke koruması için iyi bir seçim değildir. Bunun nedeni, mikro şebekenin genellikle orta veya alçak gerilim dağıtım sistemlerinde yerleşik olmasıdır. Dağıtım sistemlerinin hat uzunlukları kısadır ve arıza bölgeleri küçüktür. Dahili bir arıza meydana geldiğinde, devrenin asimetrisinden veya arıza empedansından kaynaklanan küçük bir hata, rölenin gecikmeli çalışmasına veya bazen çalışmayı reddetmesine neden olabilir.

Mikro şebekelerin mevcut koruma yöntemi adaptif korumadır. Bu modelde sistemin tüm çalışma koşulları çıkarılır ve sistemlerin tüm bileşenleri merkezi veya merkezi olmayan kontrol sistemi veya hatta dinamik yük tahmini ile sürekli olarak izlenir. Bu model merkezi bir kontrol sistemine uygulanamaz çünkü büyük miktarda veriyi yüksek bir örnekleme hızında işlemek zorundadır ve gerçek zamanlı kararlar vermek imkansızdır.

Bu gerçeklere dayanarak, bu tezde, mikro şebekenin arıza tespiti ve sınıflandırılması için yeni bir akıllı makine öğrenme tabanlı yöntem önerilmiştir. Önerilen yöntemde, arıza akım seviyesi yerine sinyalin kısa süreli geçici olay bileşenini çıkarmak için üç farklı adaptif sinyal işleme yöntemi kullanılmıştır. Verileri (özellik çıkarma) üç farklı veri alanına aktarır. Bu sinyal işleme yöntemlerinin temel özelliği, bir sinyali ayrıştırmak için önceden tanımlanmış bir temel kullanmamalarıdır. Temeller, sinyale uyarlanabilir ve bileşenlerin gürültü oranı ve sinyalin frekans bileşenlerine bağlı olarak çıkarılır.

Bu veri uzaylarında karar vermek için Brwonboost adı verilen makine öğrenme tabanlı bir yöntem kullanılır ve son karar, bu üç veri alanında bu üç makine öğrenme tabanlı yöntemin oy çokluğu ile alınır. Bu yöntemde sınıflandırıcı marj bazında çalışır. Bu, yalnızca sınıflandırma hatasını en aza indiren bir sınıflandırıcı bulmak yerine, her sınıfın verileri arasında maksimum ayrıma sahip bir sınıflandırıcı seçtiği anlamına

gelir. Önerilen yöntemin geleneksel makine öğrenme yöntemlerine kıyasla en önemli özelliği adaptif olması ve algılama ve sınıflandırma için dışbükey olmayan bir optimizasyon yöntemi kullanır. Önerilen yöntem, zayıf sınıflandırıcılardan oluşan bir topluluktur ve veri uzayını adım adım ve yinelemeli olarak öğrenmeye çalışır. Önceki iterasyonlarda yanlış sınıflandırılan verileri sınıflandırarak verilere uyum sağlamaya çalışır. Öte yandan, önerilen yöntemin benzersiz dışbükey olmayan optimizasyon özelliği, yanlış sınıflandırılmış verileri seçme veya atma konusunda karar verebilme özelliğine sahiptir. Bu adım adım işlem sırasında, algoritma, diğer sınıf alanını yoğun bir şekilde ihlal eden aykırı değerleri veya yanlış sınıflandırılmış verileri tespit edebilir ve kaldırabilir. Bu özellik, onu aşırı öğrenmeye karşı sağlam kılar ve gerçek dünyada ölçülen veriler için pratik bir yöntem haline gelir.

Toplamda önerilen yöntem, verileri üç farklı veri uzayında sınıflandırmaya çalışmaktadır. Her sınıfın verileri arasında maksimum ayrım yapan veri alanı gürültüye daha az duyarlıdır. Böylece, bir sınıflandırıcı, görünmeyen yeni verilere yönelik daha az genelleme hatasına sahiptir(daha yüksek marj). Bu nedenle, bu uzaydaki Brownboost karar vermede daha fazla oy hakkına sahiptir.

Sonuçlar, örnek test mikro şebekede değerlendirilmiştir. DÜK'ler, sinyalin gerçek detay formunu çıkarmak için ayrıntılı modelle modellenir. DÜK'lerin çeşitli tiplerde kontrol modeli ve arızalı sürüş özelliği uygulanmaktadır.

1. INTRODUCTION

The ever-increasing energy demand, the inadequacy of traditional energy production plans and environmental problems are leading energy plans for new alternative choices. This is causing a steady increase in the demand and acceptance of renewable energy sources (RES) due to the positive environmental impact that is free for fuel sources such as wind and solar. But besides these benefits, RES has presented significant challenges in adapting and controlling them to conventional power systems. With the increasing penetration of RES and the establishment of close generation (distribution networks), more sophisticated and complex controls are becoming indispensable. Also, due to the high penetration of these resources and their significant role in meeting the power demand, disconnecting them after every outages and disturbances can render the power system unstable. Therefore, it is necessary to create new control and operating methods that optimally meet power demands and are resistant to disturbances. The proposed methods require economically validated topologies and therefore introduce minimal infrastructure changes.

To meet these expectations, a new power system topology called microgrid (MG) (Figure 1.1) has been introduced in power systems. A microgrid [1] is a low or medium voltage distribution system, usually equipped with different distributed energy resources (DERs) (solar, wind, diesel, battery storage, tidal, biomass, asymmetrical and inverter-based DC system, etc.). as well as various types of loads (linear, non-linear, dynamic, static and new EV charger DC load model, etc.). These micro-resources are distributed in an area according to its surroundings according to renewable energy resources. Microgrids are a micro-scale model of power systems with a wide variety of loads and DERs (inverter-interfaces, storage systems, and rotating and…). on resources such as the storage system (charging, unloading). It can also operate autonomously (island) and feed loads with proper control of DERs. This network model is persistent against external disturbances as well as optimizing the operation of DERs. In addition, various control modes make it easy for the microgrid to pass through faults with minimal loss of generation and consumption.

This topology is mainly installed in medium voltage distribution systems. However, it has sufficient flexibility for installation in low voltage distribution networks or, in some cases, transmission systems where it is close to loads. This topology is the microscale of the power system. It can operate autonomously and meet the aggregate demand of this local distribution system. Like the SCADA power system, it has an equivalent centralized monitoring and control system. The total generation is almost sufficient for the aggregate demand of the loads converted to microgrid in the distribution system. It can operate as a standalone ecosystem separated from the main grid and is self-sufficient. The basic requirement of this topology for connecting from PCC (point of common coupling) to the main net is to increase the total inertia of the system and increase the post-failure stability zone. In addition, if this topology produces more power than the load needs, it can transfer the energy to the main system. This can reduce the stress of bulk production system (main grid). In addition, if the main upper grid fails, the micro grid can continue to supply its load by disconnecting from the grid.

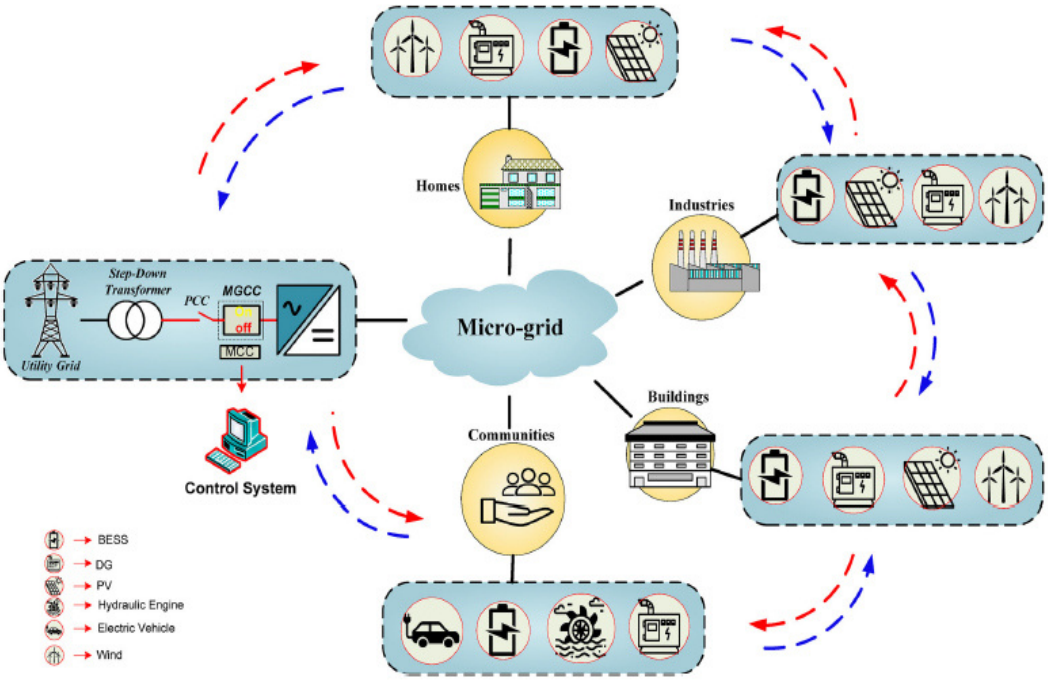

Figure 1.1 : Typical Concept of Microgrid [2].

According to these facts, control systems have to optimally share the demand power for optimum harvesting of renewable energy sources. They also have to keep stable

operation and ride-through the fault or disturbances after isolating the faulty area. These problems are exacerbated by emergance and development of MGs and with it the increasing penetration of DERs. These systems enable DERs to operate both in island and grid connection. In grid connected mode, the MG is connected to the main grid through PCC. The voltage and frequency (V-f) of the DERs are supported by the main grid and V-f control of DERs is not required. However, in islanded mode the topology operates as an autonomous energy island. It has to keep both voltage and frequency at rated value while responding to the active and reactive power demands of the loads. In this mode the system is very sensitive to disturbances due to the low total inertia of the system. İn addition, the stochastic behavior of the RES in this mode of operation results in the use of energy storage systems (ESS) or flywheel as backup generations. These ESSs also need to be charged by the DERs or main grid at appropriate time intervals, thus making the power demand management problem increasingly complex.

Various methods have been proposed for optimal control of MGs in islanded mode. The purpose of these methods is:

1- Optimum power sharing between DERs [3; 4].

2- Prevent DERs from violating operational limits [5].

3- Keep the MG stable after sudden transitions and disturbances (faults) in the MG [6].

Depending on the size of the MG, these control methods are generally classified as centralized and decentralized [7]. In centralized methods, DERs and loads are connected via communication link and the measured voltages and currents are transferred to the central decision system. Based on aggregate demand, load priority, and loading of DERs, reference values (commands) for DERs are transmitted. Although these systems are reliable and provide optimum power flow, they are not economically viable for large scale MGs. In addition, with the rapid growth of MGs and the emergence of multiple MG clusters (Figure 1.2) [8], studies have concentrated on decentralized models. As an initial attempt drop control systems are suggested for MGs. The operation of this control model is based on sampling the measurements of the DER terminal and keeping V-f at permissible values while generating the reference (required) active and reactive power (P-Q). In this method, communication links are

minimized and the control system is less complex. However, it suffers from a lack of improved power sharing between loads and DERs and poor stability performance. Other decentralized methods such as hierarchical control methods consist of primary control loop responsible for power sharing control, secondary for V-f control and zone control for optimization.

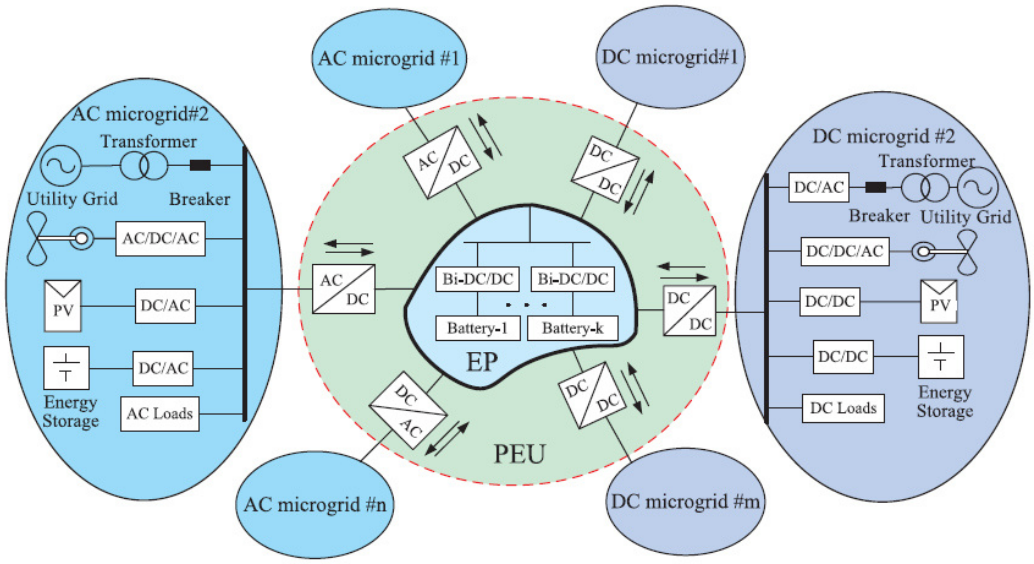

Figure 1.2 : Concept of Microgrid Clusters [9].

According the these facts, the MGs advanced operation condition create benefits and advantagous for optimal operation of the novel RES. However this toplogy and its modern operational conditions pose serious challenges that cannot be justified by traditional power system solutions. One of these key challenges is fault detection and protection of MGs. MGs are substantially established in distribution systems and unlike traditional power systems there is a high amount of uncertainty in generation and consumption (loads). The distribution system has changed from a passive network to an active dynamic network. In this system, topology, generation and consumption are changed rapidly and faster than in conventional power systems. This situation constantly changes the fault current level and direction, and the conventional overcurrent protection is completely insufficient to protect them. Also, due to the high penetration DERs sensitive to disturbances, prolonged fault current is not allowed (stability issue). These systems are mainly equipped with novel inverter based DERs in order to optimally harvest of the reneable energies. However these inverter-based DERs have a very small contribution to the fault current level.

Other suggested solution for microgrid protection is differential protection [10]. It compares the current diffrence of the two points and the decision is done by a predefined threshold. This method do not need a prior knowledge about fault current level. It is fast and simple to implement. One concern about this protection method is necessity to increase the measurement devices compare to counterparts. This in turn increase the cost. It is a coomunication based method and delays affect the performance significantly. The differential protection is used to protect a single unit in power system like busbar, transformer and so on. It is not possible to define a backup protection of the same type. Other protection methods is selected as backup protection. According to this fact when it is needed to protect complete network wih a proper method a sole differntial protection method is insufficient for whole network.[11]

The current protection method of MGs is adaptive protection. In this model, all operating conditions of the system are extracted and all components of the systems are continuously monitored by central or decentralized control system or even dynamic load estimation. This model cannot be applied to a central control system because it has to process large amounts of data at a high sampling rate and it is impossible to make real-time decisions. Dynamic status alerting and other monitoring systems in the decentralized control system (where systems communicate locally) significantly increase operating costs and need to be checked for worthwhile work.

As a result, protection methods are inadequate for fault detection and classification of MGs due to the following causes and effects:

1- Operational modes of the MGs and DERs are key parameter that are effective on fault current level. As an example in islanding mode, the type of DERs, whether rotational type DERs or full inverter based DERs, is a highly effective on fault current level. For example, DERs with inverter interface limits the fault current level to 1.2-2 times of the nominal value because of fault current limiters. This causes saturation of the limiters and distortion of voltage and current during a fault [12; 13]. Also, the location of the DERs is influential. In small MG the DERs are centralized in a small area and the fault current level and direction are more predictable. However, it is a large GO, DERs are scattered in the area near renewable energy sources. This, in turn, greatly affects the level and direction of the fault current, and a detailed study is indispensable for the proper setting of conventional protection devices. Finally,

the main sources of fault current in island mode operation are DERs. Therefore, the fault current level also depends on the loading level of the DERs.

2- Various operating modes and topologies of DERs are also effective in fault current direction and level. Unlike traditional distribution networks, MGs are an active medium voltage network. Generally, in these systems, the topology of the network (radial, mesh) is constantly changing. This leads to bidirectional power flow between the main grid or resources, causing sympathetic tripping or blinding of conventional protection relays [14; 15].

3- The novel type of the DERs utilized low voltage ride through (LVRT) equipments. This property helps them the avoid post fault instability and pass from the fault if it is not in isolated faulty area [16].

4- When a MG operate in in islanded mode the total inertia of the network decreased considerably. This leads to have higher risk of instability because a prolonged faults. Thus, a method for fast post fault recovery of MGs is indispensible (LVRT) [17].

1.1 Purpose of Thesis (Second Level Title: First Letters Capital)

In this thesis, an intelligence-based method is introduced for fault detection and classification of MGs. The proposed method provides a unique answer to the problem of overfitting, which is the main challenge of intelligence-based methods. This makes it applicable for practical purposes. Another feature of this method is decision making is done based on majority vote of multiple classifiers instead of a single classifier. In this method, a group of simple intelligence methods are utilized in the decision-making process. This condition helps it achieve the same performance as any typical strong method, along with simplicity in programming.

The test microgrid is modeled with all its details and various control and operating modes. This helps us test the proposed method with all possible protection challenges. Finally, the method is tested with real-world data shortcomings such as out-of-sync, noise, and presence of outliers.

1.2 Literature Review

In order to protect the MGs and cope with their protection challenges, many solutions have been introduced in the studies. The main goal of these solutions is minimizing the infrastructure change of protection pattern and economic consideration as well as achieving to high reliability.

The initial tries are concentrated on solving these challenges for only specific operating modes or topologies. These methods are for islanded mode equipped only with inverter interfaced [18], photovoltaic-systems [19] or voltage frequency (V/f) [20]. The method proposed In [21], is only practical for radial microgrids in small scale. These methods are fast and safe, but they do not cover all operational conditions and are not suitable for practical purposes. Thus, they are applicable for a specific porpuse MGs and if it is necessary to operate in other operational modes additional measures are necessary which increase the operatinal cost considerably. Other practical attempts are state of the arts methods [6]. The important examples of these methods are legacy distance protection, line differential protection and adaptive protection scheme with microgrid central protection. These methods help us to establish a protection method with minimum infrastructure changes. However, they are suitable for small scale microgrid with centralized protection method, or for specific topology microgrids. Therefore, they lost their justifications with increasing penetration of the growth in their scale.

Further studies have attempted to suggest solutions with existing technologies, such as or voltage-based power differentials [12]. The main goal of these methods is minimum change of the infrstructures, using exsiting grid devices and create economic justtification. These method prompt and secure, but it is necessary to have devices with considerable accuracy and sample frequency. Another suggested solution for microgrid protection is Adaptive protection [22; 23; 24], which is an continous process for monitor and change the setting of the protection relays. The condition of then is changed as the operating condition of the microgrid and DERs vary. These devices are secure enough but need extensive telecommunication infrastructure and high speed processing systems.

As it is seen, the conventional solutions are considered insufficient or uneconomical. In addition, solution based on fault current level is not a proper answer to MG's dynamic behavior. Thereby, the attempts move toward intelligence-based methods,

analyzing and extracting the transient behavior (components) of the signal instead of their level. Initial attempts are focus signal processing, and non-stationary signal analysis methods. These methods are used to extract the frequency component of the transient phenomenon at the moment of disturbance (fault). These methods set threshold(s) for the components and classify these transients according to these fixed predefined experimental values. This property gives a more robust behavior against MGs operational modes and variation in its topology. They are generally classified in the time and time-frequency domains. The methods based on the time domain analysis [25] are simple to implement and program in processing systems, but the main drawback is that they are inapplicable on noisy or out-of-sync data. Thus, these methods are not applicable for real world measured data and the time frequency methods are more preferrable. As stated, these methods are based on experimental adjustment of the threshold values which is its main drawback. If a small value is set as threshold, there is a high risk of misclassification between faults and other transient phenomena. Conversely, a high threshold prolongs the time to issue trip signals, delays the LVRT control and increases the risk of postfault instability. Furthermore, for different transient phenomena of the same class or other classes the time it takes to pass the threshold value is not equal and it not possible the properly define the detection time of these methods. S-transform [26; 27; 28], Hilbert-Huang transform [29] and wavelet transform-based [30] signal processing are prevalent methods for fault detection and classification. As an instance to these methods in ref [31] discrete wavelet transforms and singular value decomposition (SVD) is used for detecting and classification of the fault. The wavelet transform is implemented on current signal to extract high frequency component under the fault condition. Wavelet coefficients of signals under each fault condition are extracted. These coefficients are formed as a wavelet matrix. Then this matrix is decomposed by SVD and eigenvalues are extracted. For every phase of signal maximum singular value, which contains highest energy of the signal are calculated, normalize and then sum up with each other. According to these values and by empirical process the threshold of different types of faults are calculated. The main drawback of these signal processing methods and mainly the wavelet transform is it high noise sensitivity, which decrease its accuracy considerably. Also it is necessry to have multiple threshold values. Thus these methods are in applicable for practical and real world purposes. In [32] a monotreshold time time transform method it suggest for noisy data with sampling time differences. This

methods answers to some of the real world data concerns, but the risk of misdetection between transient phenomena was not solved.

According to these facts it is necessary to get rid of the setting the threshold by operator and manually. Thus, the signal processing methods are combined with machine learning method for decision making. The signal processing methods extract the outstanding features in order to be processed by machine learning methods. These methods are classified as linear and nonlinear methods depends on their operation on the data space. The linear methods are called weak learner (decision tree) and others are called strong learner (extreme learning machine). Weak learners have not enough accuracy for practical purposes and cannot cover whole operational modes of MGs. Therefore, strong classifiers are more advantageous. These methods attempt to optimize the classification error based on convex optimization methods. This type of classification main goal is only minimize the classification error at all costs. However, this behavior always have a high risk of overfitting in noisy dataspace or dataspace with outliers during training the .algorithm. In addition, these methods contain coefficients which is necessary to adjust properly in order to attain the desirable performance and there is no straightforward method to adjust them.

Ref [33] is an example of a combination of deep learning and signal processing methods for fault detection. In this paper, S-transform and decision tree based smart scheme is applied for fault detection and classification. In the preprocessing procedure, the S-transform is used for feature extraction. Time windows are used as input data to obtain the differential characteristics and only one post-cycle fault current samples of each phase from the fault are used at the bus ends of the respective feeder. The S-transform of the fault current at both ends of the respective feeders is taken and statistical properties such as mean, standard deviation, skewness, kurtosis, energy and entropy are extracted. However, in this method, data at both ends of the feeder is required for fault analysis. The above parameter of both currents is the key parameter to train the Decision Tree for fault location, classification and detection in MGs.

In ref [34] it emphasizes to existence of unsymmetrical faults in MGs and necessity of not tripping healthy phases. In this article it claims that novel methods base on machine learning is robust against fault resistance and impedance of photovoltaic systems or variation of their power factor during the fault. in feature extraction process for fault in this article fault current is divided to an active and reactive parts, where the fault

current is mainly affected from reactive component. Besides, in this article instead of fault current voltage magnitude and its phase is used.

In ref [35] combined wavelet transform and decision tree is implemented for protection of the microgrid for programming intelligent relays. The process starts by extracting current signals from relying points and extract their features by wavelet transform. Thn parameters like Shannon entropy, energy and standard deviation from the coefficients of discrete wavelet transform is calculated. In this article the purpose is to identify the fault as fast as possible to overcome the novel instability problems which emerges by implementing the MGs in power systems. Symmetrical components of differential current are used for fault identification instead of the line current, voltage, and harmonic current. This article's main drawback is only islanded mode of the microgrid is considered. The current signal is extracted from the network and processed then by decision tree classifier for fault detection. Besides that, the negative, positive, and zero components of the signal is extracted and their wavelet transforms is again given to another decision tree for detecting the fault type. A (Consortium for Electric Reliability Technology Solution CERTS) microgrid is used for test and identify our results. In this method the features of the coefficient that has vital information during fault, is calculated. The results are first change to perunit form. And try to find the most distinct deviation in detail coefficients of wavelet transform in which the 7th,11th,13th harmonic exists.

A new approach for fault classification based on combination of the machine learning and wavelet transform in ref [36] is introduced in this paper. The outstanding trait in this paper is implantation of Particle Swarm Optimization (PSO) for selecting the optimal mother wavelet function matching point to find which function is able to extract the best feature characteristics of faults. Discrete wavelet transform is applied in Both voltage and current waveform. Afterward, four classification techniques: Decision Tree, K-Nearest Neighbor, Support Vector Machine, and Naïve Bayes are implanted and compare the results with each other by using Monte Carlo stratified cross validation method.

Machine learning based on wavelet or Hilbert-Huang transform in [37; 38; 39; 40], is used for fault detection and classification. These methods are very sensitive to the network topology and the effects of noise have not been studied. In addition, their accuracy is insufficient for practical purposes and zero sequence components of

voltage or other additional measurements are used as additional features to increase accuracy to some extent.Nevertheless, these methods are strong compare to weak classifiers but they cannot provide a sufficient accuracy for practical justification. To cope with these deficiency intelligence base methods, a move was made toward deep learning algorithms. In [15] there was a combination of wavelet transforms and deep neural networks, in [41] time-time transforms and deep belief networks were given and in [42] convolutional neural networks were proposed. These methods improve the performance significantly, but often the effect of noise is not considered. Moreover, there are many parameters and multiple hidden nodes to adjust. Therefore, these algorithms are very complex, and the risk of overfitting is high when tuning these models based on error minimization, especially for noisy data.

Given these facts, it is necessary to offer an intelligence method that will respond to MGs protection challenges. The proposed method needs to be able to deal with real-world data without the risk of overfitting. Additionally, most have the desired performance and accuracy for practical purposes.

1.3 Hypothesis and Motivation

The main goal of this thesis is introducing a method which is fast, secure and reliable for fault detection and protection of the microgrid. The proposed system does not need a central data gathering and decision-making device. Instead, the fault detection and issuing trip signal happens near the faulted load. It is robust to all topologies and operating modes of the MGs. The proposed method extracts the frequency component of the current signal for decision making. It processes only the transient behavior for differential current signal of both ends of the lines for fault detection and classification in a definite time window. Therefore, it is independent from fault current level and robust to traditional overcurrent protection system challenges. As a result, this model is suitable for all operating modes (grid-connected or islanded), topologies (mesh or radial) and dynamic behavior of the MGs.

In order to extract the frequency component of the signal a signal processing method called Hilber-Huang transform (HHT) is selected. The main advantages of this method are its time-frequency based signal processing and extracting the basis (transient behaviour) and defining the decomposition level according to the signal. In this method unlike the wavelet transform the basis are not a predefined function. The

decomposition level and the extracted component are adaptive to signal and it varies from one signal to another. In order to make a fast and secure decision a non-convex optimization based sequentially ensemble of decision tree (weak learners) nemed Brownboost [43; 44] is suggested. It combines with signal processing method with adaptive basis. This method only used decision trees that facilitate it to program and it has international process that helps to monitor the training process. The non convex optimization of Brownboost make it unique compare to its counterparts. This gives it power to select and eliminate misclassified data during it training iteration. By this property it is possible to remove malicious effects of the wrongly classified data during training process. It helps to have effective results in noisy real world data spaces. In the proposed method the data are transferred to three various attribute space and data space with more discrimination have higher voting power.

.

2. SIGNAL PROCESSING BASED FEATURE EXTRACTION

Signal processing methods, especially the non-stationary signal processing, are mainly recommended to identify and classify transient behavior in electrical power systems. In deep learning-based methods, signal processing tools are useful tools for investigating the extraordinary properties of the signal. As is known, due to the nature of measuring devices in power systems, only a limited number of data can be easily measured, and measuring other data is a time-consuming and costly process, or even impossible with existing equipment. As a result, signal processing can be used as a powerful tool for extracting some features or removing noise from existing data. This, in turn, can help us achieve better training and testing results with less measured data, and more extracted specific features.

The first step in constructing a suitable classifier is feature extraction. This helps to find and discriminate the outstanding property of raw data for each class. With this it is possible to create a data space (attribute space) with maximum separation between the data of each class. The greater the separation between the data of each class, the easier it becomes to program a classifier that is less susceptible to noise and more robust to overfitting. Therefore, classifiers will have fewer generalization errors against new data that is not visible in training process. In this article, signal processing methods are discussed as a suitable method for feature extraction. They assist in decision making based on the transient behavior of the signal at the time the fault occurs. Is it therefore independent of fault current level. This section introduces some of the dominant non-stationary signal processing methods used for error detection and classification in MGs. Then, the proposed method and its advantages over traditional methods are discussed.

In the proposed method, the decision is made by transferring the data to various feature spaces of the same type. The last part of this section discusses the reason and benefits of creating various data fields for decision making.

2.1 Wavelet Transform

The main motivation for the wavelet transform [45] is that a signal is believed to consist of different properties in terms of time and frequency. The high-frequency component is believed to have a short time interval, while the low-frequency components are believed to have a longer duration. Therefore, wavelet transform is introduced to get good resolution for both high frequency transient and low frequency periodic components. In mathematics, a continuous wavelet transform (CWT) is used to divide the continuous time function into wavelets. Unlike the Fourier transform, the continuous wavelet transform is capable of generating a time-frequency representation of a signal that offers very good time and frequency localization. The continuous wavelet transforms of a function x(t) on the scale ($a > 0$) and the translated value of $b \in \mathbb{R}$ are expressed as:

$$X_{a,b}(t) = \frac{1}{\sqrt{a}} \int_{-\infty}^{+\infty} x(t)\psi\left(\frac{t-b}{a}\right) dt \tag{2.1}$$

where is a continuous function in both the time and the frequency domain called the mother wavelet. Also, in this function a is called scaling parameter which is a degree of compression for mother wavelet. The b is translation parameter which determines the time location of the wavelet. The main purpose of the mother wavelet is to provide a source function to generate the daughter wavelets which are simply the translated and scaled versions of the mother wavelet.

2.2 Discrete Wavelet Transform

The goal of decamping a signal is mainly study it at different level of the resolution. The resolution of a signal is a parameter to describe it with its frequency components.

The practical application of wavelet transform is performed using discrete wavelet. Any time signals x(t) can be completely decomposed into approximations by using a dyadic scaling function $\phi_j(t)$which is also known father wavelet. The signal can decompose into detailed coefficients using mother wavelet $\psi_j(t)$ as depicted in Figure 2.1 and as follow:

$$\phi_{jk}(t) = 2^{-\frac{j}{2}}\phi\left(2^{-j}t - n\right) \tag{2.2}$$

$$\psi_{jk}(t) = 2^{-\frac{j}{2}}\psi(2^{-j}t - n) \tag{2.3}$$

Where $n \in \mathbb{Z}$,j and k are integers.

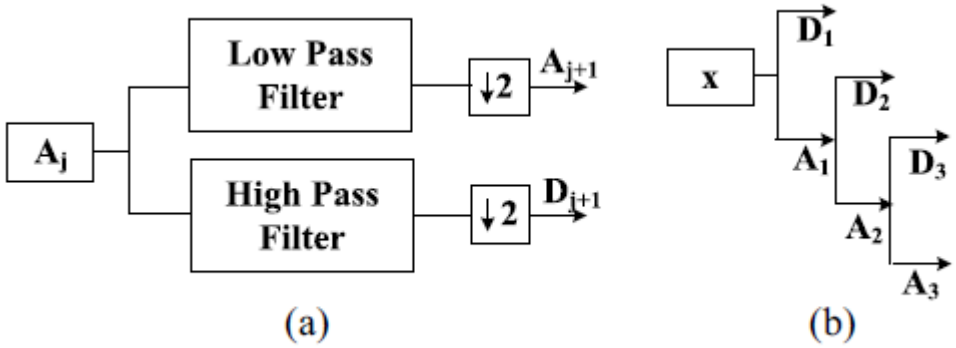

Figure 2.1 : Discrete Wavelet Transform.

As j and k are integers and the basis function is scaled by factor 2^{-j} and translated n units of time. The scaling function associated with low pass filters with filter coefficients $H = \{h_n\}$ and the wavelet function is associated with high pass filter coefficients $G = \{g_n\}$. It is important to note that G is reverse of H interleaved with sign changes. The two-scaling function give a rise to filters:

$$\phi(t) = \sum_n h(n)\sqrt{2}\phi(2t - n) \tag{2.4}$$

$$\psi(t) = \sum_n g(n)\sqrt{2}\psi(2t - n) \tag{2.5}$$

A signal x(t) having length 2^M, then there is maximum "M" levels of decomposition. The expression for the signal using wavelet transform is given as follows:

$$x(t) = \sum_{k=0}^{2^{M-j-1}} a_{jk}\phi_{jk}(t) + \sum_j \sum_{k=0}^{2^{M-j-1}} d_{jk}\psi_{jk}(t) \tag{2.6}$$

Where $a_{jk}$and d_{jk} are known as the approximation and detail coefficients of the signal at level j, respectively. The signal is passed through high and low pass filters. Then the outputs of both filters are down-sampled by a factor of 2. The approximation and detailed coefficients for level 1 (A1 and D1) are obtained. This process continue until a predifined desired decomposition level is reached.

2.3 Stockwell Transform (S-Transform)

S-transform [46] is a combination of Gabor transform and wavelet that scales and localize the Guassian window. It is able to have multiresolution analysis because of variable window. The standard deviation is an inverse function of frequency, thus reducing the dimension of the transform. Moreover, the S transform doesn't have a cross-term problem and yields a better signal clarity than Gabor transform. However, the S transform has its own disadvantages: the clarity is worse than Wigner distribution function and Cohen's class distribution function. To avoid some of these disadvantages, various adaptive forms of the S-transform have been introduced.

The expansion for S-transform of continuous signal $x(t)$ in time domain is given as:

$$s(t,f) = \int_{-\infty}^{+\infty} x(t)w(\tau - t, f)e^{-j2\pi ft}dt \tag{2.7}$$

Where f is the frequency, t is the time and τ is a parameter that control position of Gaussian window on the t-axis. The window function can be expanded and the S-transform in time domain is given as follows:

$$s(t,f) = \int_{-\infty}^{\infty} x(t)\frac{|f|}{\sqrt{2\pi}}e^{\frac{-f^2(\tau-t)^2}{2}}e^{-j2\pi ft}dt \tag{2.8}$$

The discrete S-transform of the signal is given as:

$$S\left(jT, \frac{n}{NT}\right) = \sum_{m=0}^{N-1} X\left(\frac{n+m}{NT}\right)e^{(-\frac{2\pi^2m^2}{n^2})}e^{j\frac{2\pi nj}{N}} \tag{2.9}$$

And $j = 1, \dots, N-1$, $n = 0, 1, \dots, N-1$. Here j and n indicate the time samples and frequency steps respectively. $X(n+m)$ is obtained by shifting $X(n)$ by m, whereas $X(n)$ is Fourier transform of $x(k)$ and given as:

$$X(n) = \frac{1}{N}\sum_{k=0}^{N-1} x(k)e^{-j(\frac{2\pi nk}{N})} \tag{2.10}$$

Now the discrete S-transform can also be represented in terms of amplitude and phase spectrum as:

$$S(j,n) = A(j,n)e^{i\phi(j,n)} \tag{2.11}$$

Where $A(j,n)$ is the amplitude spectrum and $\phi(j,n)$ is the phase spectrum of the original time series signal.

2.4 Proposed Adaptive Based Decomposition with Hilbert Huang Transform

In the above-mentioned time-frequency signal processing methods, the signal is essentially decomposed according to a predefined basis. However, in this thesis, various types of Hilbert-Huang Transform (HHT) are used for feature extraction. The main reason for choosing this method is its adaptability to the signal. Unlike wavelet transform, we do not define the decomposition level before we start decomposing the signal. Instead, this method changes the component numbers based on the signal frequency component and the noise penetration level. We just define the maximum decomposition level, which is also an optional choice. In fact, the key features of the transformations used in this paper are their nonlinearity and adaptive basis. They do not use a predefined base function to properly decompose the signals.

In these methods, the aim is to decompose these signals into components with Hilbert transform to extract meaningful instantaneous frequencies. Three well-known and appropriately chosen methods to achieve this goal are Empirical model decomposition (EMD), variational mode decomposition (VMD) and empirical wavelet transform (EWT).

The first step of the proposed adaptive based signal processing method is synthesize the signal and extract K numbers of various monocomponent oscillating signals called intrinsic mode functions (IMFs). These functions are defined as amplitude modulated-frequency modulated signals as follows:

$$u_k(t) = A_k(t)\cos\left(\varphi_k(t)\right) \tag{2.12}$$

Where $A_k(t)$ are envelopes and $\varphi_k(t)$ are phases.

2.4.1 EMD, VMD and EWT Based Adaptive Signal Processing

In EMD [29; 39], an iterative process is used to synthsized the signal into IMFs. The high frequency mode is extraced from every iteration and the remainder is the other low frequency components. This extracts monocomponents and symmetrical components by a process called sifting, as follows:

1- Extract the local extrema (minimum and maximum) of the signal.

2- Construct the lower $e_l(t)$ and upper $e_u(t)$ envelopes of the signal by using the local extrema and cubic spline interpolation method. Then, calculate their mean value $e_m(t)$.

3- Subtract the mean value from the main signal $x(t)$ and find the IMFs $I_i(t)$.

$$I_i(t) = x(t) - meat(e_m(t)) \tag{2.13}$$

Extract the residue $r_i(t) = x(t) - I_i(t)$. If the residue is lower than a predefined value, the stop criteria are granted; otherwise, the process is repeated to extract more IMFs.

Variational Mode Decomposition (VMD) [47] is a method inspired by EMD. It creates time series by decomposing a signal into several modes with specific sparsity properties and calculate the IMFs in frequency domain. It synthesizes the signal by a non-recursive method and determine the center frequency and bandwidth for K number of narrowband IMFs. These modes have positive and slowly changing envelopes $A_k(t)$. Each IMFs are calculated by iteratively searching for the optimal solution of the variational model. Then the original signal is decomposed adaptively into sum of individual IMF components. To calculate the IMF waveforms, the following constrained variational problem is minimized:

$$\begin{gathered}\min_{(u_k,\omega_k)}\left\{\sum_{k=1}^{K}\left\|\frac{d}{dt}\left[\left(\sigma+\frac{j}{\pi t}\right)*u_k(t)\right]e^{j\omega_k t}\right\|^2\right\} \\ s.t.\ \sum_k u_k(t) = s(t)\end{gathered} \tag{2.14}$$

In this equation, $s(t)$ is the main signal, * is convolution, $\|f(.)\|^2$ is norm-2, and $\omega_k = \frac{d\varphi_k(t)}{dt}$ is the central frequency.

Finally, the EWT[48] extracts the modes of a signal by designing an appropriate wavelet filter bank. A family of wavelets are adapted for processed signals. From the Fourier transform point of view, these bandpass filter banks can be considered to be IMFs. Depending on the location of signal information, these filter banks can be

considered to be adaptive supports (basis). Therefore, these constructed adaptive bases (IMFs) are accepted as compact supports around the central frequencies.

In the first step of the EWT, the Fourier spectrum is calculated for the signal. It normalized between $[0, \pi]$ and N adaptive frequency bands $\Lambda_n = [\omega_{n-1}, \omega_n]$ with various bandwidths are constructed. Bandpass wavelet filter banks are constructed in the next step. In ref [48], the author utilized Meyer's wavelet to design a group of mutually orthogonal trigonometric functions. Accordingly, for an empirical multiresolution analysis, the scaling function $\Phi(\omega)$ and the empirical wavelet function $\Psi(\omega)$ are defined as follows:

$$\Phi(\omega) = \begin{cases} 1 & if \quad |\omega| \leq (1-\gamma)\omega_n \\ \cos\left[\frac{\pi}{2}\beta\left(\frac{1}{2\gamma\omega_n}(|\omega| - (1-\gamma)\omega_n)\right)\right] & if \quad (1-\gamma)\omega_n < |\omega| < (1+\gamma)\omega_n \\ 0 & otherwise \end{cases} \tag{2.15}$$

$$(\omega) = \begin{cases} 1 & if\ (1+\gamma)\omega_n < |\omega| < (1-\gamma)\omega_{n+1} \\ \cos\left[\frac{\pi}{2}\beta\left(\frac{1}{2\gamma\omega_{n+1}}(|\omega| - (1-\gamma)\omega_{n+1})\right)\right] & if \quad (1-\gamma)\omega_{n+1} < |\omega| < (1+\gamma)\omega_n \\ \sin\left[\frac{\pi}{2}\beta\left(\frac{1}{2\gamma\omega_n}(|\omega| - (1-\gamma)\omega_{n+1})\right)\right] & if \quad (1-\gamma)\omega_n < |\omega| < (1+\gamma)\omega_n \\ 0 & otherwise \end{cases} \tag{2.16}$$

In these equations, $\beta(x) = x^4(35 - 84x + 70x^2 - 20x^3)$, $\gamma < \min\left(\frac{\omega_{n+1}-\omega_n}{\omega_{n+1}+\omega_n}\right)$.

In the final step, similar to the traditional wavelet transform, a signal is decomposed into approximation coefficients and detail coefficients. Hence, for an arbitrary signal $S(t)$:

$$S(t)=W_f(0,t) * \Phi_1(\omega) + \sum_{n=1}^{N} W_f(n,t) * \Psi_n(\omega) \tag{2.17}$$

In this equation:

$$W_f(0,t) = \langle S(t), \Phi_1(t) \rangle = F^{-1}(S(\omega)\widehat{\Psi_n}(\omega)) \tag{2.18}$$

$$W_f(n,t) = \langle S(t), \Psi_n(t) \rangle = F^{-1}(S(\omega)\widehat{\Phi_1}(\omega)) \tag{2.19}$$

In equations (2.18) and (2.19), F^{-1} is the inverse Fourier transform and $\langle . \rangle$ is the inner product.

2.4.2 Hilbert Transform

The next step in the HHT is to calculate the Hilbert transform of the mono component IMFs. In mathematics the Hilbert-Transform is a linear operator that take a real value function and produces another real value function. It extracts an analytic representation of a real valued time domain signal as a complex function. This transform maps all the amplitude modulated-frequency modulated cosine functions to their sine function. Therefore, an imaginary part of an IMF is:

$$\bar{I}(t) = \frac{1}{\pi} p.v. \int_{-\infty}^{+\infty} \frac{I(\tau)}{t-\tau} d\tau \tag{2.20}$$

The $p.v.$ is Cauchy principal value. Accordingly, the analytical signal is:

$$F(t) = I(t) + j\bar{I}(t) = D(t)e^{j\theta(t)} \tag{2.21}$$

In this equation, $D(t)=\sqrt{I(t)^2 + \bar{I}^2(t)}$ is the amplitude and $\theta(t) = tan^{-1}\frac{\bar{I}(t)}{I(t)}$ is the phase.

3. INTELLIGENCE BASED FAULT DETECTION AND CLASSIFICATION

The protection challenges of MGs lead research to find a fast and safe method that is operator independent. The proposed methods should have high reliability and be adapted to the various dynamic conditions of MGs. These dynamic conditions allow MGs to have a broad spectrum of fault current level. Therefore, in the first attempt, faults are detected and classified with the help of signal processing methods. In these methods, it is tried to extract all operating modes of the MGs and manually set a threshold value for different fault scenarios in the extracted component of the signal. However, the proposed method does not cover all data (scenarios) in the data space(dynamic behavior). This means that since you cannot cover all scenarios, there is no guarantee that you can detect all fault types with the defined threshold. Also, the threshold (detection time) differs between classes, and you don't have a fixed timeframe for all scenarios. If the largest time window is chosen for all scenarios, this will result in large detection time for severe faults and delay in activation of LVRT systems, which can cause instability of post-failure operation of MGs. Also, a greater detection time causes other transient scenarios to be misclassified as fault scenarios and fault trips or trips of relays. All these problems have revealed the necessity of using a method that detects and classifies transient scenarios in a fixed short time window, independent of fault current level. Covering and classifying all data in the data space is imperative, and the detection time is fast enough and completely independent of manually setting the threshold. All these conditions make us recommend the combination of signal processing methods and intelligent machine learning methods. Signal processing methods help us infer the transient behavior of the signal and construct the data spcae accordingly (feature extraction). Intelligence-based methods help us to create data space for classification and fast detection of various transient scenarios. In this paper, an ensemble of intelligence methods is used for fault detection and classification. The main feature of ensemble methods is that they consist of groups of basic weak and linear learners (decision trees) with varying voting power. Therefore, setting up and adjusting the data space is easy and there is a lower risk of overfitting. In addition, they are capable of achieving classification

performance very close to strong nonlinear classifiers such as neural networks. On the other hand, to have the same quality performance for real-world noisy data, a non-convex optimization-based method called Brownboost [43; 44] is used for error detection and classification. It helps to create a overfit proof model with a unique solution for non-convex data fields (data fields with noise and outliers). This makes the method practical and suitable for real-world data from measuring devicess.

3.1 Ensemble Learning

In machine learning, ensemble learning methods use multiple learning algorithms to obtain better predictive performance than could be obtained from any of the strong machine learning algorithm alone. It consists of finite sets of basic(weak) learners with various voting powers, but typically allows much more flexible structures to exist among those alternatives. In this method more than one machine learning method tries to learn the problem. In traditional method only one train data space is selected. However in ensemble method various subspaces are selected to have various models and combine them to have final decision.

An ensemble contains a number of learners which are usually called base learners. The generalization ability of an ensemble is usually much stronger than that of the base learners (deep learners). Actually, ensemble learning is appealing because it is able to boost weak learners which are slightly better than random guess to strong learners which can make very accurate prediction.

Ensemble learning algorithms are generally constructed by combination of single type of the algorithms like decision tree or neural networks and so on. If only a single type of the algorithm is selected, the generated ensemble method is called homogenous ensemble of the base learners. But it is also possible to construct an ensemble of heterogeneous learners to make decision simultaneously.

Typically, an ensemble is constructed in two steps. First, a number of base learners are trained, in a parallel style(bagging) or in a sequential(boosting) style. In sequential learning the generation of a base learner has influence on the generation of subsequent learners. It is tried to classify the misclassified data in previous step and minimize the generation error. Then, the base learners are combined to use, where among them

models with higher voting power (lower classification error) have majority voting for classification and weighted averaging for regression.

Generally, to get a good ensemble, the base learners should have highest possible accuracy and diversity. In order to achieve this goal, there is various tests, such as cross-validation, hold-out test, etc. However, there is no rigorous definition about diversity. Roughly, an ensemble model with high diversity needs to span all aspects of the dataspace properly. For practical purposes the diversity can considered from various aspects like adding randomness to traning process, utilizing multiple methods, subsampling and so on. The selection of the various base leaners results to have different type of the ensembles.

The ensemble methods are generally classified as Bagging and Boosting. Here, binary classification is considered for simplicity. That is, let X and Y denote the instance space and the set of class labels, respectively, assuming $y = \{-1, +1\}$. A training data set $D = \{(x_1, y_1), (x_2, y_2), \dots, (x_m, y_m)\}$ is given, where $x_i \in X$ and $y \in Y (i = 1, \dots, m)$.

Boosting [49] is in fact a family of algorithms since there are many variants. Adaboost [50] and gradient boosting [51; 52] are two outstanding examples of this method. In Adaboost the goal is minimization of the classification errors iteratively step by step. In this process in every iteration the misclassified data influence and the possibility of their selection to train the next base learner is increased. On the other side in In Gradient boosting (Figure 3.1**)** instead of emphasizing on misclassified data, the classification error for whole data is defined as a function to minimize in every iteration. First, a simple prediction model is defined as probability of data belongs to a class or not. The goal is minimizing a differentiable loss function (mean square error) by optimization method called gradient decent algorithm (first order iterative optimization algorithm to find minimum of a differentiable functions). In this method an ensemble of the regression models in used instead of classification models.

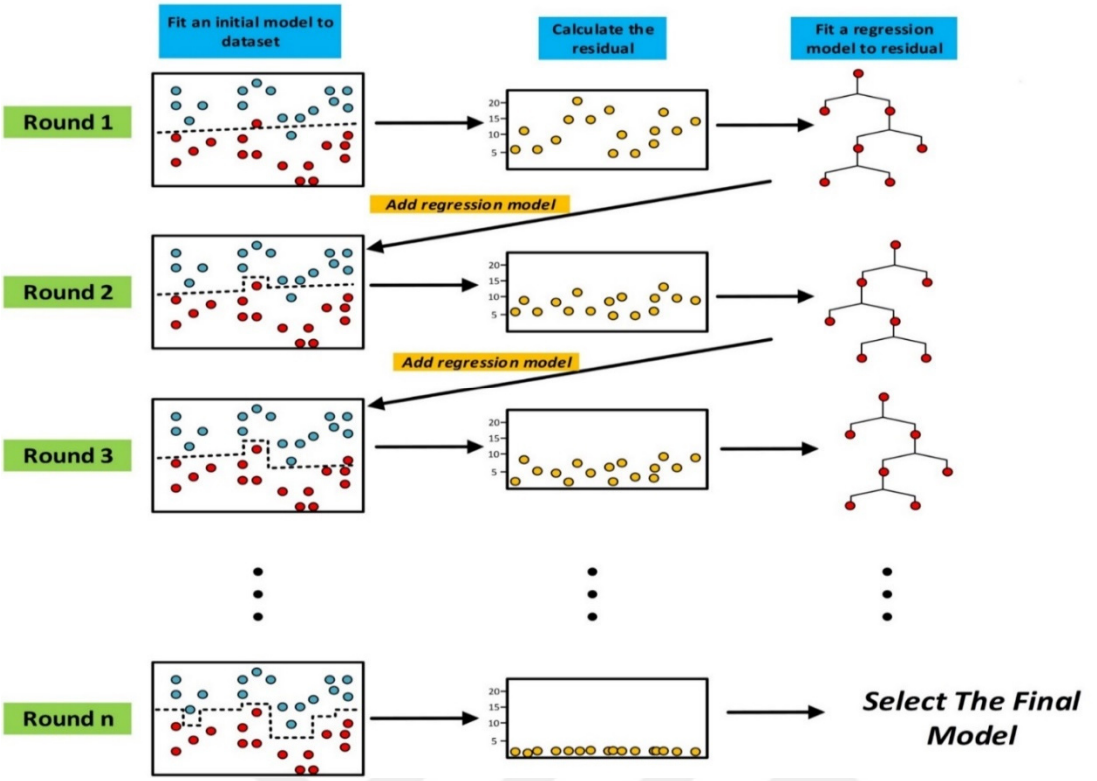

Figure 3.1 : Sequential Learning of Gradient Boosting [52].

In order to explain the main difference of the proposed Brownboost method compare to tradtional machine learning and conventional ensemble learnning method, first in this part as an example the Adaboost method is explained. In Adaboost, first, equal weights is assigned to the all training data. Then a subspace of trained data are selected randomly according to their wights. In the first step the data have the same weights and therefore the have the same chance of the selection. In this process the selected data distribution in t-th learning round denoted as D_t. A base learner h_t is trained by this D_t and the weighted sum of the errors is calculated for selected data. According to this sum of the errors (performance of the base learner) the voting power of the base learner α_t is calculated. Then the weights of the selected data are updated in manner that the selection possibility of the misclassified data increase and the other one is decrease. This process can cause that in the final steps the base learners main concentration become the misclassed data, if they are not classified in steps(rounds) of training process. In this algorithm the training process continues for a predefined number of base learners (rounds) or until the total decision error of the base learners are become smaller than a defined threshold. Finally, the decision is done by total voting of the base learners. The pseudo-code of AdaBoost is:

Table 3.1 : Pseudo Code of Adaboost Algorithm

Adaboost Algorithm

Input: Given dataset $\mathcal{D} = \{(\boldsymbol{x}_1, \mathcal{y}_1), (\boldsymbol{x}_2, \mathcal{y}_2), \dots, (\boldsymbol{x}_m, \mathcal{y}_m)\}$;
Define the base model to construct ensemble(decision tree) $\mathcal{L}$;
Define number of iterations (rounds) T .

Process:

$w_1(i) = \frac{1}{m}$. *%give intial weight to every data*

for $t = 1, \dots, T$:

$h_t = \mathcal{L}(\mathcal{D}, \mathcal{D}_t)$; *%Select subsapce $\mathcal{D}$ and train h_t % using distribution $\mathcal{D}_t$*

$\epsilon_t = Pr_{i\sim D_i}[h_t(\mathbf{x_i} \neq y_i)]$; *%Measures the error of h_t*

$\alpha_t = \frac{1}{2}\ln\frac{1-\epsilon_t}{\epsilon_t}$; *%Determine the weight of h_t*

$$w_{t+1}(i) = \frac{w_t(i)}{Z_t} \times \begin{cases} \exp(-\alpha_t) & \text{if } h_t(\mathbf{x_i}) = y_i \\ \exp(\alpha_t) & \text{if } h_t(\mathbf{x_i}) \neq y_i \end{cases}$$

$$= \frac{w_t(i)\exp(-\alpha_t y_i h_t(\mathbf{x_i}))}{Z_t}$$

%Update the distribution, where Z_t is % a normalization factor enables w_{t+1} % to be a distribution

End

Output: $H(\mathbf{x})=\text{sign}(f(\mathbf{x}))=\text{sign}\sum_{t=1}^{T}\alpha_t h_t(\mathbf{x})$

Bagging [53] trains, a number of base learners each one is independently. They can be the same base learners or various types machine learning algorithms. The decision is done by average voting of the learners. In this model every learners have the same power in decision and the purpose of the Bagging ensemble is construct the models robust to overfitting. The general pattern of the bagging and its difference from boosting is depicted in Figure 3.2.

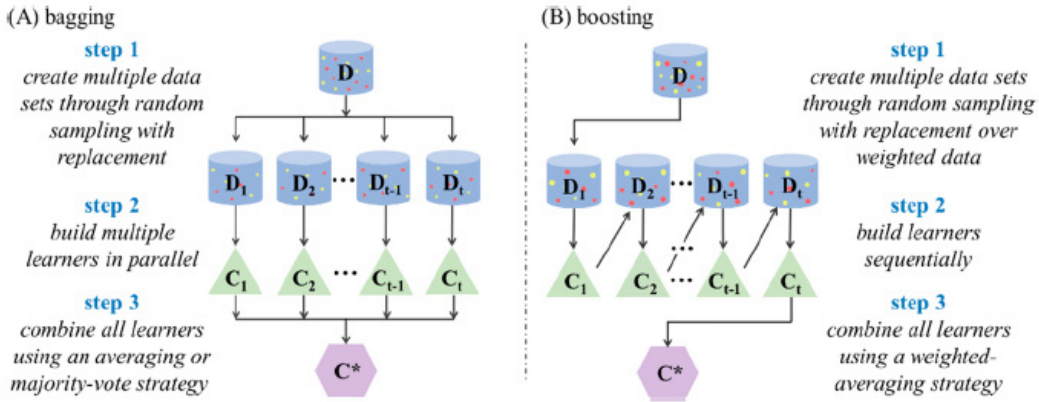

Figure 3.2 : Illustration of Bagging and Boosting.

3.2 Brownboost Ensemble Algorithm

One of the key features of ensemble methods is that decision making is done by majority vote of the learners. In this algorithm, basic learners are tried to be adapted to the data space step by step or iteratively. At any given iteration, if a model has a better adaptation to train data in the data space, it should definitely have more power in decision making. However, ensemble learners like Adaboost, gradient boosting or any other Bagging or Bossting ensemble methods use convex optimization method for classification same as what is used in traditional weak and strong machine learning method like artificial neural networks, support vector machine or extreme learning machine etc. In convex optimization-based algorithm training, the process starts with an initial guess and the sole goal is to minimize the classification error or classifier margin (the maximum separation between data for each class and classifier) at all costs. As shown in Figure 3.3, this condition increases the risk of overfitting in a noisy data domain or data domain where there is minimal discrimination between the data of each class. As illustrated the data of each class are very close to each with a samll discrimination between the data of each class. In addition, some data is violated due to noise and penetrates the area of the other class. If a well-trained convex optimization-based model is used for these data, there is a high risk of overfitting since the sole purpose is to minimize the classification error at all costs. This can result in high training accuracy and very poor performance for new invisible data. Therefore, traditional machine learning methods are not suitable for real-world data. These data are not as perfect as synthetic data. They contain noise and many outliers and are a non-convex optimization problem. Therefore, it is imperative to choose a method with sufficient intelligence which is able to select or discard data for classification among the problematic misclassified data that may be encountered in real system data gathering devices. In data space some of the data are violated to other class area but some of data are close to other class area. A desirable classifier must discard the first group of the data in training process to avoid the overfitting, but it have to be strong enough to classify the second group properly. there are always outliers or errors for many reasons. If we insist on classifying some of them at all costs, this will result in overfitting and unsuitable performance of the algorithm.

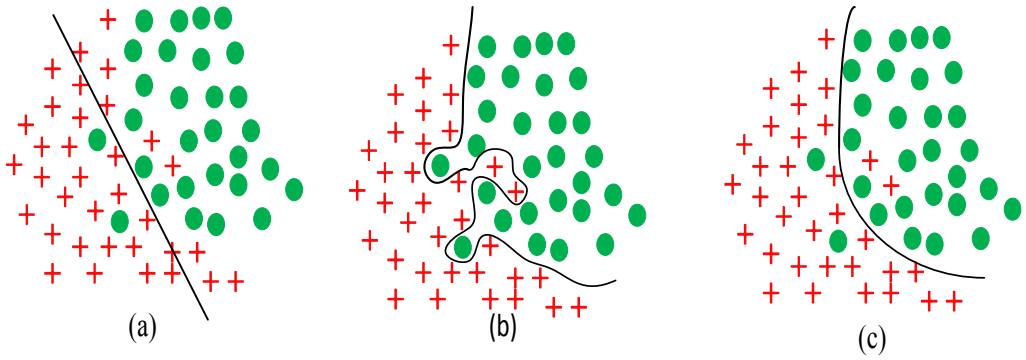

Figure 3.3 : A Classifier in Nonlinear Dataspace with Noise (a) Classifier for Linear Performance (b) Overfitted Classifier, and (c) Appropriate Classifier.

The general performance of the ensemble methods is based on minimization of margins for data of every class in dataspace alongside minimization of the classification error. This means they train a classifier to attain maximum discrimination from the data of each class in the data space (Figure 3.4**).** These methods are not only select a method that has minimum error, but also has maximum margin. This condition helps the classifier to have lower classification error for unseen new data and classify the data space in possible optimal form (lower generalization error). The importance of classification based on maximum margin is depicted in Figure 3.5.

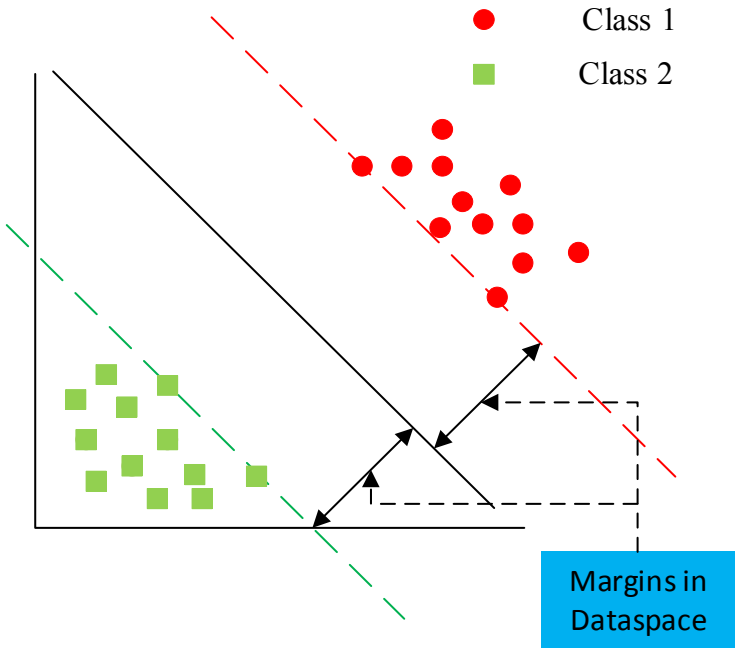

Figure 3.4 : Margin of a Classifier in Dataspace.

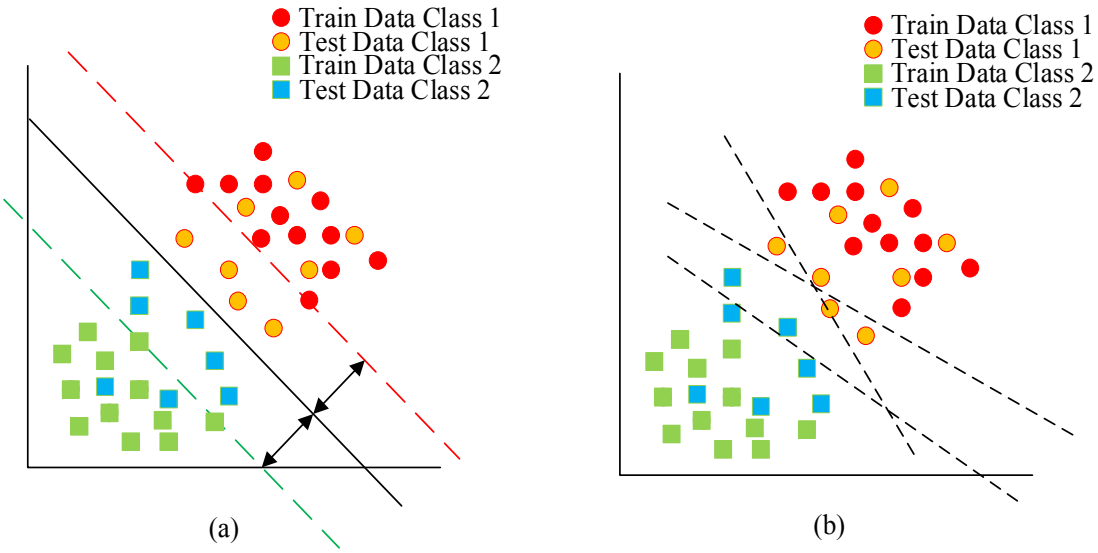

Figure 3.5 : (a) Margin Based Classification of the Data (Maximum Margin Yields to Have Lower Error Posibility Against Unseen New Data), (b) Classification Error Based Classifier (Although Is May Have 100% Accuracy for Train Data, There is Risk of Low Accurcy for Test Data).

Herein a non-convex optimization-based ensemble method called Brownboost is introduced. Brownboost is an adaptive ensemble machine learning algorithm. This algorithm uses a nonconvex potential loss function. The operation of this algorithm is not just to minimize the classification error at any cost. It presents a solution to traditional machine learning challenges like overfitting in noisy datasets. In the Brownboost ensemble, in each iteration the weights of the data do not solely depend on their misclassification in the previous iteration. Unlike the traditional boosting ensemble algorithm where the iteration is a discrete parameter, in Brownboost there is a parameter called time to manage the iteration. However, this parameter is not a discrete value. It a continuous value and in every training round it can have totally difference values compare to previous rounds. This parameter change in every step(round) plays a critical role in increasing the possibility of selection or discard of a misclassified data in the next round. In addition, this parameter is also effective in voting power a trained model in a specific round. The general concept and meaning of the time parameter are as following:

If, in a training round, it takes longer to train a base learner, it means that the base learner is dealing with noisy and outlier misclassified data in its trained subspace. In this case, it is difficult to classify correctly, but the long classification time means that it cannot perform well and it struggles to classify it properly. In this case, the model

should have lower voting power and the weights of the selected data should reduced not increased. İf they persist in misclassification in subsequent iterations, it is necessary to exclude this data step by step in the training process. With this process, if a misclassified data is correctly classified in a shorter time and in a limited number of iterations, its weighted value is increased until it is correctly classified. On the other hand, annoying outliers and noisy data that have a longer classification time and constantly insist on not being properly classified are suppressed in subsequent iterations. During this process, in subsequent iterations, these data are gradually ignored and the probability of being selected in the basic learner's training is significantly reduced.

According to Brownboost theory, weak learners need various times to learn the training data. In this algorithm, the weights of the misclassified data are increased if the violations are not high. This process is an iterative process and the weight adjustment is an adaptive process. In each iteration, a weak learner is trained on the data, and the learner's voting power and elapsed time are calculated simultaneously. To do this, a system of two nonlinear equations is solved by bisection or any nonlinear root-finding method such as Newton-Raphson. Next, the distance of each data point from the decision boundary, called the margin, is calculated. Then the weights of the training data are updated accordingly. The only parameter that can be entered manually is the cutoff time$c$. A large value is chosen if the data is less noisy; conversely, a small value is chosen for a noisy dataspace. The algorithm stops when the clock reaches a predefined time. The Brownboost algorithm is explained as follows:

Table 3.2 : Pseudo Code of Brownboost Algorithm

Brownboost Algorithm
Input:
Take N training set $(\mathbf{x_i}, \mathrm{y_i})$
Define target error $\epsilon \in (0, \frac{1}{2})$
Define clock cutoff $c \in (0,1)$
Define potential function $\Phi(m,t) = \frac{1}{2} erfc(\frac{m+\rho(1-t)}{\sqrt{2\rho(1-t)}})$
%%*erfc is the complementary error function*
Initialize:
Find parameter ρ that satisfies: $\epsilon = \Phi(0,0)$
Set start time $t_1 = 0$, initial margin of N train data $m_{1,i} = 0$, $i = 1, \dots, N$, iteration number $k = 1$,
While $t_k > 1 - c$

Table 3.2 : (continued)

1: Set weight of each train data, giving:

$$\omega(m_{k,i}, t_1) = \exp\left(-\frac{\left(m_{k,i} + \rho(1 - t_k)\right)^2}{2\rho(1 - t_k)}\right)$$

2: Normalize the weight of train data

$$D_k(i) = \frac{\omega(m_{k,i}, t_k)}{Z_k} for\ i = 1, \dots, N$$

%%Where $Z_k = \sum_{i=1}^{N} \omega(m_{k,i}, t_k)$ *is the normalization factor*

2: Define distribution over N training dataset and train a weak learner $h_k: \chi \to \{-1,1\}$, which has some advantage over random guessing:

$$\boldsymbol{min}\left(\sum_{i=1}^{N} \omega(m_{k,i}, t_i)\, h_k(x_i) y_i\right) > \mathbf{0}$$

3. Solve system of two nonlinear equation find $\Delta t_k > 0$ and $\alpha_k \in \mathbb{R}$

$$\sum_{i=1}^{N} \Phi(m_{k,i}, t_k) = \sum_{i=1}^{N} \Phi(m_{k,i} + \alpha_k\, y_i h_k(x_i), t_i + \Delta t_k)$$

$$\sum_{i=1}^{N} \omega(m_{k,i}, \alpha_k y_i h_k(x_i), t_i + \Delta t_k) y_i h_k(x_i) = 0$$

$$(t_i + \Delta t_k \leq 1 - c)$$

4. Update the values

Update the time $t_{k+1} = t_k + \Delta t_k$

Update the margin of the train data

$$m_{k+1,i} = m_{k,i} + \alpha_k y_i h_k(x_i) \qquad for\ i = 1, \dots, N$$

Update the learning round $k = k + 1$

Output of the final hypothesis

$$H(x) = sign\left(\sum_{k=1}^{K} \alpha_k h_k(x_i)\right)$$

%%K is the total number of trained weak learners (total number of algorithm iterations)

3.3 Proposed Method

Only a single ensemble learning method can cover (adapt) train data from various aspects in just one dataspace. On the other hand, Brownboost or any other ensemble algorithm gives us a criterion to evaluate its performance in the dataspace which is called margin. The margin tells us how much classifier is away from data of each class in a dataspace. So, if it is possible to map raw data to several processed spaces of the same type, there is an evaluation parameter between them. Therefore, in this thesis, three different adaptive-based signal processing methods named EMD-HHT, VMD-HHT and EWT-HHT are used to transfer data to various feature spaces. In fact, different feature extraction is used to train three different Brownboost algorithms to create an additional ensemble in various dataspaces. This helps the elite to have more

voting power in deciding on data belonging to a particular class when making a decision with the votes of various decision making methods (various Brownboost). In this process, the dataspace (HHT-based Brownboosts) for a particular class with higher margin has higher voting power. This is because a data field with a higher margin means higher separation between the boundaries of that class compared to others and is less likely to misclassify a typical unseen new data. Also, in a noisy dataspace, if there is a higher margin between each class's data, there is a lower risk of noisy data breaching and entering another's domain.

It is important to remember that the one-to-all method is used for multiclass classification by each Brownboost for each signal processing input. Therefore, 13 Brownboost clusters are trained for 13 different classes for a single dataspace (feature space). Therefore, for a particular class in the data field (for example EMD-HHT), when there is different decision between these three Brownboost clusters, it is possible that this class has a higher margin compared to other dataspaces (EMD-EWT, EMD-VMD). Here, a data field or data fields with a higher total margin (with the same vote) takes precedence. This is because a data field with a higher margin means higher separation between the boundaries of that class compared to others and is less likely to be misclassified due to noise or other disturbances.

The proposed fault detection and classification scheme is depicted in Figure 3.6. In the proposed method, fault detection and classification are attempted with the minimum measured parameters and maximum feature processing. Thus, currents are subtracted from both ends of the line and their difference is used for processing and feature extraction. In the first stage, features are extracted by signal processing method. It helps to extract data from the transient behavior of the signal at the time the fault occurs, providing a fast fault detection method. Adaptive-based signal processing methods help extract features based on the shape of the present signal, the intensity of the noise, and the synchronization delay. It is not on a predefined basis for all signals as in Wavelet. At this level IMFs are extracted separately up to 5 levels for the same training data via EMD, VMD and EWT. Next, Hilbert transforms for the IMFs are calculated and the standard deviation, skewness and energy of these coefficients are calculated.

In this method, a signal with limited time around the fault is used. However, in real world application, the method is applied for a discrete, uninterrupted continuous signal

with a given sampling frequency. Therefore, a sliding time window with a limited number of samples is mandatory for online application. A cycle time window of 64 samples/period is selected for feature extraction to show that only the transient behavior of the signal is sufficient for fault detection and classification. In this study, in the worst case, fault detection is required in a period time window from the beginning of the fault. Therefore, this time window is chosen to train and test the algorithm. In this way, it is known that the method can detect the fault in a maximum of one period. Also, this method has a fixed maximum detection time, unlike methods in which the threshold is set experimentally, where the detection time varies with the dynamic behavior of the microgrid.

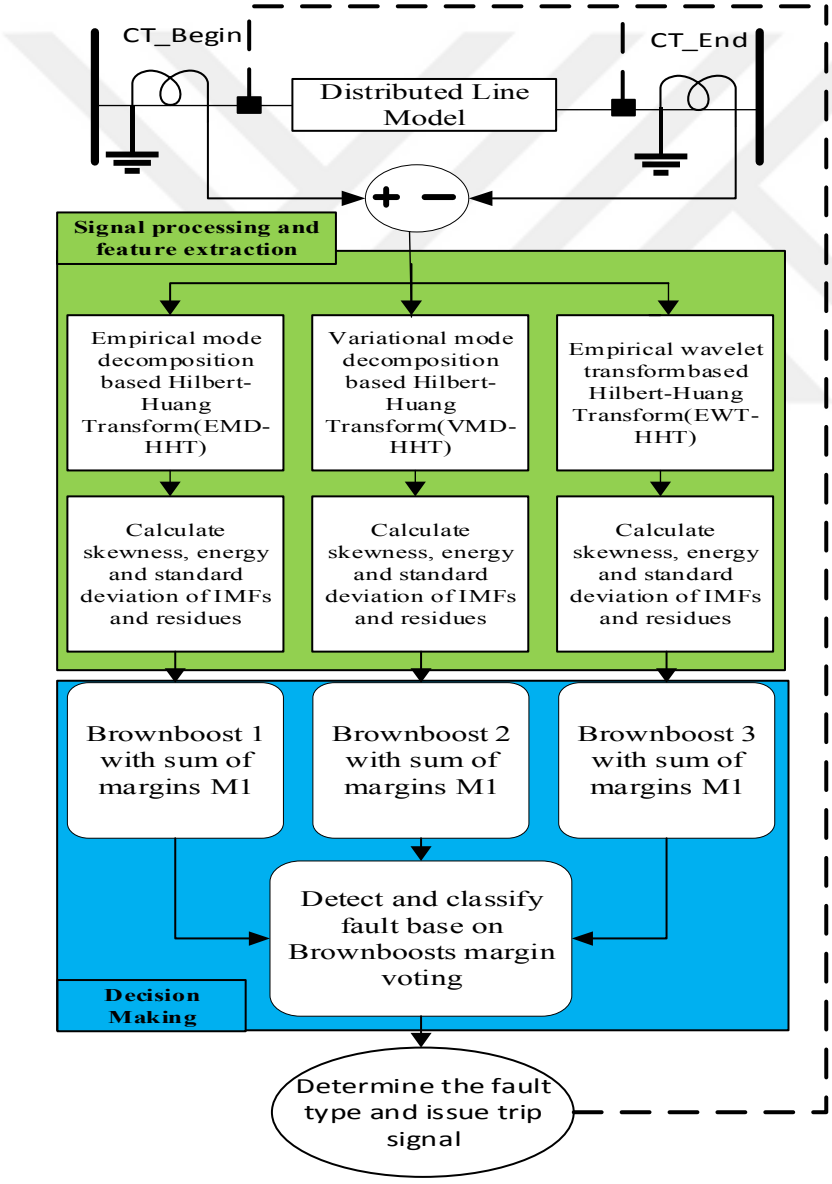

Figure 3.6 : Brownboost Margin Based Proposed Fault Classification Algorithm.

Next, a totally different Brwonboost is trained for every dataspaces. The performance of the Brownboost is evaluted by the criteria called margin. Thus the total margin of the data in every space is calculated. A classifier with higher margin have higher discrimination between data for every classes. It has lower generalization error and this make it less sensible and affected from noise.As a result a classifer with higher margin should have more voting power and decision priority. This step of the algorithm helps to have an ensemble of the dataspaces and check performance of the model in various dataspaces simultanously.

4. MODELING RENEWABLE ENERGY SOURCES OF MICROGRID

In this section, the energy sources used in the micro-grid are explained in detail. The various control modes and how they are implemented are described. Each element of the RES and their operating modes according to the microgrid operating mode are discussed. In the following subsection, firstly, the control systems of non-rotating inverter-based DERs (PV, BESS) are described in grid-tied mode and islanded mode. Power control mode and voltage control modes are explained in detail with their mathematical models. In addition, embedded fault ride through or low voltage ride through (LVRT) control blocks are explained in detail to control the system during fault occurrence and to control post fault stability. In the next step, the detailed model of the DFIG based wind turbine is explained. Finally, the various control modes, equipment used for LVRT, and unsymmetrical fault transition and post-fault stable operation are explained in detail.

4.1 Inverter Based Converters

One of the key features of new renewable-based power systems is the emergence of distributed energy sources (DER) with inverter interface. The energy sources include a DC bus connected to the main grid via inverters (Figure 4.1) which are mainly the predominant types of DER in microgrids. As it is mentioned they this novel topologies creates several challenges of traditional power systems protection schemes. Besides that challenges, they have a complex control system and can operate in both grid-tied mode and island mode. The control system of these DERs is generally divided into two main groups [54]:

1- Power control mode which is also known as grid following type of inverters.

2- Voltage control mode which is known as grid forming types of inverters.

Almost all of the current DERs connected to the current grid are in power control mode. The main purpose of running DERs in this mode is the maximum harvesting of

renewable energy sources (wind, sun, etc.). Or control the active and reactive power injected into the network in elements such as battery energy storage systems (BESS).

Power control mode DERs use a current control loop and phase lock loop to control the inverter output current. It allows voltage source converters (VSC) to have a similar behavior to current sources (Figure 4.2). They can be arranged quickly. However, since they cannot control the voltage and frequency, they are dependent on the mains voltage sources and frequency and and they are not capable to operate and supply the load solely (Islanded).

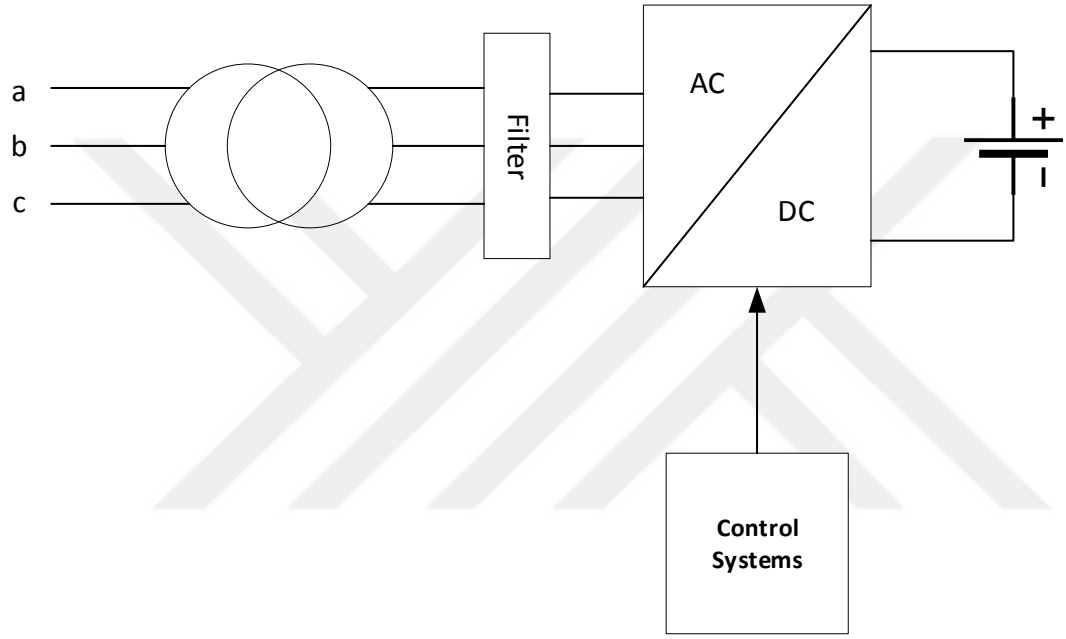

Figure 4.1 : Typical Grid Connected Converter Configuration.

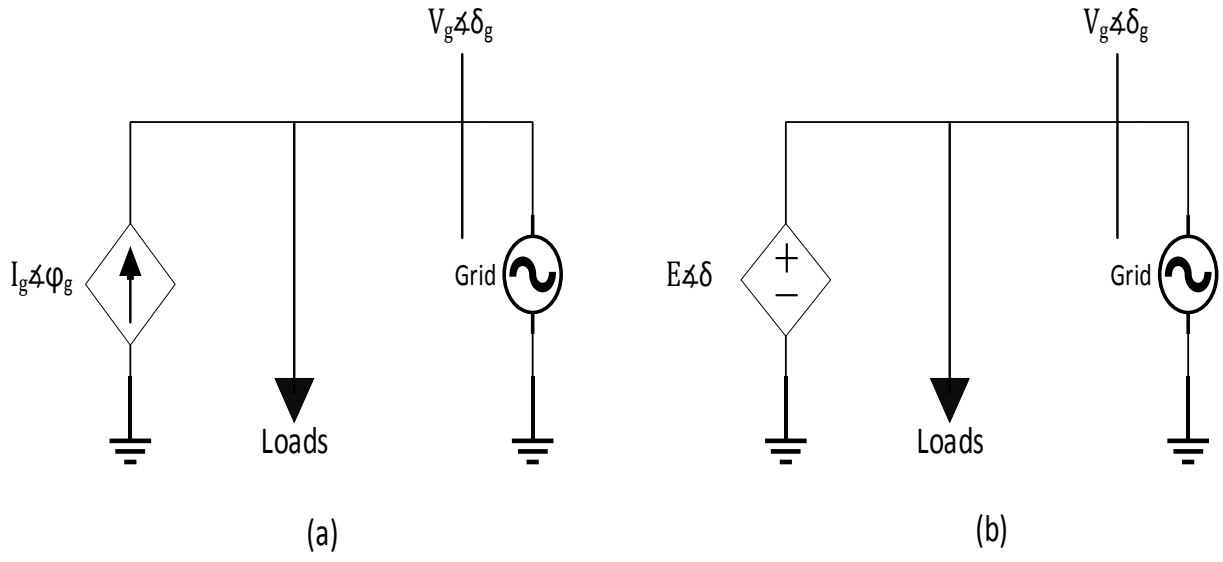

Figure 4.2 : Concept of (a) Grid Following and (b) Grid Forming.

On the other hand, the voltage control mode operating DERs can operate in island mode and adjust the active and reactive power to track the load pattern. There are various voltage control strategies. Some of these main methods are droop control, virtual oscillator control, and virtual synchronous machine and so on [54].

Two perspectives are generally used in modeling the dynamic behavior of based inverter based system: the detailed model and the average model [55]. Average models are used to simulate the electromechanical transition of the system. This model is used to study voltage and frequency stability or optimum power sharing between DERs. In this model, power electronics elements of inverters such as IGBT of VSCs are modeled as equivalent voltage sources. They are useful for studying long-term dynamic behavior and produce AC voltage averaged over a cycle frequency.

On the other hand, the detailed model is used to study short-term electromagnetic transients such as faults in power systems. This model consists of a detailed representation of power electronics switching elements such as IGBTs. This model helps us to extract the detail model of the signal (full waveform of the signal) during the transition event and also to observe the effects of the harmonic caused by the switching frequency of the inverters. As a result, in this thesis, the detailed model of the inverters and higher order dynamic model of the elements are used to extract the electromagnetic model of the systems.

4.1.1 Control Reference Frames for Grid-Connected Inverters

The first conventional operational mode of inverter-based DERs is grid connected mode. In this mode, the VSC is usually controlled by two different control methods. The first method transfers the measured mains currents to the fixed reference frame (αβ frame) and controls the current with a resonance controller. The configuration of this controller is as follows:

$$\mathrm{PIR}(s) = k_p + \frac{k_i s}{s^2 + \omega^2} \tag{4.1}$$

In this controller k_p and k_i are the controller's gain and ω is the grid frequency. According to Figure 4.3 the grid voltage is measured and transferred to stationary reference frame. Then, by a PLL system the phase angle of the grid voltage is estimated and reference current values in synchronous reference frame (dq-frame) are transferred to stationary frame and the output is control by a resonant controller. This is the main

current loop or internal controller of the inverters. In order to operate the controller in power control mode an outer control loop is also necessary.

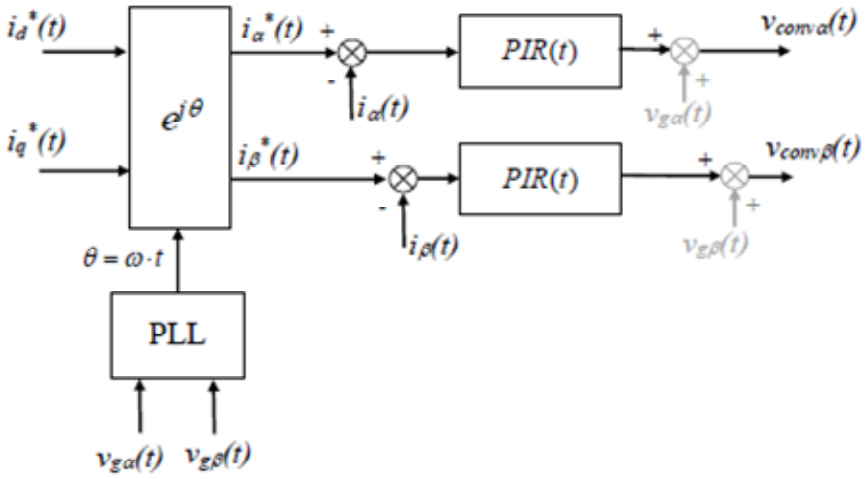

Figure 4.3 : Current Control Diagram in Stationary Reference Frame [56].

Another method which is more preferable for current control of grid connected inverters is controlling in rotating reference frame (dq-frame). In this method PI(s) controllers are used to track the reference current value and the configuration of this controller is as follows:

$$\mathrm{PI(s)} = \mathrm{k_p} + \frac{\mathrm{k_i}}{\mathrm{s}} \tag{4.2}$$

In this method the current is transferred to synchronously rotating reference frame and the output closed loop signal is controlled by a PI(s) controller. Afterwards it is possible to apply the output signal with cancellation the coupling terms (Figure 4.4) or without cancellation of the coupling terms (Figure 4.5). The coupling terms are emerged due to transfer the signal to dq-frame (Figure 4.6).

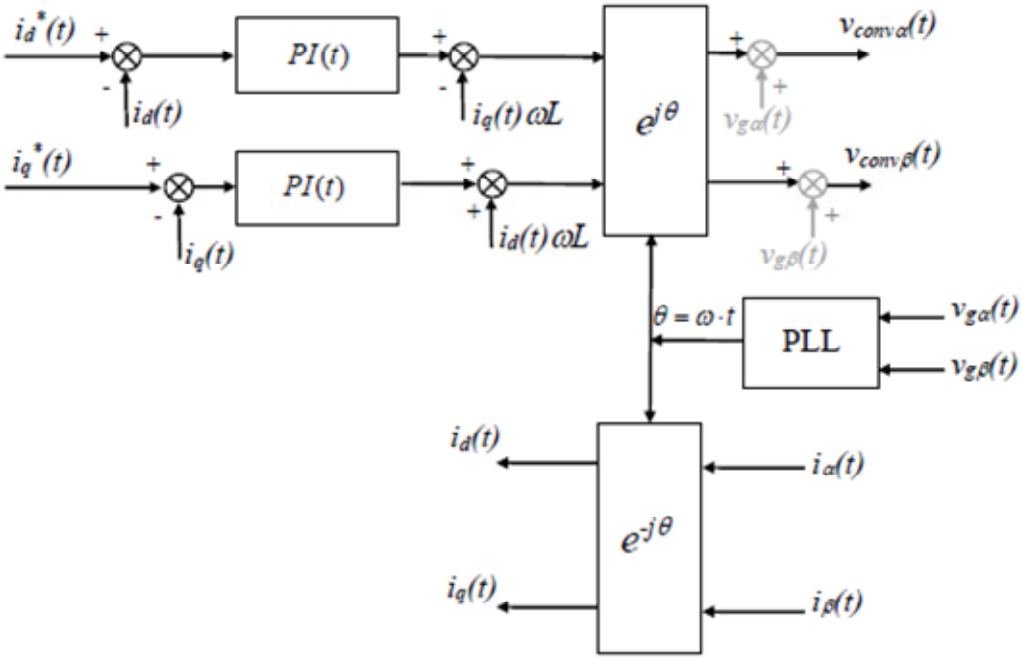

Figure 4.4 : Current Control Diagram in Synchronously Reference Frame with Cancellation of the Coupling Terms [56].

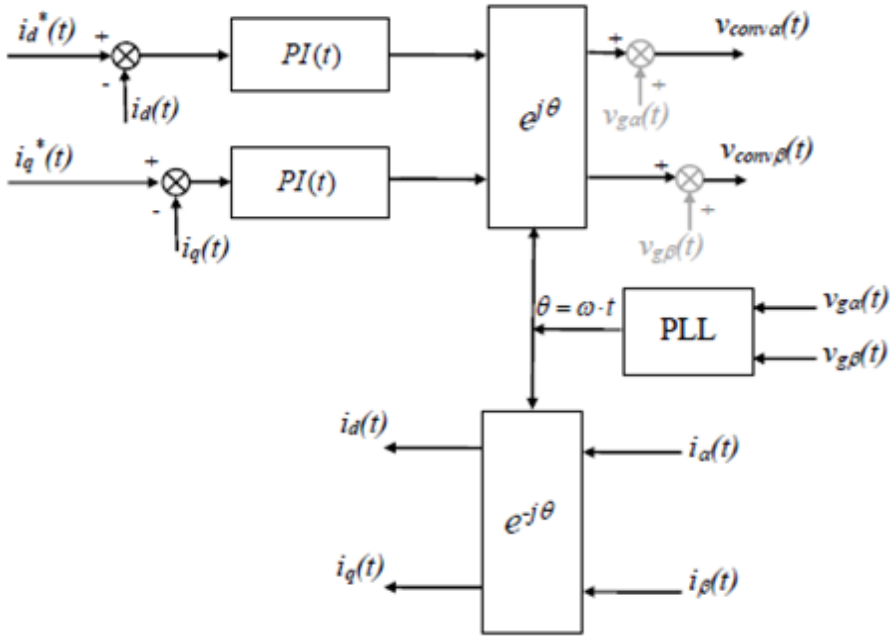

Figure 4.5 : Current Control Diagram in Synchronously Reference Frame Without Cancellation of the Coupling Terms.

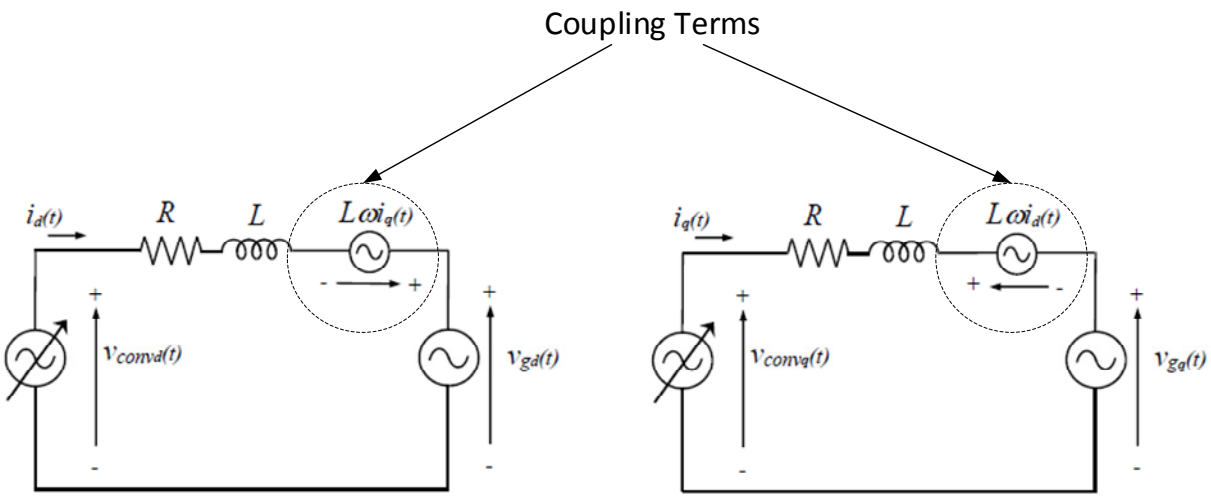

Figure 4.6 : Equivalent Circuit of Grid-Connected Inverters in dq-frame.

As illustrated, there are three possible control methods for grid-connected converters in grid-forming mode. The time domain unit step response for these three types of systems is presented in Figure 4.7. In this figure the output current and converter voltage are shown in the fixed (αβ) reference frame for all these control methods. Also, the damping natural response is depicted for the step input. According to this figure, a resonant PIR(s) controller has higher overshoot compared to the other two controllers and needs more time for damping. On the other side for currents controlled in the dq-frame without canceling the reference frame, the higher the overshoot remains, but the response is damped faster. Finally, a dq-reference frame in which the coupling terms are canceled has lower overshoots and shorter damping time. In a network where DERs are connected to the main power system (power grid) and feed the loads together, the effect of noise and harmonics is negligible. Therefore, there is no risk of instability in any of these control methods. However, there is a high risk of instability in this network during load changes or other types of disturbances when these DERs are connected to a weak grid or when other voltage control mode DERs feed island mode loads alongside these DERs. As a result, in this thesis, in the modeling of the network element, power control mode inverters are modeled in the dq frame with the cancellation of the coupling terms.

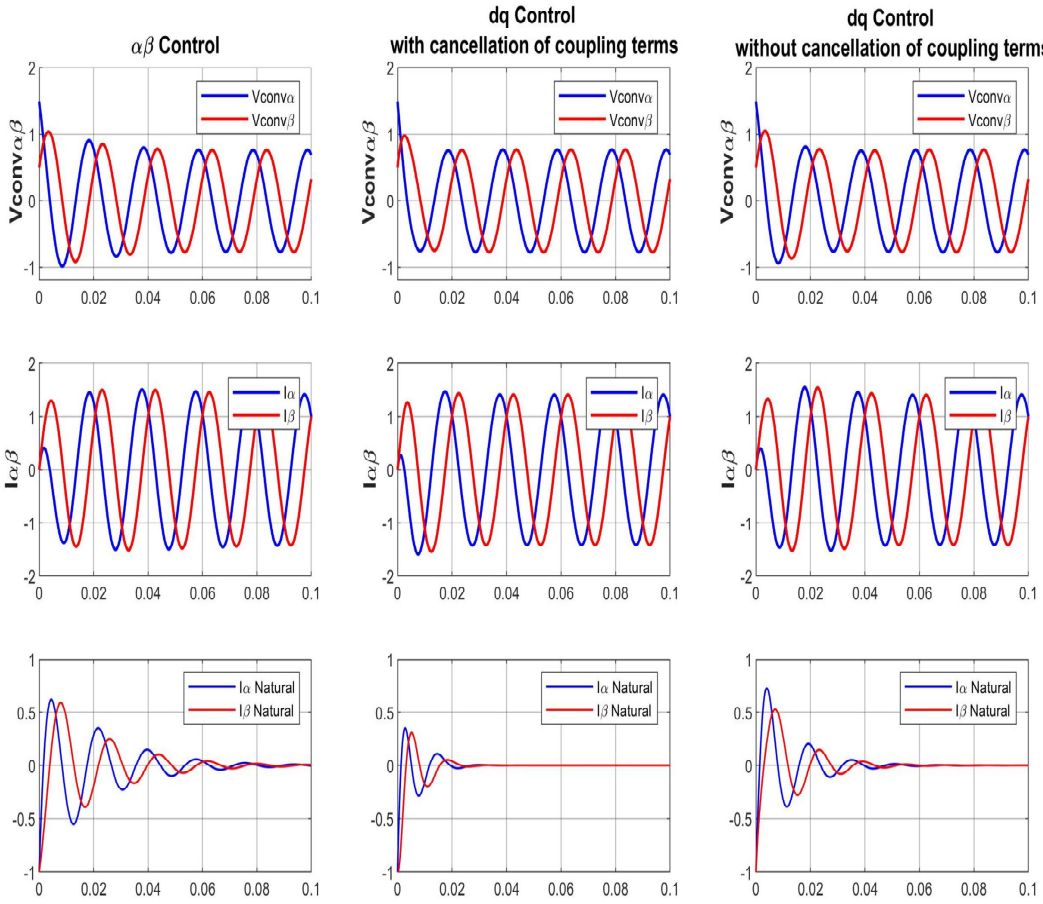

Figure 4.7 : Step Response of Grid-Connected Inverters Current Control for 3 Types of Control Methods.

4.1.2 Mathematical Formulation of Current Control in Synchronously Rotating Reference Frame (dq-frame) with Cancellation of Coupling Terms

As stated in this thesis the dq-frame with cancellation of the coupling terms is selected to model grid-connected inverters. According to equivalent circuit in Figure 4.6 the following voltage equation can be derived:

$$v_{convd}(t) = R.\,i_d(t) + L.\frac{di_d(t)}{dt} + v_{gd}(t) - \omega.L.\,i_q(t) \tag{4.3}$$

$$v_{convq}(t) = R.\,i_q(t) + L.\frac{di_q(t)}{dt} + v_{gq}(t) + \omega.L.\,i_d(t) \tag{4.4}$$

According to Figure 4.4 the close-loop control of the system is as follows:

$$[i_d^*(t) - i_d(t)] \otimes PI(t) + v_{gd} - \omega.L.\,i_q(t) = v_{convd}(t) \tag{4.5}$$

$$[i_q^*(t) - i_q(t)] \otimes PI(t) + v_{gq} + \omega.L.\,i_d(t) = v_{convq}(t) \tag{4.6}$$

($\otimes$ is convolutional)

If the value of $v_{convd}(t)$ and $v_{convq}(t)$ is added to this equation the result is:

$$[i_d^*(t) - i_d(t)] \otimes PI(t) + v_{gd} - \omega . L . i_q(t) = R . i_d(t) + L . \frac{di_d(t)}{dt} + v_{gd}(t) - \omega . L . i_q(t) \quad (4.7)$$

$$[i_q^*(t) - i_q(t)] \otimes PI(t) + v_{gq} + \omega . L . i_d(t) = R . i_q(t) + L . \frac{di_q(t)}{dt} + v_{gq}(t) + \omega . L . i_d(t) \quad (4.8)$$

If the equal terms are removed from both side of the equations and the equations transferred to a Laplace space:

$$[I_d^*(s) - I_d(s)] . \left(k_p + \frac{k_i}{s}\right) = R . I_d(s) + L . s . I_d(s) \quad (4.9)$$

$$[I_q^*(s) - I_q(s)] . \left(k_p + \frac{k_i}{s}\right) = R . I_q(s) + L . s . I_q(s) \quad (4.10)$$

If we rearrange these two equations, the transfer function of each current control loop yields:

$$\frac{I_d^*(s)}{I_d(s)} = \frac{I_q^*(s)}{I_q(s)} = \frac{(k_p s + k_i)/L}{s^2 + \frac{(k_p s + R)}{L} s + \frac{k_i}{L}} = \frac{(k_p s + k_i)/L}{s^2 + 2\xi\omega_n s + \omega_n^2} \quad (4.11)$$

This equation is second order transfer function of a system and it is possible to adjust the controller values k_p and k_i for a specific natural frequency ω_n and damping ratio ξ as follows:

$$k_p = 2\xi\omega_n L - R \quad (4.12)$$

$$k_i = \omega_n^2 L \quad (4.13)$$

4.1.3 Maximum Power Point Tracking (MPPT) in Photovoltaic Systems

A photovoltaic system is the interconnection of parallel and series PV cells. This series and parallel connection increases the voltage and current respectively and creates the PV system current-voltage (V-I) and power voltage (P-V) curve Figure 4.8, which depends on the variation of temperature and radiation. According to this curve, the cell can operate at a certain voltage and current at any time. For a unique irradiance and temperature, the system has a variety of voltages and currents accordingly. Therefore, in this case it has its own power curve, it depends on the voltage and current set. From Figure 4.8 it is concluded that for a given temperature and radiance in the P-V curve, the maximum power is harvested at a certain voltage. Therefore, it is necessary to force the PV to operate at its corresponding maximum power point (MPP). This is usually done by forcing the voltage or current of the PV module to its maximum point (the peak value of the P-V curve). However, with the change in temperature and irradiation (Figure 4.9) [57] , the peak of the MPP changes constantly and it is necessary to monitor the point to find new MPP. This process is called maximum power point tracking (MPPT). Consequently, it is imperative to install a device that will implement the MPPT algorithm.

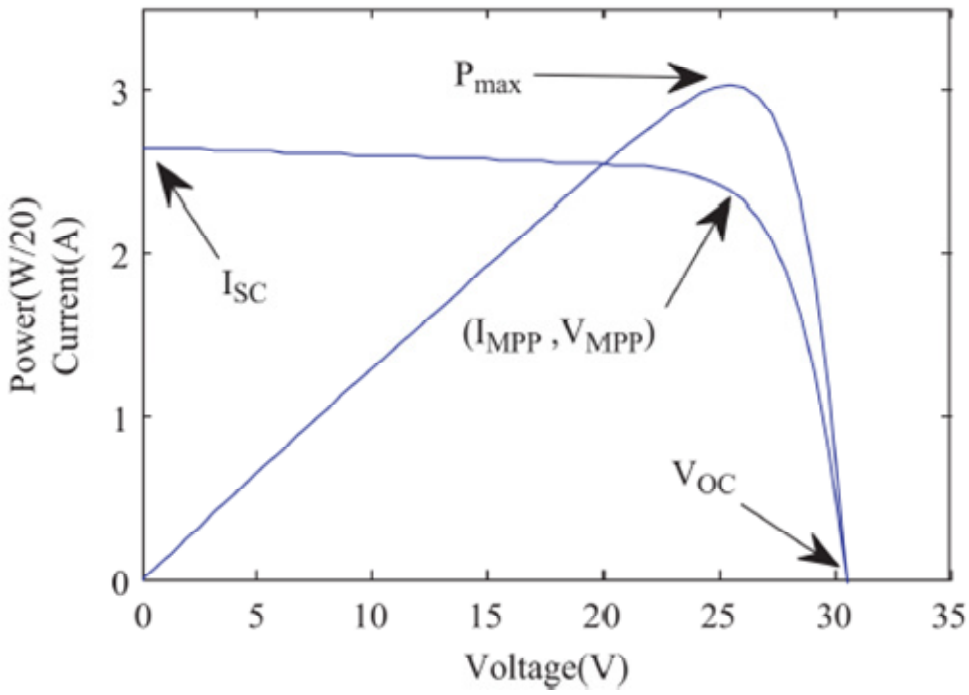

Figure 4.8 : Voltage Current (V-I) and Power Current (P-V) Curve of a PV-cell [58].

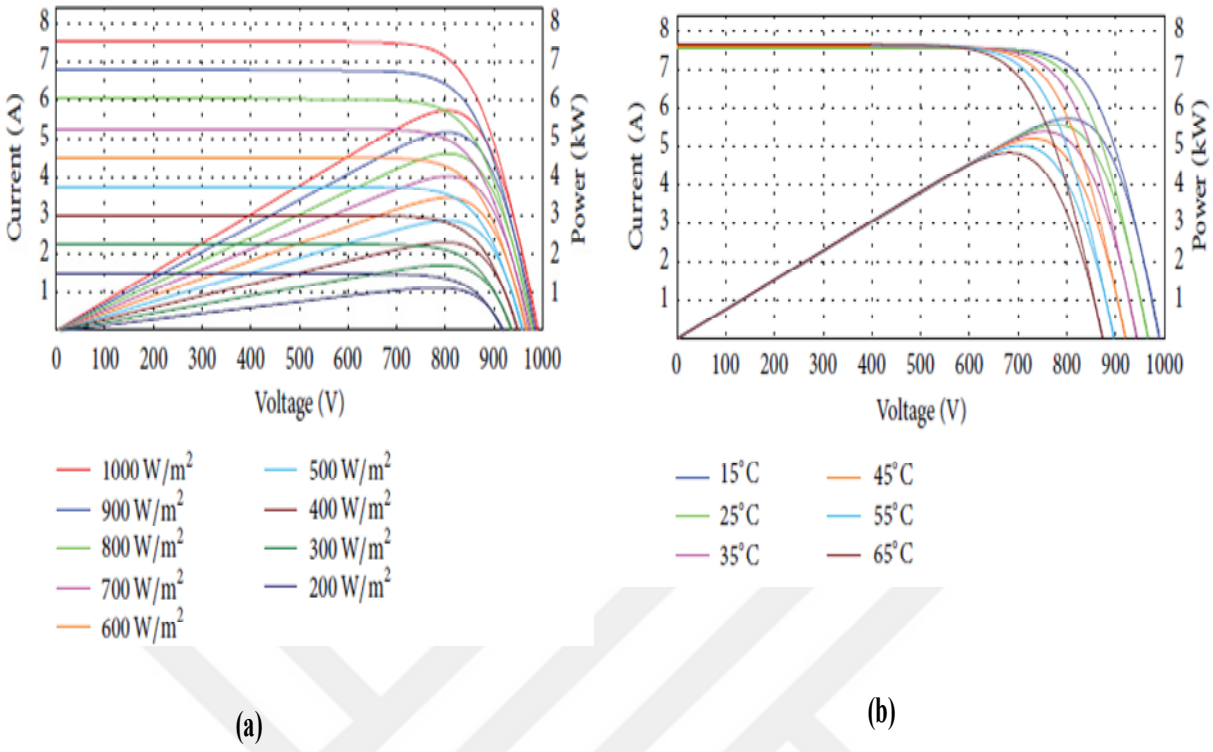

Figure 4.9 : V-I and P-V Curve Variation According to (a) Irradiation (b) Temperature [57].

The MPPT algorithms are generally divided as two categories [57] :

1- Indirect methods: Fixed value, fractional open circuit voltage method.

2- Direct Methods: Perturb and observed method, incremental conduction method.

The method preferred in this paper is from direct methods, the perturb and observed method. The direct methods involve measurement of voltage and current to calculate power. They help us to have more fast and accurate response compare to indirect ones.

In perturb and observed algorithm, for a value of the temperature and irradiation, the value of the voltage and current is measured and the power is calculated. Then, the value of the voltage is increased (decreased) and again the power is calculated. This condition continue until any further perturbation in the voltage leads to decrement of the power. At this moment we catch the MPP or the peak value of the power. This reference voltage is kept constant until a variation happens in irradiation or temperature.

4.1.4 Dynamic Model of the Grid Connected Inverters in Power Control Mode (Grid Following)

In previous section the current control model of the grid-connected inverters in explain in detail. However, in order to operate the system in power control mode it is necessary to add an out active and reactive power (PQ) outer loop to the system. In systems like the BESS the generation or consumption of the active and reactive power is controlled by operator. Therefore, and outer loop to control reactive power (power factor) and adjust the DC-bus voltage to control active power is sufficient.

On the other side in PV system the generation of active power (DC-bus voltage) is not controllable by the operator. Hence, when the PV system is connected to the grid, in power control mode a MPPT system is implemented to the DC-bus for maximum harvest of energy and guarantee to generate maximum power at any irradiation and temperature. At this condition the only adjustable value by the operator is the reactive power (power factor) of the PV system.

The fully control system of the grid connected inverter (photovoltaic system) is depicted in Figure 4.10. According to this system the voltage and current of the PV unit is measured and by MPPT system the reference voltage value is generated in manner that the system generates the maximum power and the reference d-axis current made the inverter to supply the network. In addition, the outer loop of the q-axis current is used to generate reactive power when there is imbalance of the reactive power between generation and consumption. This condition is more evident is islanded mode operation of the microgrid. Here it is possible to compensate the microgrid reactive power imbalance by the inverters operating in power control mode.

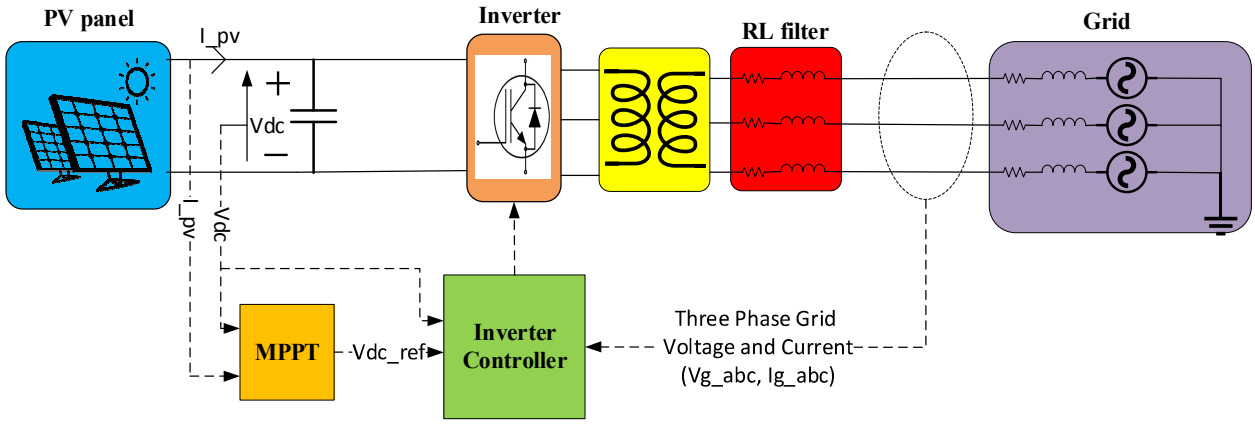

Figure 4.10 : Generic Control Structure of Grid-Connected PV System.

According to these facts the inverter control of a PV system and BESS in power control mode are depicted in Figure 4.11. As stated in power control mode of the PV system the generated active power is dependent on irradiation and temperature and it is not controllable. It is only possible to maximally harvesting the power by MPPT. However, in BESS system in power control mode it is possible to control and adjust the active power between limits. In addition, it is possible to operate in discharging mode (supply network active and reactive power mismatch) or charging mode (consume active reactive power). According to this fact the only difference of the system in power control mode compare to PV system is instead of reference dc voltage V_{dc}^{*} the reference active power is used in outer loop.

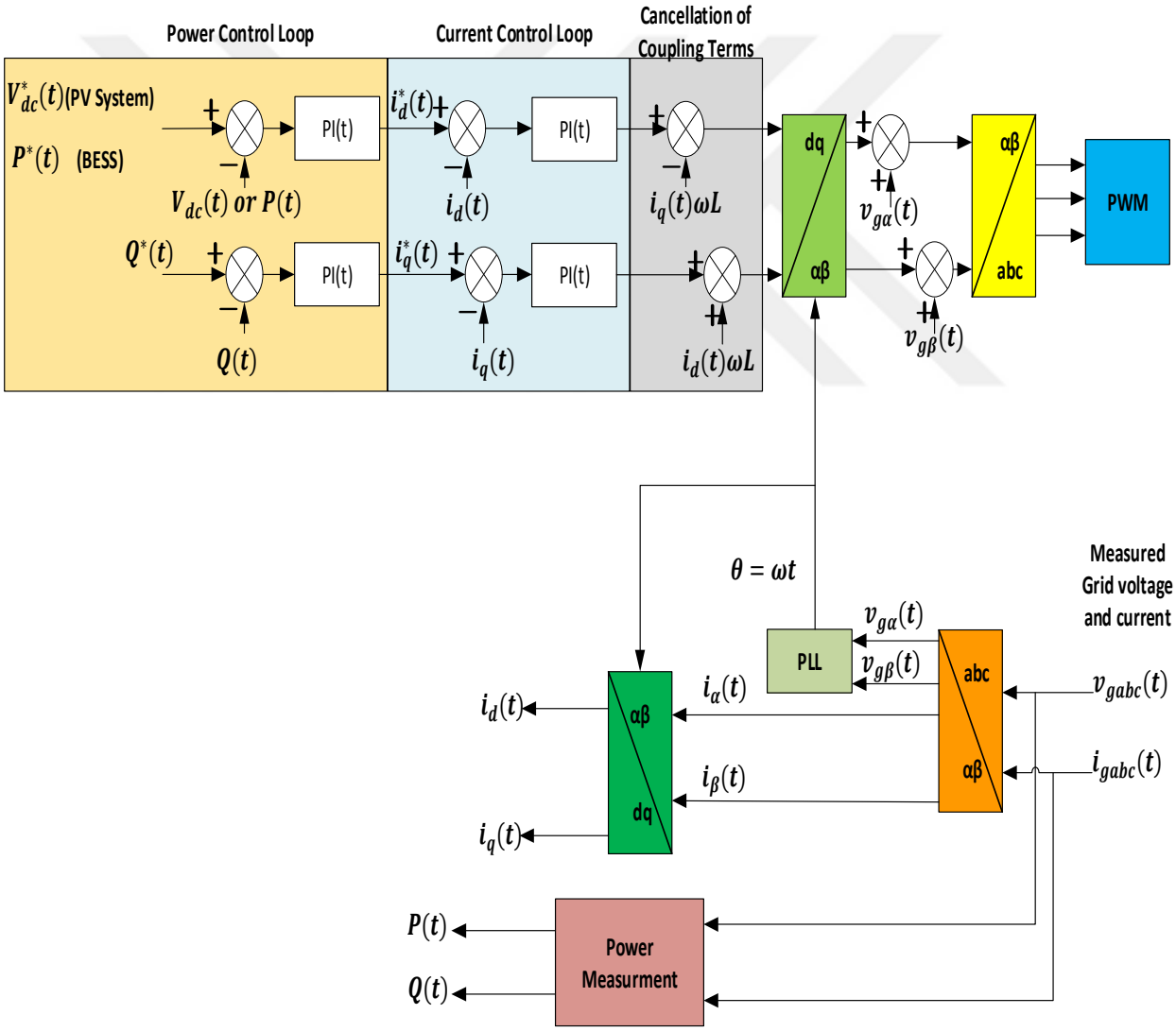

Figure 4.11 : Control Scheme of PV System (BESS) in Power Control Mode (Grid Following).

4.1.5 Dynamic Model of Islanded Inverters in Voltage Control Mode (Grid Forming)

As mentioned, when an inverter system is operated in power control mode, the main goal is to harvest maximum energy from renewable sources. In this condition the main grid compensate the active and reactive power mismatch between loads and generation units in microgrid as well as increasing the system stability. However, the main feature of MGs is their ability to operate in islanded mode and follow the load pattern. If all DERs operate in power control mode, in islanded operation of microgrid, there will be a power mismatch in the system and microgrid loss voltage frequency (V-f) stability. Therefore, during islanded operation of microgrids, at least one of the DERs must operate in voltage control mode and compensate for the active and reactive power mismatch. These DER(s) act as slack bus (voltage bus) and automatically check the active and reactive power mismatch and keep the system (V-f) stable. In a microgrid, when an inverter operates in voltage control mode (grid formation), it improves system stability [54] . However, it is not possible to use the MPPT system in this operating mode, and the system's active and reactive power generation depends on the load model. Therefore, it is impossible to harvest the energy source at the maximum level. Given this fact, it is important to compromise between maximum energy harvest and stability, especially when a microgrid operates in islanded mode. Therefore, operating all DERs in voltage control mode is not an economical and rational choice. As a result, the voltage control (grid forming) mode operation of the control scheme of DERs is shown in Figure 4.12 [59; 60; 61]. In this mode, instead of the reference active and reactive power valuesin the outer loop, the voltages measured from the network are compared with the reference voltage values in the dq-axis. In this control mode the d-axis reference values utilized to control voltage peak value and the q-axis reference values is suitable to control the reference voltage phase (the reference voltage value is generally selected as $1\angle 0$ and thus the q-axis reference value is equal to zero). Finally, in order to keep the frequency synchronization, the angle value that is extracted from PLL system to utilized in the transforms (dq and αβ). It is set to fixed reference value according the network operation frequency (50 or 60 Hz). This reference frequency value is used to generate the voltage source converter reference sinusoidal signal. In this way it is possible to generate a sinusoidal reference voltage with a fixed frequency.

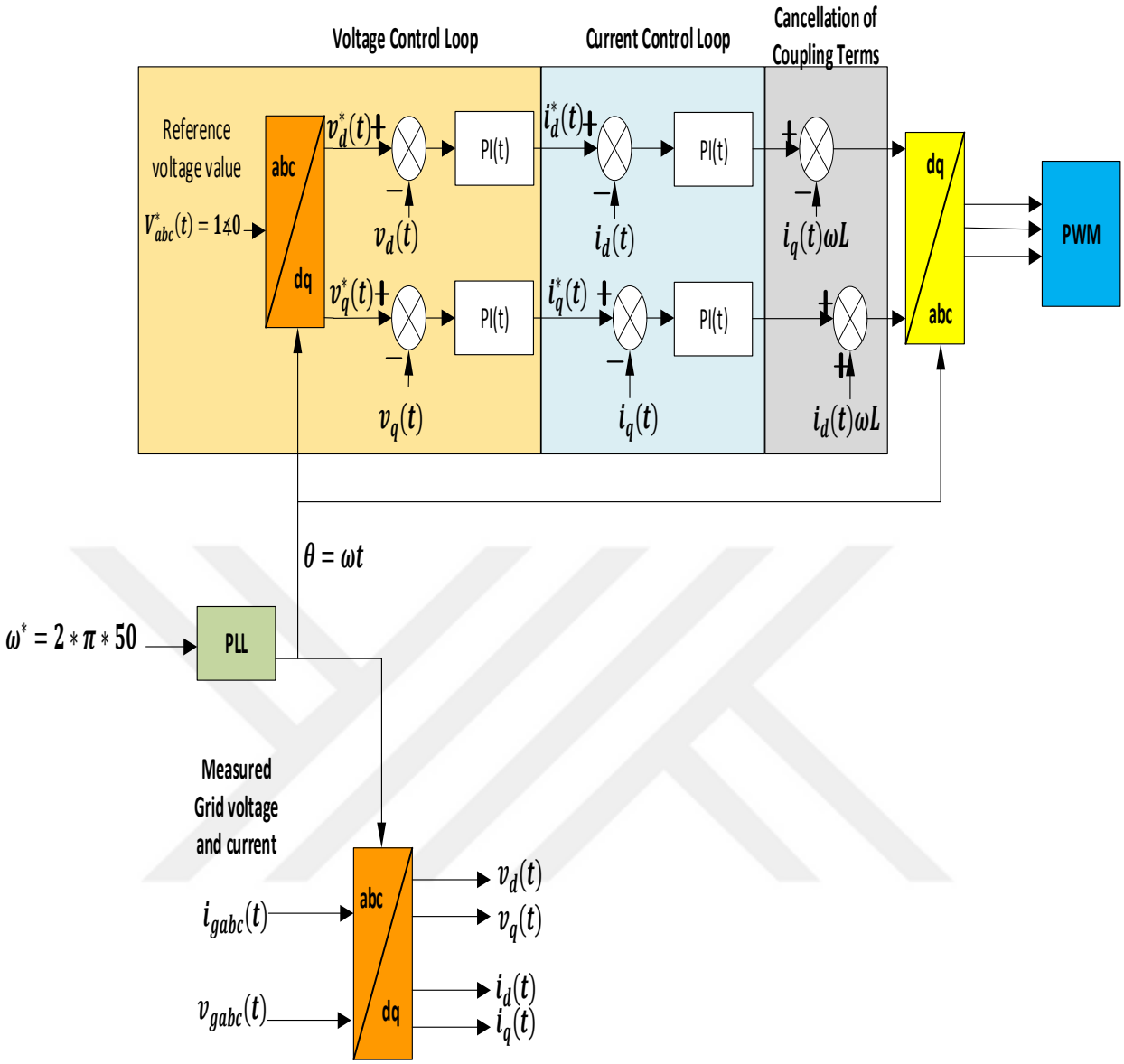

Figure 4.12 : Control Scheme of PV System in Voltage Control Mode (Grid Forming).

4.1.6 Dynamic Model of the Inverters for Low Voltage Ride Through (LVRT)

In conventional power systems, the main energy source is mass production synchronous generators. Renewable energy sources (RES) do not have a significant contribution to the total electricity production and supplying of the loads. Accordingly, when a disturbance (fault or voltage sag) occurs in the grid, these RES are disconnected from the grid and reconnected manually. Since their contribution to the network is low, they do not cause stability problems due to production and consumption mismatch. However, with the increasing penetration of RES and the emergence of MGs ensures that RES can make a significant contribution to meeting

the load demands. Therefore, disconnecting all RES after any disturbance (fault or voltage drop) can lead to total system instability due to generation and consumption mismatch. Consequently, these RESs need to be capable of ride through disturbances. This means that when a fault or any disturbance occurs in the network these RESs need to control the voltage drop and once the faulted area is isolated they can continue to operate and supply the loads. According to these facts, inverter control systems are getting more complex and equipped with low voltage ride through control systems.

For stable operation in the balanced voltage condition, as mentioned, the dq-frame control system is selected with the cancellation of the coupling terms. This model is more resistant to noises and high-frequency current surges. In addition, it has a shorter oscillation time and reaches the steady-state state faster [56]. Finally, it is possible to inject reactive power into the grid during the occurrence of severe three-phase disturbances (faults) that cause high voltage drops. This is done by varying the reference reactive power values $Q^*(t)$ or the reference q-axis voltage $v_q^*(t)$ in power control mode and voltage control mode, respectively. In this way, it is possible to reduce the risk of post-failure instability of inverters.

The common and well-known method for unsymmetrical disturbances or unbalanced voltage condition is dual vector control [62]. In this method, the measured mains voltage and currents are decomposed to positive (index 1) and negative sequences (index 2) and compared with reference values. In this system, the reference negative values are kept at zero, and if the system rotates at an angle of θ in the positive order when transferred to other reference frames, it will rotate as (-θ) in the negative order. Dual vector control in power control mode and voltage control mode of the system is offered in Figure 4.13 and Figure 4.14.

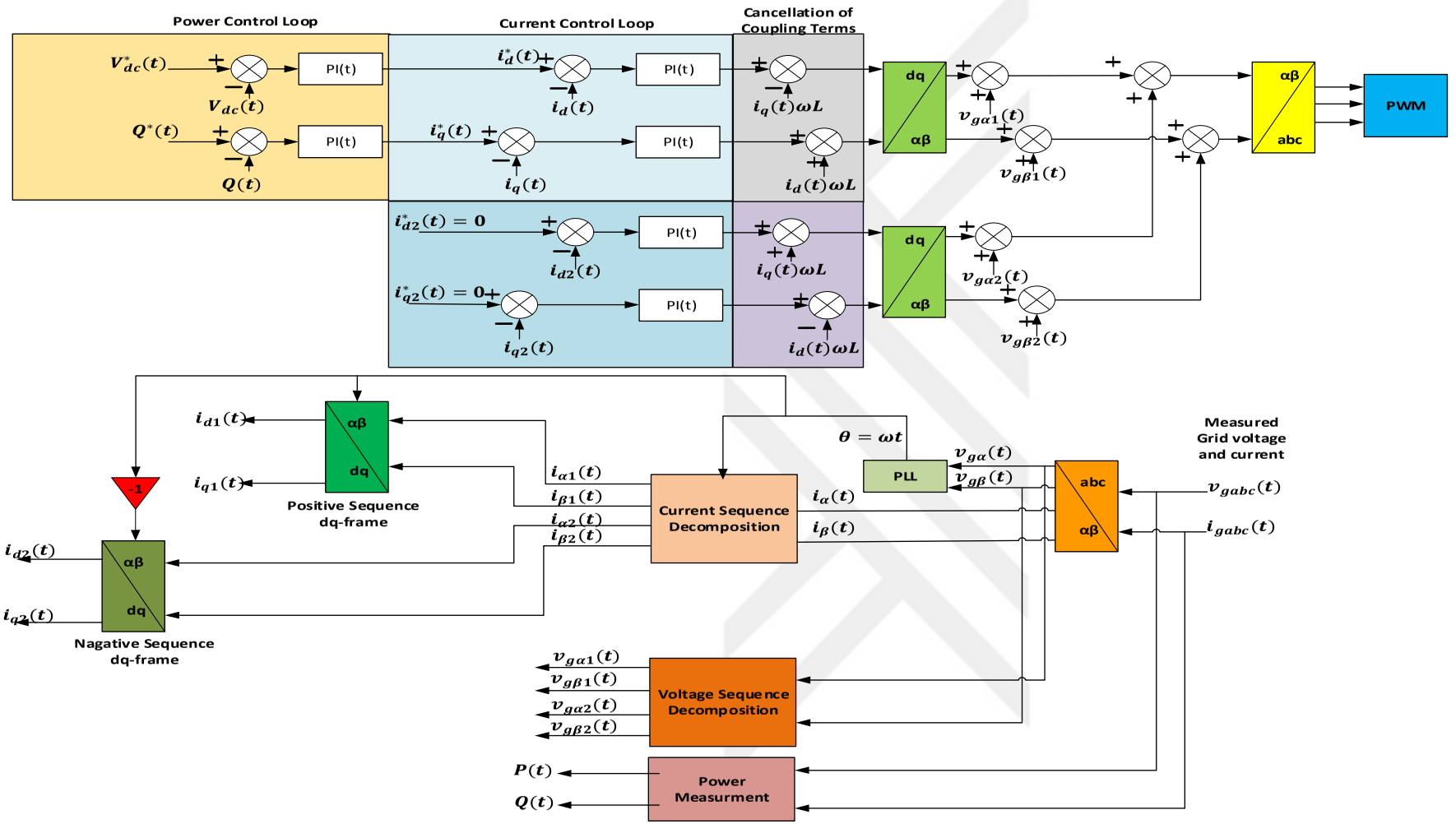

Figure 4.13 : Dual Vector Control of Grid Following (Power Control Mode) Inverter.

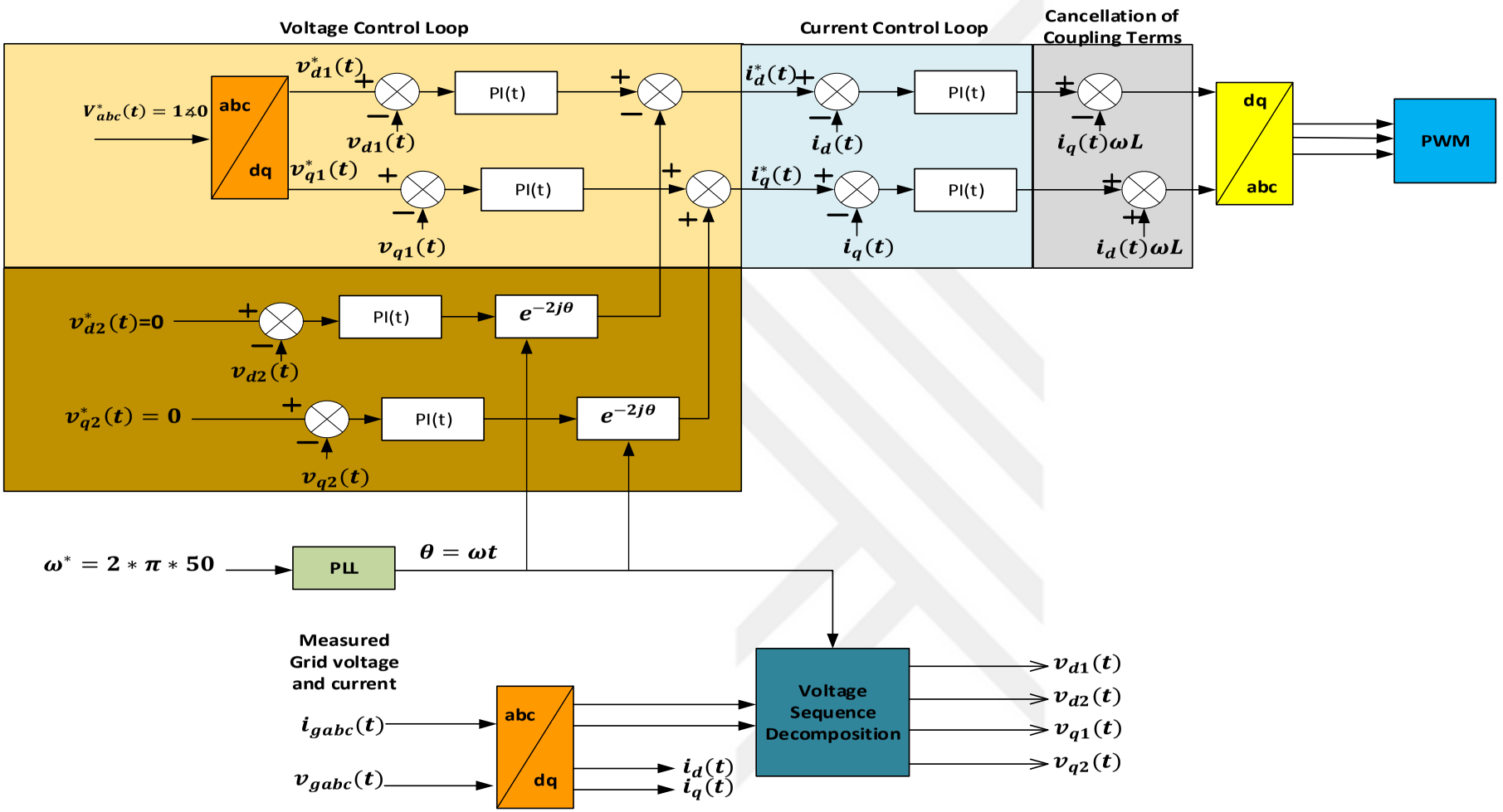

Figure 4.14 : Dual Vector Control of Grid Forming (Voltage Control Mode) Inverter.

4.2 Wind Farm

Another predominant renewable energy source widely used in power systems and MGs is wind turbines. The first types of these turbines are fixed speed wind turbines. There are less reliable and do not show any flexibility towards wind speed variation. This is because, as shown in Figure 4.15, these turbines use a soft starter and step-up transformer and a synchronous or induction generator directly connected to the network, without any converter interface. Therefore, it is necessary to always keep them at a constant synchronous speed. This leads to constant power generation at various wind speeds and cannot harvest wind energy optimally. Also, it lacks LVRT capabilities. Therefore, widespread use of such turbines is not economical and practical. The new generation wind turbines are variable speed wind turbines. Using power electronic components such as inverter (back-to-back) converters helps us collect wind energy at the maximum power point at various wind speeds. In fact, with back-to-back converters, the power generated at various frequencies (depending on the wind speed) is first converted to DC power and then converted to power grid frequency. This helps us to operate the wind turbine at various speeds above and below the rated speed with optimum harvesting of wind energy.

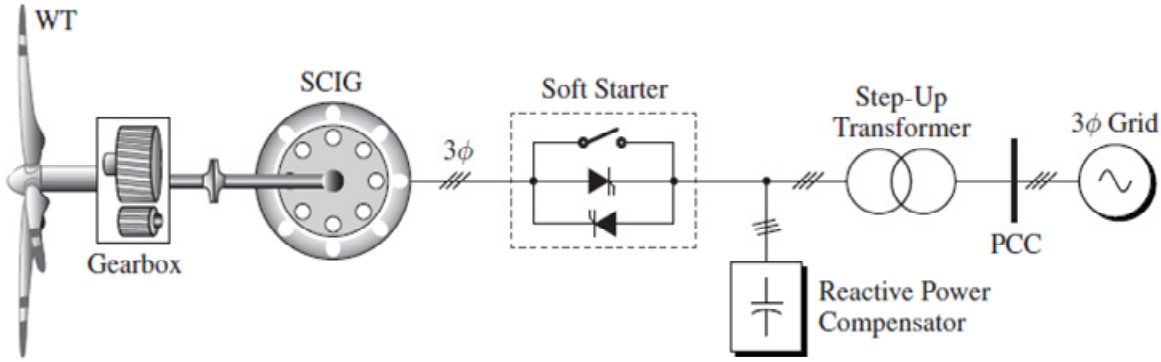

Figure 4.15 : Type 1 Fixed Speed Wind Power Generation Systems [63].

In order to overcome the type 1 wind speed conversation system and with development and prevalence of power electronic components, other type of wind power conversion systems are become popular. The second generation of these converters are doubly fed induction generators (DFIG). As presented in Figure 4.16 the stator is connected to the grid directly and the rotor is connected by a bidirectional back-to-back converter. This condition helps us to operate the generator in $\pm 30\%$ of below or above the

synchronous speed. In addition, it is economic due to use of small-scale power electronic devices (they are connected only on rotor side) and it has complete control of the active and reactive power exchanged with the grid [64].

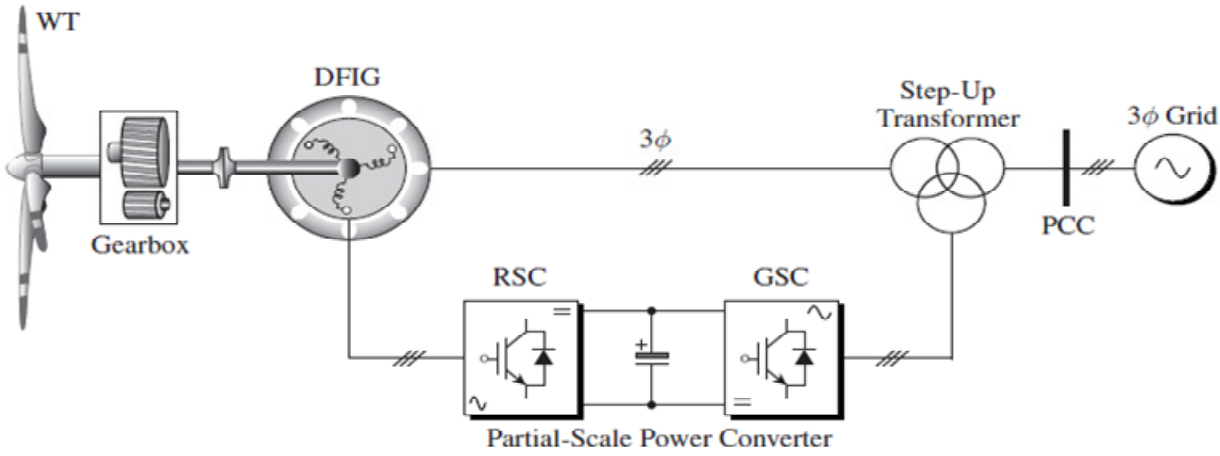

Figure 4.16 : DFIG Based Configuration of the Wind Conversion System [63].

The other type and the most novel variable speed wind power conversion system is full scale conversion system. In this configuration the wind generator are generally permanent magnet synchronous generator (PMSG) and squirrel cage induction generator (SCIG). These systems are fully decoupled from the grid by converters and there is no direct connection between generator and grid (Figure 4.17). This condition enables the smooth grid connection, helps to have full operating power range (100%) and complete control on active and reactive power exchanged with the grid.

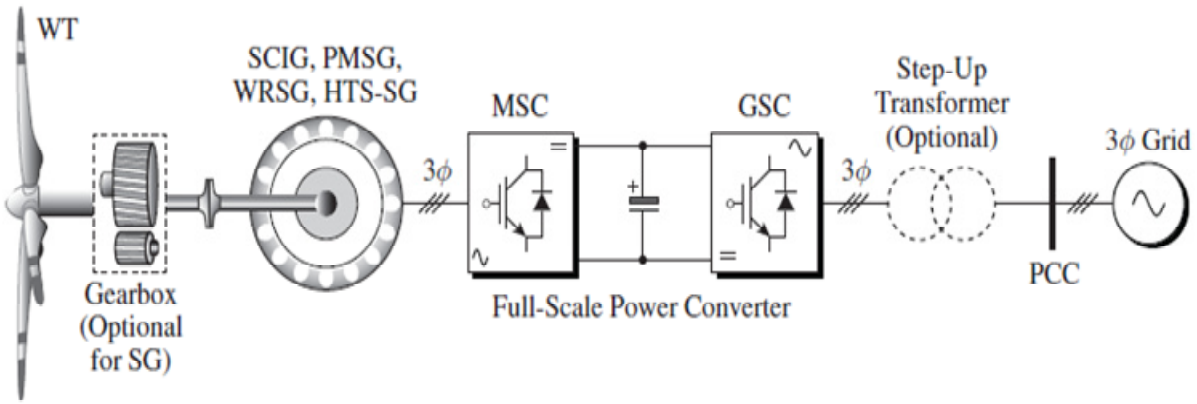

Figure 4.17 : Full Scale Converter of the Wind Energy Conversion System [63].

In this thesis, only DFIG-based wind energy conversion system is modeled as an element of microgrid systems. It works at various wind speeds and loads. It is explained in detail following various dynamic control models of DFIG wind speed, including voltage control mode (grid formation) and current control mode (grid follow). Finally, a hardware solution called crowbar protection for serious faults (3-phase fault) and LVRT capability is described.

4.2.1 Dynamic Model of Grid Connected DFIG Wind in Power Control Mode

Doubly fed induction generators are wound rotor induction machines. Their rotor is connected to the grid by back-to-back converter and the stator is connected to the grid directly. In Figure 4.18 the general control configuration of this system in presented. In this system the stator is connected to the grid directly with constant voltage and frequency. The rotor is supplied by a back-to-back converter with two different rotor-side and grid-side control systems.

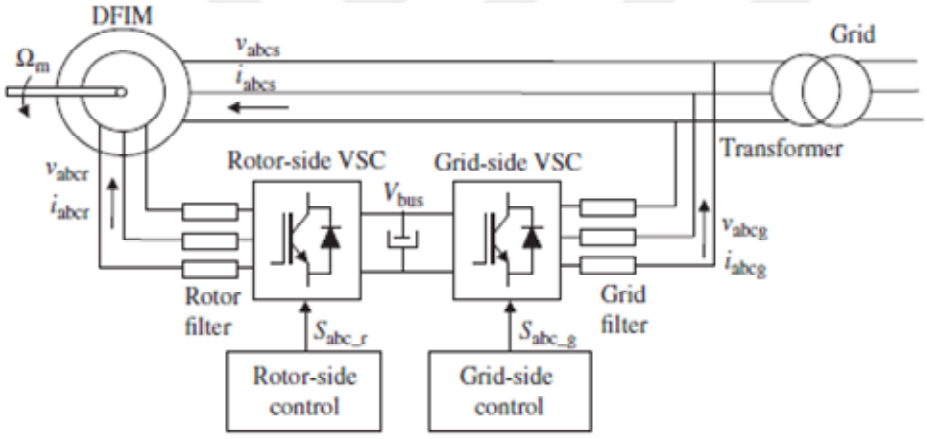

Figure 4.18 : General Control Configuration of DFIG [65].

This control system helps us to supply the rotor by different voltage frequency and amplitude. According to this fact if ω_s is the synchronous frequency and the ω_r is rotor's voltage and current frequency, then the rotor electrical speeds ω_m become:

$$\omega_m = \omega_s - \omega_r \tag{4.14}$$

If the rotor has p pole pair, then the relation of the shaft mechanical speed and rotor electrical speed is:

$$\omega_m = p\Omega_m \tag{4.15}$$

The slip of the machine is defined:

$$s = \frac{\omega_s - \omega_m}{\omega_s} = \frac{\omega_r}{\omega_s} \tag{4.16}$$

According to these equations the stator frequency is fixed synchronous frequency. However, the rotor frequency depends on rotor electrical speed, which creates three operating modes for the machine [66]:

$$\text{subsynchronuos operation } \omega_m < \omega_s \Rightarrow \omega_r > 0 \Rightarrow s > 0$$

$$\text{supersynchronuos operation } \omega_m > \omega_s \Rightarrow \omega_r < 0 \Rightarrow s < 0$$

$$\text{synchronuos operation } \omega_m = \omega_s \Rightarrow \omega_r = 0 \Rightarrow s = 0$$

Therefore, the rotor side control, including inner loop control (current control) and power control is depicted in Figure 4.19. In the rotor side control, the stator active and reactive power is measured and compared with the reference value. The reactive power reference value is generally set to zero and it is used to inject reactive power in fault condition to the network and avoid voltage collapse. In this control system the reference active power is generated by wind turbine MPPT system and by active power and d-axis rotor current relation $P_s = -\frac{3}{2}\frac{L_m}{L_s} V_s i_{rd}$ the d-axis rotor side reference value is generated. The reactive power reference value is compared with grid measured value and q-axis reference value is generated. By this way the rotor side controller generates the active power that is maximally harvested from the wind speed with desired power factor (reactive power) and injects to the grid. In this system the system measured value are transferred to dq-reference frame that is rotating in rotor electrical speed ω_m.

The grid side converter control system main purpose is to maintain the DC bus voltage in order to supply the active power. This controller is operating in unit power factor (q axis reference value is equal to zero) unless a severe fault happens in the network. In this condition the reacttive power is injected to avoid voltage collapse. As presented in Figure 4.20 the outer loop is used to regulate the DC voltage and the input of inner d-axis loop is the output of the voltage regulator and q-axis refence value input is the output of reactive power regulator [62; 67]. The grid side converter outputs are measured and compared transferred to dq-reference frame rotating with rotor electrical speeds ω_m. The values are compared with reference dq-axis values and the PWM output is generated.

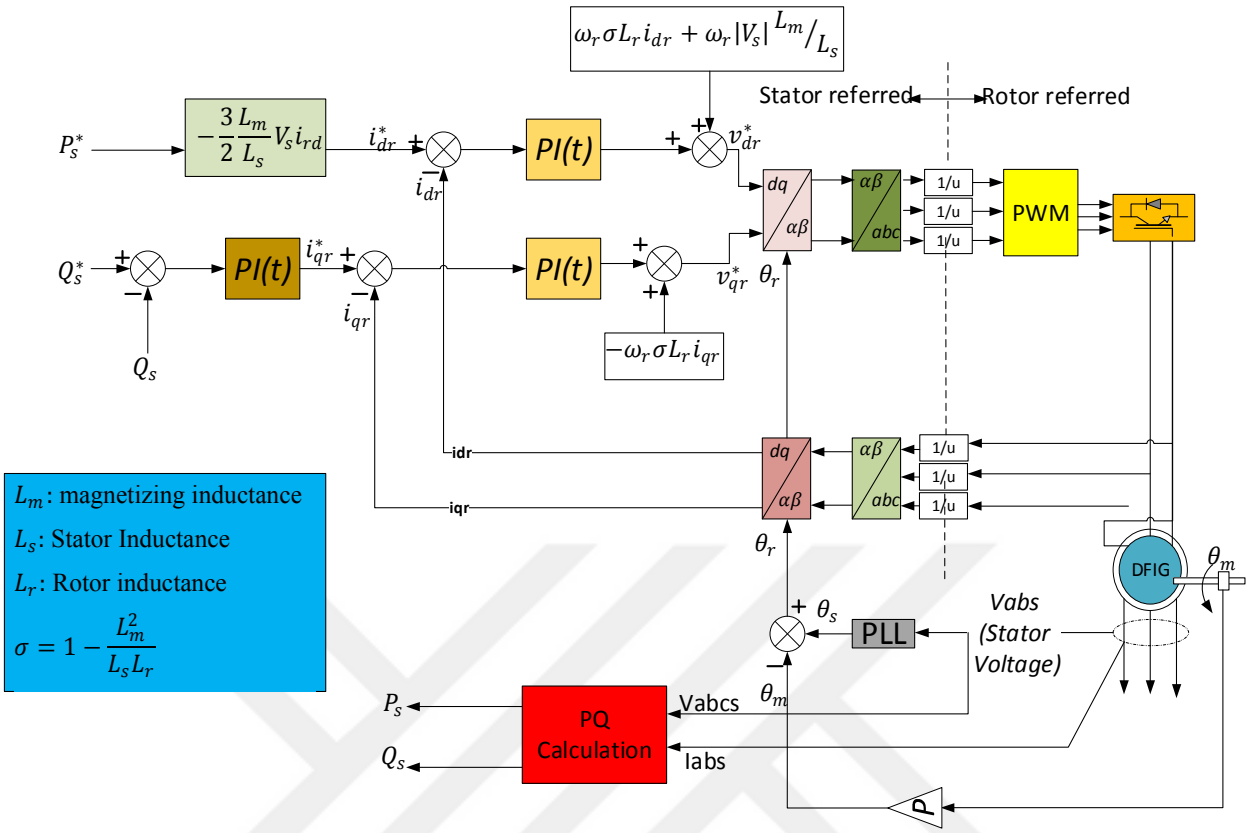

Figure 4.19 : Rotor Side DFIG Controller in Power Control Mode.

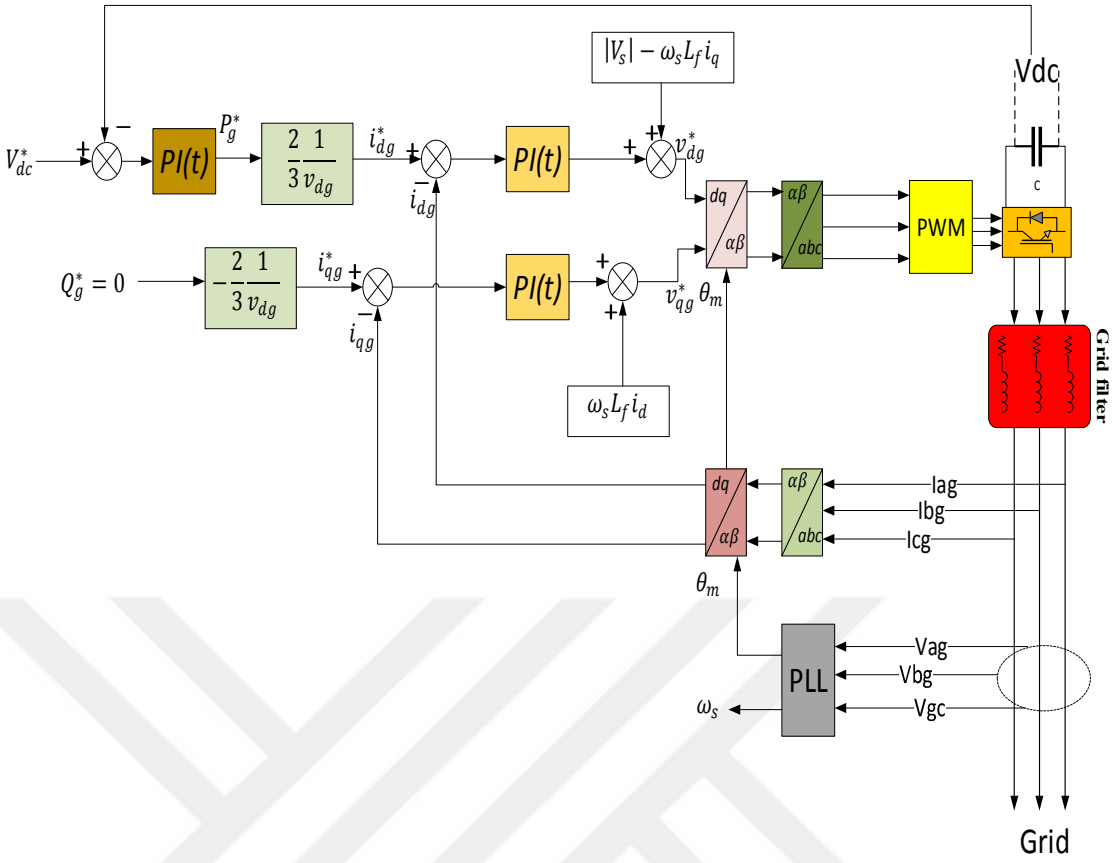

Figure 4.20 : Grid side DFIG Controller in Power Control Mode.

4.2.2 Wind turbine operational zones, model and MPPT control

A wind turbine in wind farm is system used to capture the kinetic power from the wind and convert to mechanical power on the shaft. The kinetic power of wind can be expressed:

$$P_w = \frac{1}{2}\rho\pi R^2 v_w^3 \tag{4.17}$$

In this equation ρ is the air density, R is the radius of the blade and v_w is wind speed. For a given wind turbine, this kinetic energy cannot extract completely and the extracted value is smaller than this value and it is equal to:

$$P_{turbine} = C_p(\lambda, \beta)\frac{1}{2}\rho\pi R^2 v_w^3 \tag{4.18}$$

Where $C_p(\lambda, \beta)$ is called the power coefficient and it varies according to turbine's tip speed ratio λ (depends on rotational speed of wind turbine Ω_t) and pitch angle , β. Therefore, for a given wind speed value, as presented in Figure 4.21 it is possible to harvest desired level of the wind energy and generate various powers according to

wind speed and wind turbine adjustment. Therefore, when a DFIG wind turbine is operated in power control mode, if it is not exceeded the durable rotational speed limit, it is preferable to adjust operating in maximum power coefficient $C_{pmax}(\lambda, \beta)$. This condition help that in every wind speed harvest the maximum possible power from the wind.

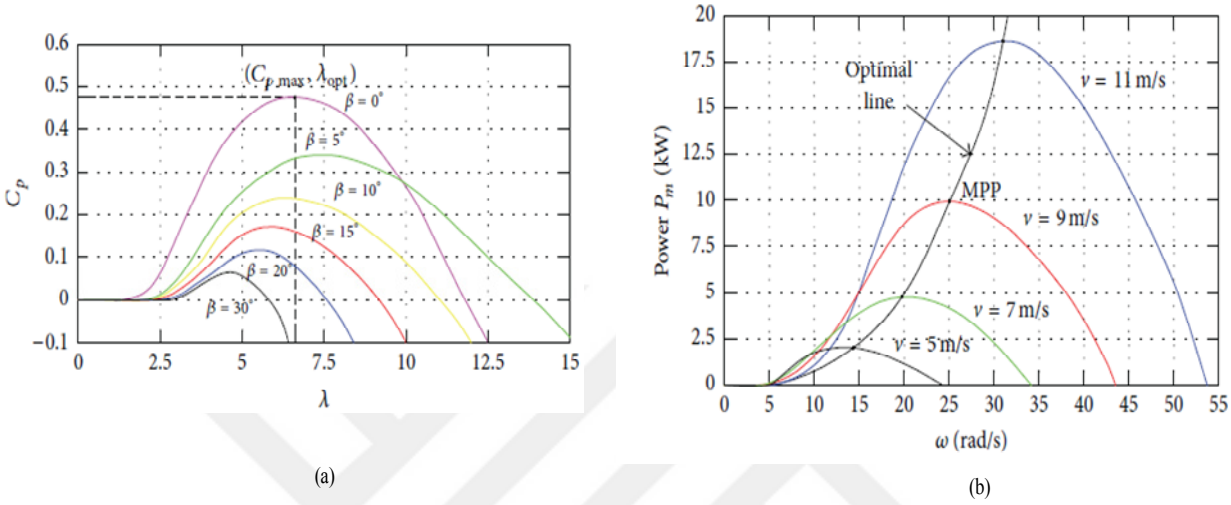

Figure 4.21 : Relation Between Wind Turbine Power Coefficient, Tip Speed Ratio and Pitch Angle (b) Relation Between Power and Wind Speed [68].

In power control mode operation of a wind turbine, it is always preferable to harvest maximum possible kinetic power from wind. However, every wind turbine has minimum and maximum rotational speed and it is not always possible to operate a wind MPPT. According to wind speed a typical wind turbine operation divided into four operating zone (Figure 4.22) [63; 65]:

Zone1: The rotational speed is kept constant and fixed value of power is generated. In this zone the maximum power of the wind is not extracted.

Zone 2: in this zone the rotational speed of the wind turbines varies according wind speed. Thus, the MPPT strategy is applicable.

Zone 3: this zone is not valid for all type of the turbine design. In this zone the turbine maximum rotational speed is reached. However, the turbine is not let to operate at maximum point of the power curve.

Zone 4: in this zone the turbine power is reached to rated power and the rotational speed is reached to maximum value. In this zone the rotational speed and power are maintained constant by system called pitch control. The pitch angle of the wind turbine

is not equal to value of it in maximum power coefficient $C_{pmax}(\lambda, \beta)$ which is $\beta = 0$. The pitch angle value continually adjusted to keep the speed and power constant.

According to these operating zones a wind turbine is need to have 3 different control strategies. When the turbine operating in zone 1 or zone 3, the rotational speed needs to set the minimum or maximum rotational speed Ω_t respectively. In these operating zones the pitch control $\beta = 0$ is set to its optimal value.

When the turbine is operating in zone 2 the MPPT strategy is implemented and according to wind speed and its result the rotational speed, maximum kinetic power is harvested at optimum pitch angle.

When the turbine operates in zone 4 the pitch angle is regulated by the PI controller in order to maintain the turbine's generated power at its nominal values.

The control strategies of wind turbine various operating zones is presented in Figure 4.23.

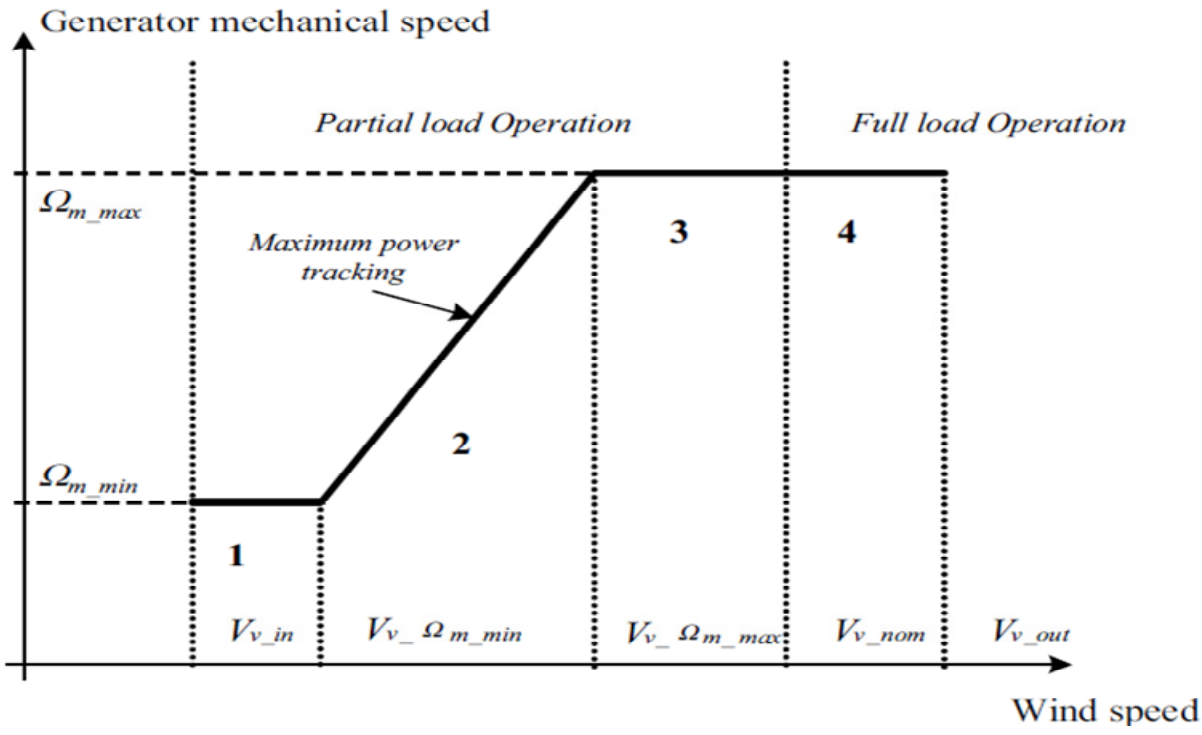

Figure 4.22 : Operational Zones and Range of a Wind Turbine [64].

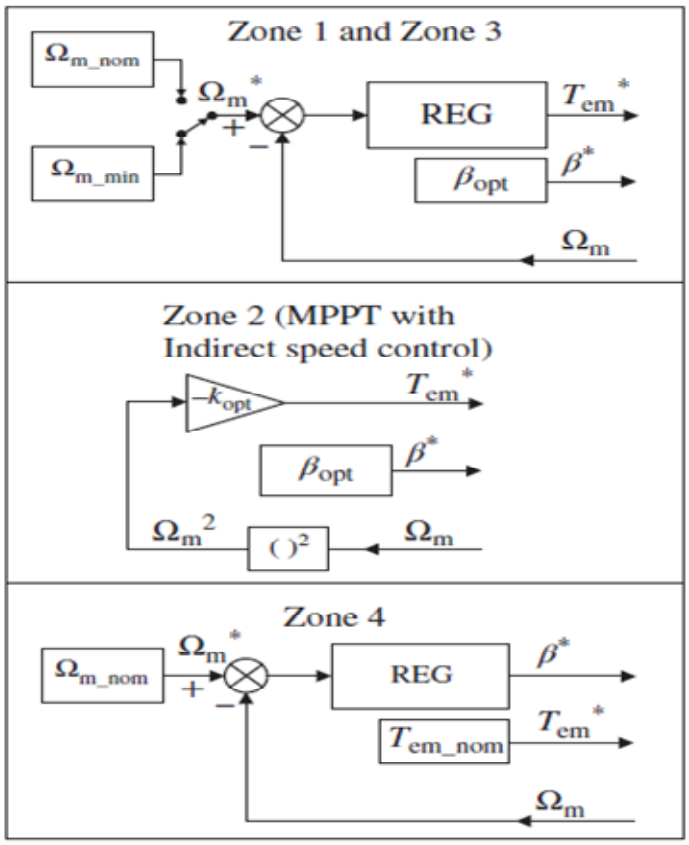

Figure 4.23 : Wind Turbine Model and Control Strategies in Various Operating Zones [65].

4.2.3 Dynamic Model of Islanded DFIG Wind in Voltage Control Mode

Like the grid forming inverter based DERs the wind turbines are also capable to operate in voltage control model. During this condition the rotor voltage is no longer set by the main grid. Furthermore, the wind turbine power generation is no longer pursing the MPPT point for harvesting the maximum wind energy. It tries to keep the stator voltage stable and pursue the demand patten. In this condition, it is necessary to make modification in control loop of the machine and add a voltage loop instead of power control loop. In DFIG wind turbine the rotor side controller is responsible for machine behavior and significant amount of the production. Therefore, the outer power control loop of the rotor side controller is replaced with a voltage control loop. On the other side, the grid side controller main role is maintenance of the DC bus voltage. During islanded operation mode of the DFIG wind this role is kept unchanged. Thus, there is no need to manipulate the grid side controller. In addition to these control system improvements, the stator is equipped with capacitor filters as depicted in Figure 4.24. This property helps to improve the voltage quality and compensate partially a

reactive power of the machine or load [65]. According to this fact the rotor side control of the DFIG wind in voltage control mode is presented in Figure 4.25.

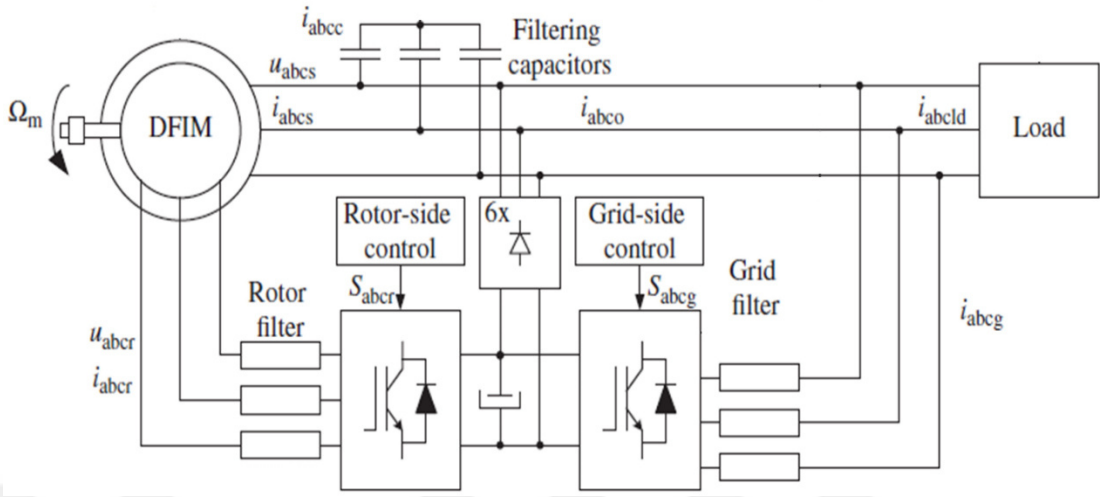

Figure 4.24 : General Scheme of the Islanded DFIG [65].

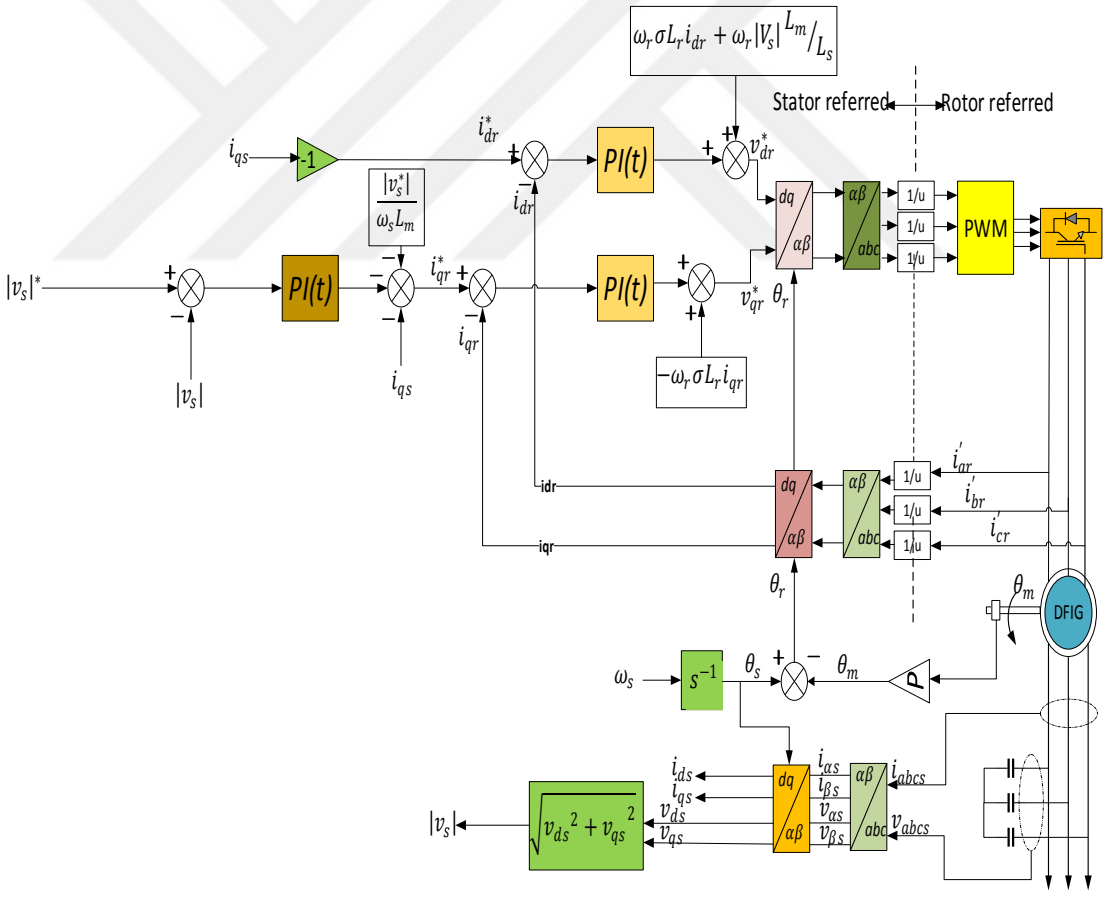

Figure 4.25 : Rotor Side DFIG Controller in Voltage Control Mode.

4.2.4 Hardware Implementation of the DFIG-Wind Turbine for Severe Voltage Drop and LVRT

Similar to inverter based DERs, it is necessary to consider properties for LVRT of the wind turbines in microgrid to stably operate for post fault condition. In this condition, for severe voltage disturbance the dual vector control system or cancellation of the coupling terms in control system is not sufficient. In inverter-based wind system when a severe voltage dip (Three phase fault) happens in the system, the stator flux cannot evolve to its new steady state value as fast as stator voltage. As a result, the rotor voltage which is dependent to stator flux cannot accompany the stator voltage drop and leads to high increase of current mainly in rotor. This severe condition is happened particularly at the first few periods from beginning of the fault. In other words, after a severe voltage dip, during evolve of the stator flux, there is a short period that the control of the machine is lost. This condition produces over currents in rotor and stator of the machine and leads to loss DC bus voltage control. This undesirable condition maintains to exist until the flux reaches to the level which is controllable by voltage converters [65]. In order to avoid this situation, the control strategies are divided in to two groups of the 1- improving the control system of the machine 2- Hardware solution. The control [69; 70].

The improvement of the control strategies main methods are demagnetizing current control, flux linkage control and feed forward control [70]. These methods have lower costs because establishment of an additional device is not needed. However, they make the control system more complex and the are not reliable to have desirable performance for all the severe voltage dips.

The hardware solution, main strategies are rotor-side crowbar, DC chopper, series dynamic breaker resistance and dynamic voltage restore methods [69; 70]. These methods impose additional costs for the system. However, they more reliable and applicable for severe symmetrical and unsymmetrical voltage drops.

In this paper, a commonly used hardware solution method called crowbar protection is selected for LVRT control of DFIG wind system. The crowbar control configuration is shown in Figure 4.26. This configuration consists of three-phase resistors with three-phase power electronics switches. In the event of a fault, the crowbar protection short-circuits the rotor winding when one of the stator voltages, the DC link voltage falls far below the limits, or the rotor current exceeds the limits. In this situation(the limits are

determined by each country grid code) the transitions of the rotor current are limited when crowbar protection is activated in the first few cycles of the fault.

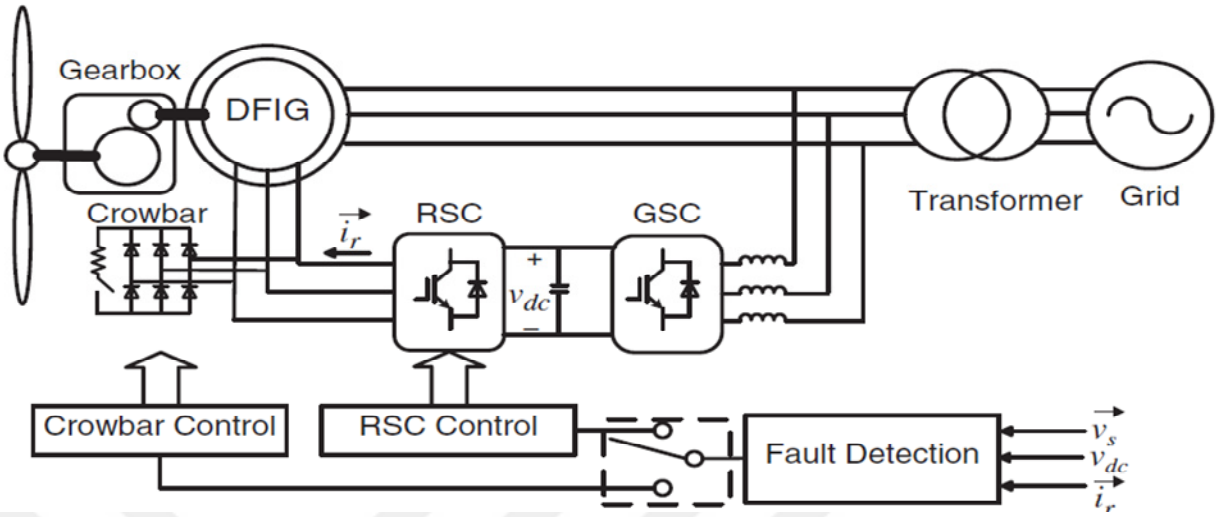

Figure 4.26 : General Presentation of the Crowbar Protection for LVRT Control of the DFIG Wind System [70].

A grid codes for LVRT operation means the tolerable voltage dips at the terminal of the wind turbine remain connected to the grid and support voltage and frequency after faults. The grid codes are varying from country to another. This condition is presented in Figure 4.27. According to this figure when the voltage drop (symmetrical or asymmetrical) is above the zones defined by the line, the wind systems must remain in system and supply the grid without tripping. Therefore, is this thesis during the all-fault simulation the zero right through condition is considered and the LVRT crowbar protection is activated. In addition, when the voltage drops are more than 10% t, the turbine provides reactive power backup.

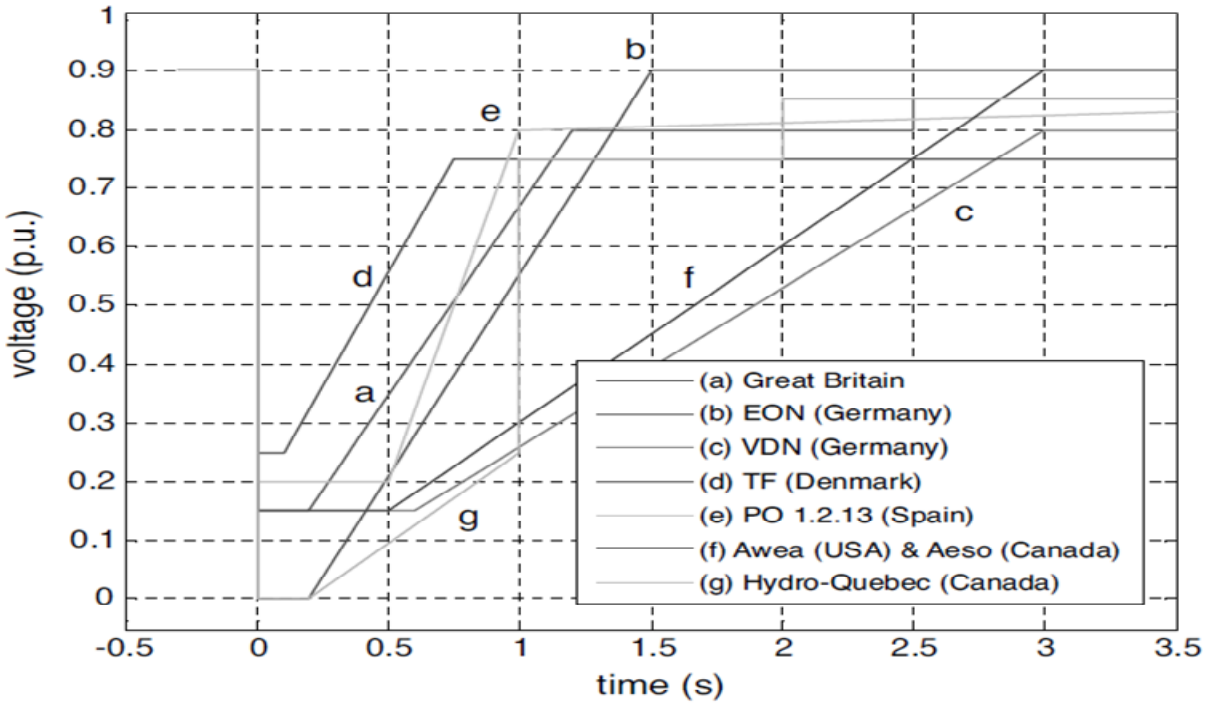

Figure 4.27 : LVRT Requirement for Different Grid Codes [16].

5. STUDY TEST BENCHMARK SYSTEM: IEC TEST MICROGRID

A standard microgrid called IEC microgrid 61850-7-420 [32; 39; 41; 42] as shown in Figure 5.1 is used to testify and validate the proposed intelligence-based method. This microgrid consists of two fully inverter interfaced 2.5 MW PV farms and a rotating 3 MW DFIG-wind farm DER. Also, two BESS are installed on bus 5 and bus 2 to simulate the elements with bidirectional power flows. PV farm and DFIG wind can operate in both power control and voltage control modes. However, BESS is only modeled as a power control mode and injects or absorbs active or reactive power(bidirectional power flow). A detailed electromagnetic model of DERs including higher order state space equations is used to simulate the microgrid.In addition, the lines are modeled based on frequency dependent Bergeron's propagation wave method. In this simulation, the full model of the inverter's DER and PWM voltage source is modeled. Such a model makes it possible to extract the higher order switching frequency that generates the harmonic and distorted current signal. Additionally, it helps us model short-time transients and extract frequency components. Our main concentration was on accurately modeling the dynamic behavior of the microgrid to obtain high-detail signals, even though all these conditions significantly slowed down the simulation speed.

In this microgrid, an attempt is made to model all the protection challenges of conventional protection systems. The microgrid can operate in both grid-connected and islanded mode. During these operations, DERs are modeled in 3 different loading conditions to control their varying contribution in the fault current level mainly in islanded mode: full load (100% nominal), half load (50% nominal), and minimum load (25%) nominal. During these loading conditions, BESS can operate in bidirectional power flow and as a backup energy source (discharge mode) or load (charge mode). A crowbar protection is used for modeling the LVRT capacity of the DFIG-wind. Also, a dual vector control [71] mode implemented for inverter-based DERs to have LVRT capability during voltage disturbances. All DERs are considered as power control mode for grid connected microgrid. This helps to have maximum energy harvest due

to activation of MPPT. In islanded mode a DERs is assumed as slack bus and it is necessary the at least one of the DERs operate as voltage control modes and adjust power mismatches. This helps to have stable performance for the microgrid. İt is also optional to have more than one DERs in voltage control mode to have better stability performance. The test network operates in various meshed and radial topologies by switching the S1 and S2 switches.

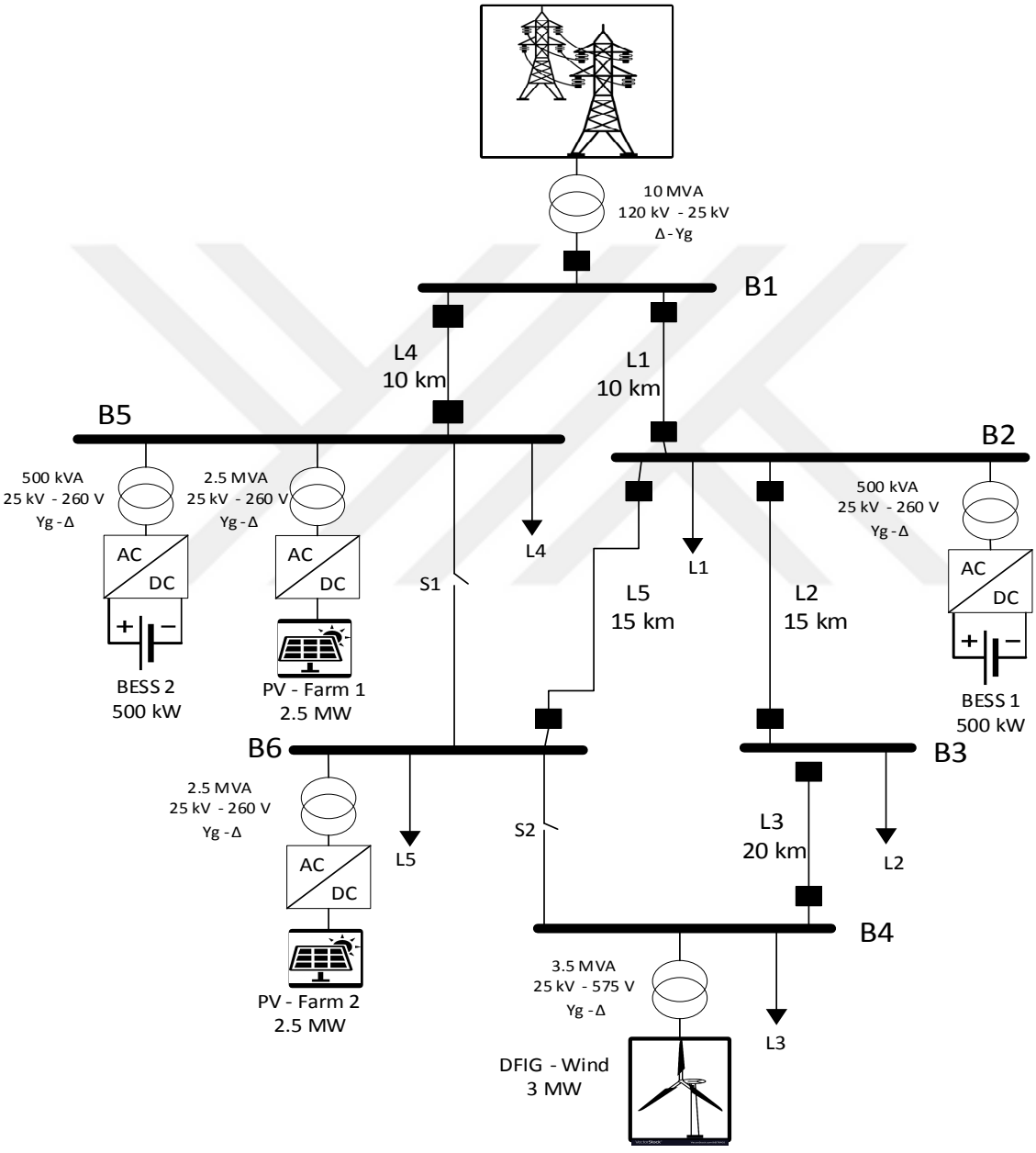

Figure 5.1 : IEC Test Microgrid.

Fault in power systems is a fast and swift change in state of the siganl. It contains electromagnetic high frequency transients in current and voltage. Every one of them have unique frequency components as well as fundamental componenet. The main

purpose of signal processing methods is to extract these components and facilitate learning and boost the training of intelligence-based methods. But besides faults in power systems, there are other transients as well. These phenomena components are not in the frequency spectrum of the faults. But some of its components may overlap. For many of these phnomena there is no need to trip the protection relays. Therefore, it is necessary to model these additional transients to check whether our model can be correctly distinguished from fault simulations. In total, 19965 fault scenarios were simulated. To prove the algorithm's ability to distinguish the non-defect scenario, 825 non-defect test cases are also simulated. The data is split 70 percent and 30 percent for the train and test of the model, respectively. The main reason for this distinction is that increasing the train data helps the model to classify the feature (data) space better. On the other hand, it is necessary to have enough data to test the algorithm performance and measure the error accurately. According to machine learning articles, a ratio of 70 to 30 is the preferred choice when there is enough amount and variation of data. Train and test data are randomly selected and the algorithm is run 300 times. There is no significant variation in the accuracy of the algorithm. This means that the attribute space has sufficient diversity and there is no great separation between the data of any class in the attribute space.The scenarios are described in TABLE 5.1. 11 fault secario is considered for Brownboost algorithm to classify them. In order to check performance of model in distiguishing other transient scenarios from fault scenario, addtional non fault sceanrios are also added as described in the table. In total, there are 13 classes in the algorithm, and for binary coding the and multiclass classifaction of Brownboost error-correcting output code (ECOC) methods withand one versus all is used.

Table 5.1 : Simulated Fault and No-Fault Scenarios

Simulated Fault Scenarios
• Location of the Fault 10%,20%,…90% of line
• Fault Happen Line L1,L2,…,L5
• Type of the Fault AG, BG, CG, AB, AC, BC, ABG, ACG, BCG, ABC, ABCG and external faults (faults happen outside the line under study line)
• Variation in Fault Penetration Level (full loading, half loading and min loading)
• Microgrid Operational Mode (grid connected or islanded)
• DERs Operational Condition in Microgrid (voltage control mode or power control mode, charging or discharging of BESS)
• Change in Microgrid Topology (mesh or radial)
• Fault Resistance (0.01,1,10,100 Ω)
• Fault Inception Angle $0^{\circ}, 30^{\circ}, 60^{\circ}, 90^{\circ}$

Table 5.1 (continued)

Simulate Other Transient No-Fault Scenarios • Sudden Change in System Topology (mesh or radial) • Change in Microgrid Operating Mode (islanded, grid-connected) • Sudden Change in Load ($\pm 10\%, \pm 15\%, \pm 20\%$) • Change in Penetrationor Generation of the DERs (full loading, half loading and min loading) • Switching Capacitor Bank (100 kvar, 200 kvar, 500 kvar, 1000 kvar, 1500 kvar) • Inject External Disturbances (voltage sag and swell)

5.1 Results and Discussion

In this section the results of simulation and implementation of the proposed method is discussed. In proposed method the differential current of the both end of the lines is extracted and then they are transferred to 3 various but same type signal processing based HHT feature spaces. The algorithm is trained and the voting power of the Brownboosts called margin in every one these feature space is calculated for every class of the data to others (one vs all). Finding the training margins of the algorithms for a given data helps us find the higher discrimination for a given class. Thus, is has lower risk of violating the boundary of the other data space in existence of noise and other disturbances like harmonic. In addition, a Brownboost model with higher margin means it shows lower struggle to deal with outliers and noisy data violated data due to well separation of the data in data space.

Beside to margin that is extract by Brownboost for every feature space the main property of this ensemble algorithm is its non-convex optimization method. It helps the have unique behavior for real world non-convex problems. This peculiarity provides the algorithm enough intelligence to iteratively continue to discard or continue to classify problematic misclassified data that may face in real system data-gathering due to misclassified and noisy data. This is what give the algorithm robustness against test and train data uncertainties and overfitting.

In a typical fault protection system, it is necessary that the system is capable to detect and trip for all fault scenarios. It is also beneficial that it is capable to discriminate other transients from faults scenarios or differ external and internal fault to avoid false and nuisance tripping and constructing a backup protection. In addition, because the fault detection is done by differential current of both end of the line it is better that the performance the algorithm is testified for synchronization delays.

For any type of the simulated noise and synchronization delays, the proposed algorithm can detect the faulty scenarios flawlessly. However, the noise and delays make some unfaulty scenarios to be considered as faulty one. A good classifier needs to avoid these data during the training process because the increase the risk overfitting considerably.

The proposed algorithm is tested on the data extracted from the test network. Both ends of the differential current are used to distinguish between the external and internal faults. In order to test accuracy of the algorithm for a class C, the following equation is used:

$$classifer\ C(\%)accuracy = (1 - \frac{N1+N2}{N}) * 100 \quad (5.1)$$

In this equation:

N1: number of the data classified incorrectly.

N2: Total number of other scenarios (other classes) that are falsely classified as class C.

N: Total number of test scenarios.

Various real world devices uncertainties are tested by the algorithm. These uncertainites are contain loss of synchronizm and various levle of noise penetration. Therefore, a multiresolution time-frequency adaptive signal processing method is preferred.

The main feature of these adaptive basis signal processing methods compared to methods such as wavelet is their decomposition level is not a predefined value before starting decomposition. Based on the transient signal component, the penetration level of the noise, and the decomposition methods, these adaptive basis signal processing methods automatically decompose the signal until a monotonic signal is obtained. Therefore, it can have various levels of dissociation for each signal. The only parameter controlled by us is the maximum decomposition level, which is also an optional choice, and it is a optional choice. However, in this paper, in order to have the same vector size input for the intelligence-based method, the maximum level of decomposition is considered to be 7. Almost none of the results have this amount of separation, and the monotonic signal is capture as lower levels of decomposition (other values are considered zero). In the proposed method, various noise penetration levels are tested with signal-to-noise ratio (SNR) of 10, 20 and 30 dB. Also, various

synchronization delays (time sample differences) of quarter, half and one cycle are tested between the output signals. An example the performance of the method under various uncertainties in line 2 is depicted as bargraphs in Figure 5.2 to Figure 5.5 for synchronization delays.

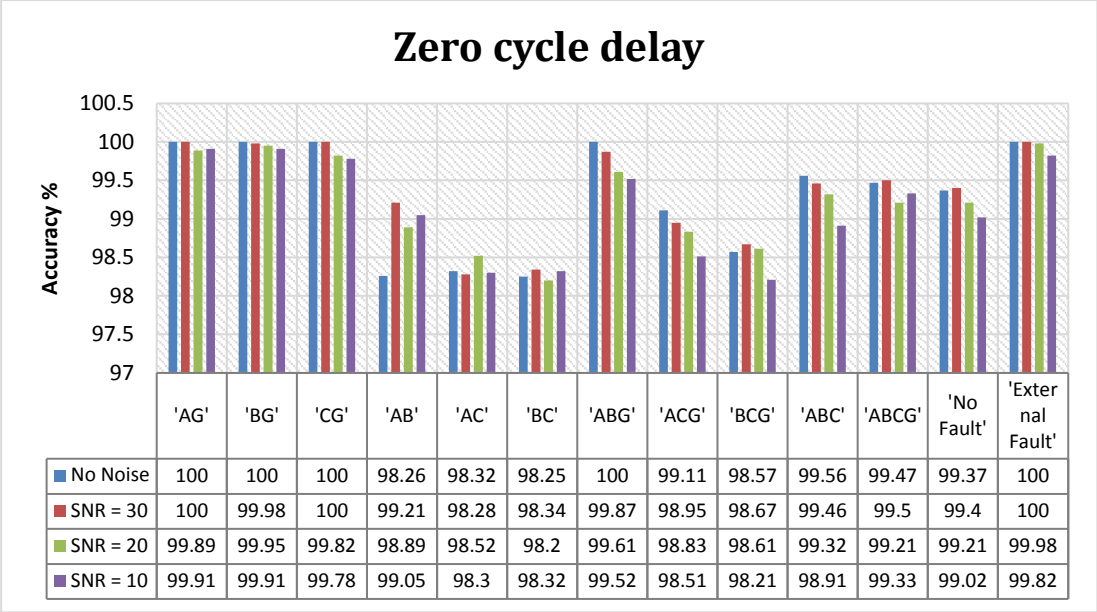

	'AG'	'BG'	'CG'	'AB'	'AC'	'BC'	'ABG'	'ACG'	'BCG'	'ABC'	'ABCG'	'No Fault'	'External Fault'
No Noise	100	100	100	98.26	98.32	98.25	100	99.11	98.57	99.56	99.47	99.37	100
SNR = 30	100	99.98	100	99.21	98.28	98.34	99.87	98.95	98.67	99.46	99.5	99.4	100
SNR = 20	99.89	99.95	99.82	98.89	98.52	98.2	99.61	98.83	98.61	99.32	99.21	99.21	99.98
SNR = 10	99.91	99.91	99.78	99.05	98.3	98.32	99.52	98.51	98.21	98.91	99.33	99.02	99.82

Figure 5.2 : Line 2 Zero Cycle Synchronization Delay.

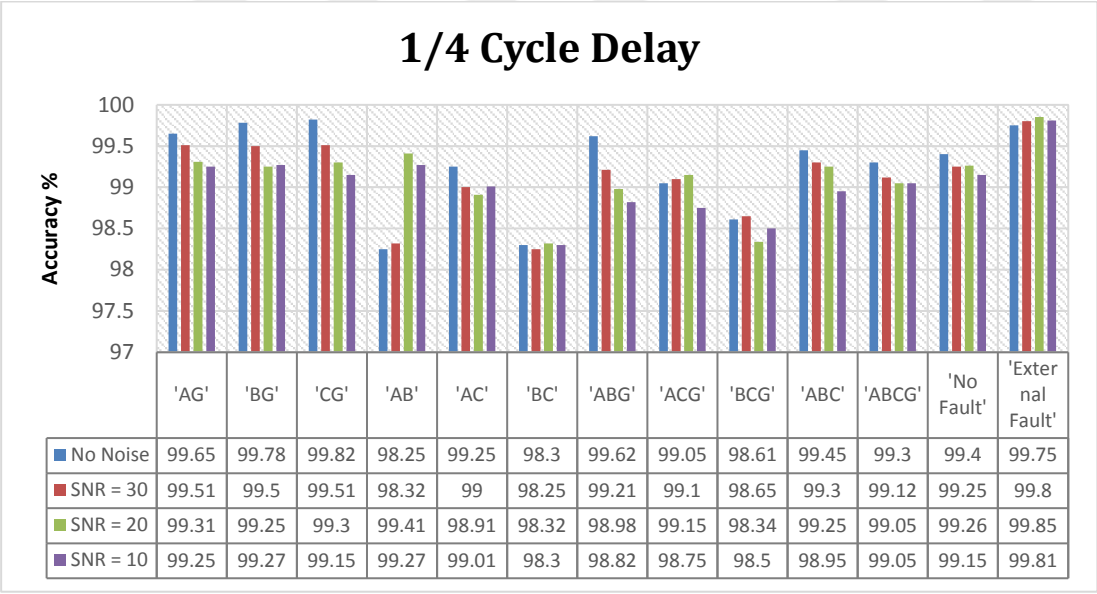

	'AG'	'BG'	'CG'	'AB'	'AC'	'BC'	'ABG'	'ACG'	'BCG'	'ABC'	'ABCG'	'No Fault'	'External Fault'
No Noise	99.65	99.78	99.82	98.25	99.25	98.3	99.62	99.05	98.61	99.45	99.3	99.4	99.75
SNR = 30	99.51	99.5	99.51	98.32	99	98.25	99.21	99.1	98.65	99.3	99.12	99.25	99.8
SNR = 20	99.31	99.25	99.3	99.41	98.91	98.32	98.98	99.15	98.34	99.25	99.05	99.26	99.85
SNR = 10	99.25	99.27	99.15	99.27	99.01	98.3	98.82	98.75	98.5	98.95	99.05	99.15	99.81

Figure 5.3 : Line 2, ¼ Cycle Synchronization Delay.

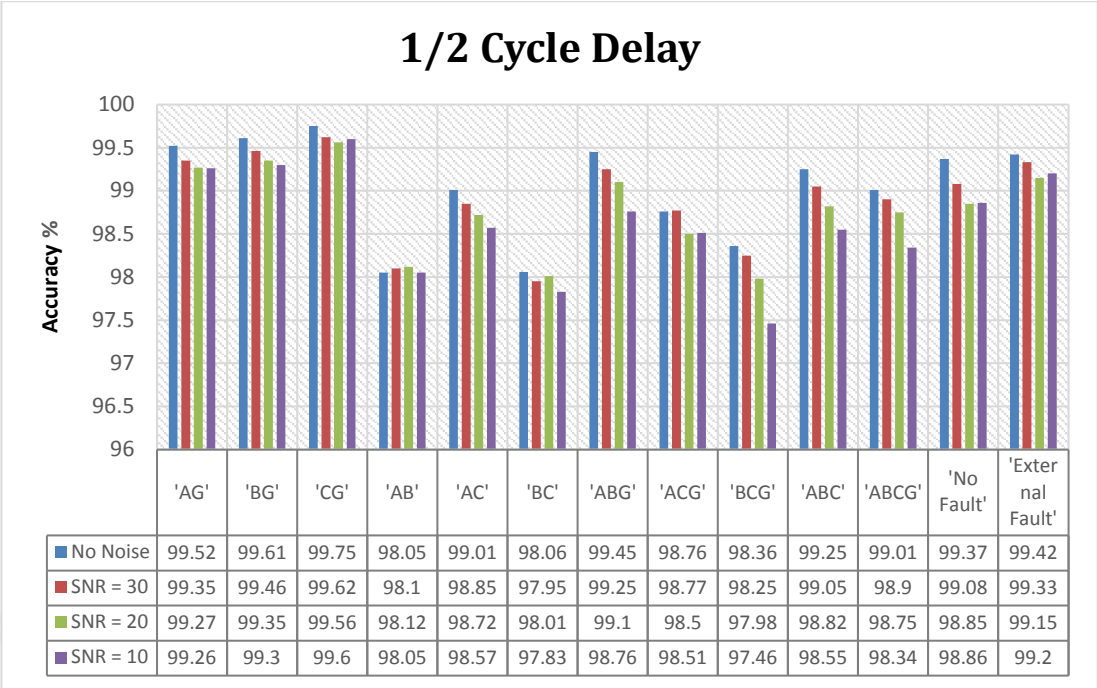

	'AG'	'BG'	'CG'	'AB'	'AC'	'BC'	'ABG'	'ACG'	'BCG'	'ABC'	'ABCG'	'No Fault'	'External Fault'
No Noise	99.52	99.61	99.75	98.05	99.01	98.06	99.45	98.76	98.36	99.25	99.01	99.37	99.42
SNR = 30	99.35	99.46	99.62	98.1	98.85	97.95	99.25	98.77	98.25	99.05	98.9	99.08	99.33
SNR = 20	99.27	99.35	99.56	98.12	98.72	98.01	99.1	98.5	97.98	98.82	98.75	98.85	99.15
SNR = 10	99.26	99.3	99.6	98.05	98.57	97.83	98.76	98.51	97.46	98.55	98.34	98.86	99.2

Figure 5.4 : Line 2, ½ Cycle Synchronization Delay.

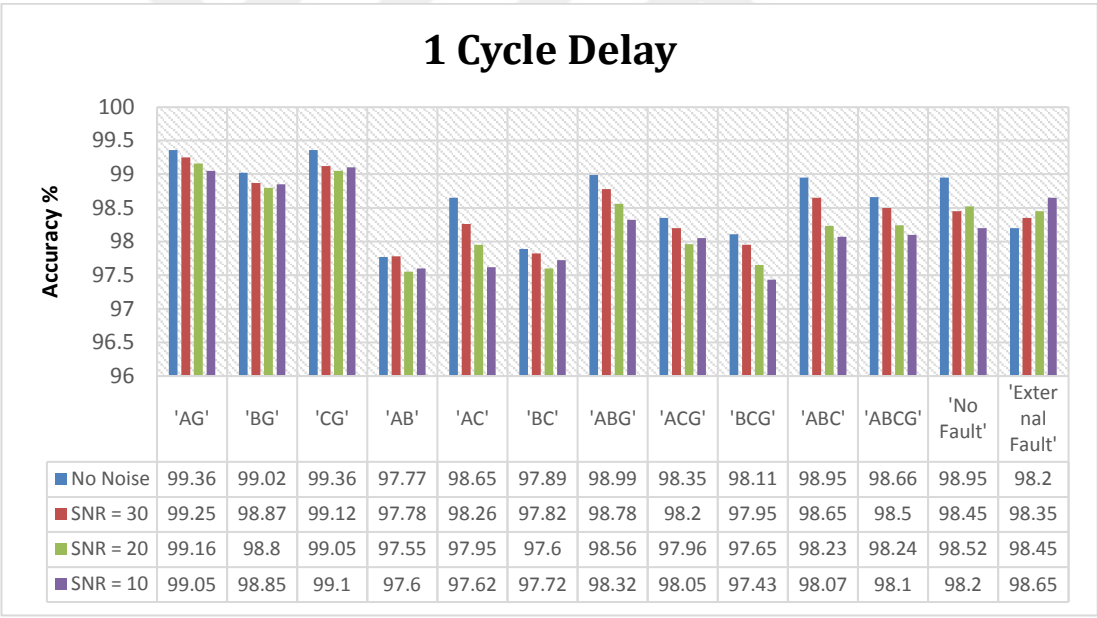

	'AG'	'BG'	'CG'	'AB'	'AC'	'BC'	'ABG'	'ACG'	'BCG'	'ABC'	'ABCG'	'No Fault'	'External Fault'
No Noise	99.36	99.02	99.36	97.77	98.65	97.89	98.99	98.35	98.11	98.95	98.66	98.95	98.2
SNR = 30	99.25	98.87	99.12	97.78	98.26	97.82	98.78	98.2	97.95	98.65	98.5	98.45	98.35
SNR = 20	99.16	98.8	99.05	97.55	97.95	97.6	98.56	97.96	97.65	98.23	98.24	98.52	98.45
SNR = 10	99.05	98.85	99.1	97.6	97.62	97.72	98.32	98.05	97.43	98.07	98.1	98.2	98.65

Figure 5.5 : Line 2, 1 Cycle Synchronization Delay.

The total performance of the all other lines is presented in Table 5.2 briefly. For various levels of noise penetration, the model appears to have an almost stable performance. In addition, the synchronization errors degrade the performance, to some extent, due to violation of other transient phenomena with into faulty scenarios boundaries. However, they are still suitable for practical purposes.

Table 5.2 : Test Microgrid Total Lines Accuracy

Line	Total Accuracy %		
	Signal without noise and delay	Noise penetrated Siganl	Signal Noise and Delay
Line No. 1	99.22	99.13	98.54
Line No. 2	99.24	99.09	98.61
Line No. 3	99.11	98.98	98.64
Line No. 4	99.12	99.04	98.48
Line No. 5	99.24	99.11	98.53

The simulation results are compare with other traditional and intelligence based methods in various studies in Table 5.3. In this table the traditional overcurrent and differential protection systems are testified in test microgrids. It is seen that due to dynamic behaviour of the MGs, they have a weak performance. In addition some of the strong methods may have have better performance compare to the proposed method in perfect signal. However, most of the do not tested in real world data with msclassified and noisy ones. According to these facts, it is seen that the proposed method is outperformed compare to traditional or convex optimation methods when face with real world data.

Table 5.3 : A Comparison of the Proposed Method with other Methods

Scheme	Accuracy %		
	Perfect signal	Signal with Noise	Signal with Synch. error
Proposed Method	99.2	99.05	98.55
Bagging [38]	93.47	--	--
WT-DT [40]	90.40	90.27	--
WT-KNN [40]	95.63	95.30	--
WT-SVM [40]	93.30	91.86	--
WT-NB [40]	94.24	93.63	--
WT-DNN [15]	97.92	97.69	
TT-DBN [41]	99.32	99.02	98.33
TT-SVM [41]	86.92	90.85	96.43
TT-DT [41]	87.83	91.34	95.24
TT-RF [41]	94.08	96.95	98.57
HHT-ELM [39]	93.68	--	--
HHT-SVM [39]	90.40	--	--
HHT-NB [39]	91.16	--	--
TKEO [72]	96.49	96.49	
CNN [42]	99.30	--	--
Overcurrent relay [32]	60.57	--	--
Differential relay [32]	81.57	--	--

6. ILLUSTRATION THE RESULTS AND SIGNAL PROCESSING DECOMPOSITION OF SOME CASE STUDIES

In this section, IMF decomposition for some fault scenarios and HHT for some of these IMFs are presented as an example for the test microgrid. The results are illustated for a variety of perfect signals and signals with noise and synchronization delay.

6.1 Case Study 1: A Two Phase to Ground Fault for Line 3

IMFS of EMD, VMD and EWT are available in Figure 6.1-4for double phase to ground fault up to 4 decomposition levels. The results are compared for a signal with no time difference at both ends of the line and a signal with a quarter cycle and time difference in SNR value of 10. The fault occurs at time t=0.1 seconds.

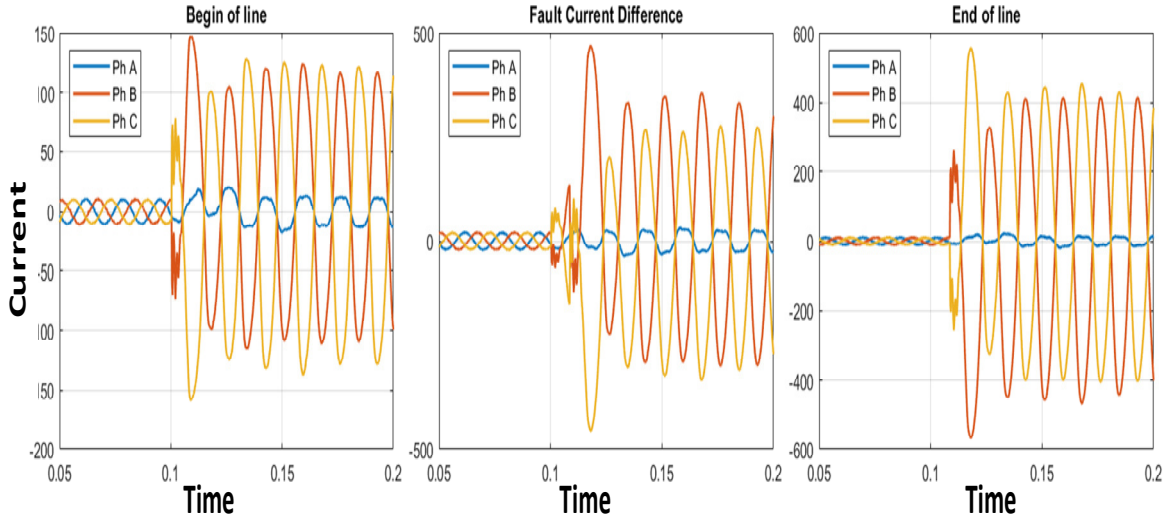

Figure 6.1 : Two Phase to Ground Fault at Line 3 and the Fault Current at Beginning and End of the Line and the Diffrential Fault Current. Fault Time = 0.1 sec SNR = 10 Delay= ¼ Cycle.

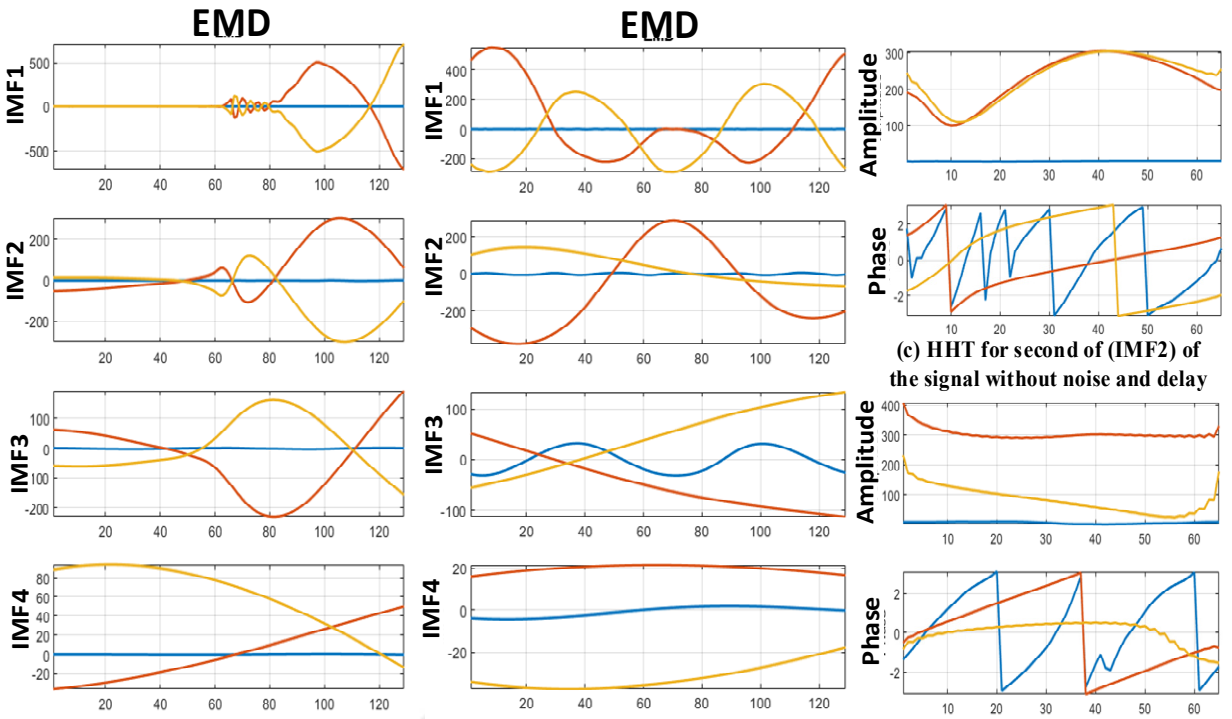

Figure 6.2 : IMFs for Empirical Mode Decomposition (EMD) and HHT of the Second IMFs for Both Signals with Noise and Delay and Wthout Noise and Delay.

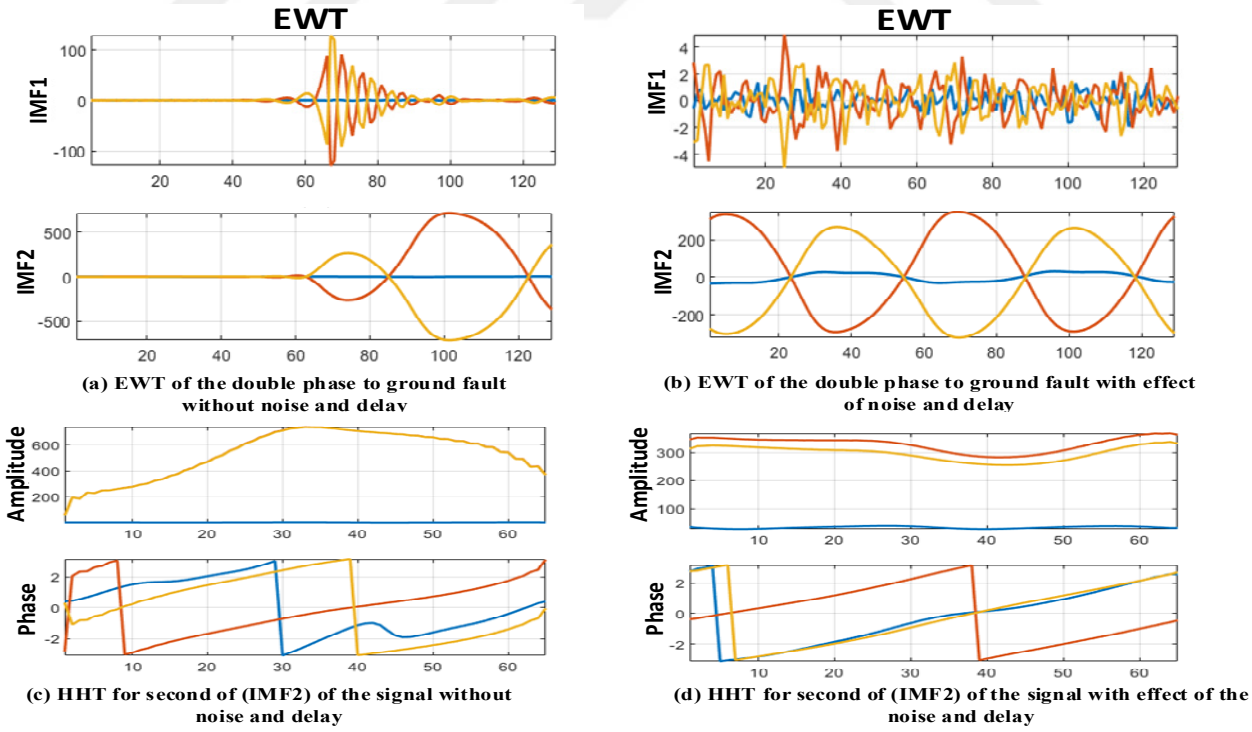

Figure 6.3 : Extracted IMFs of Empirical Wavelet Transform (EWT) for Perfect Signal and Signal with Noise and Delay and HHT of the IMF2 for Both Condition.

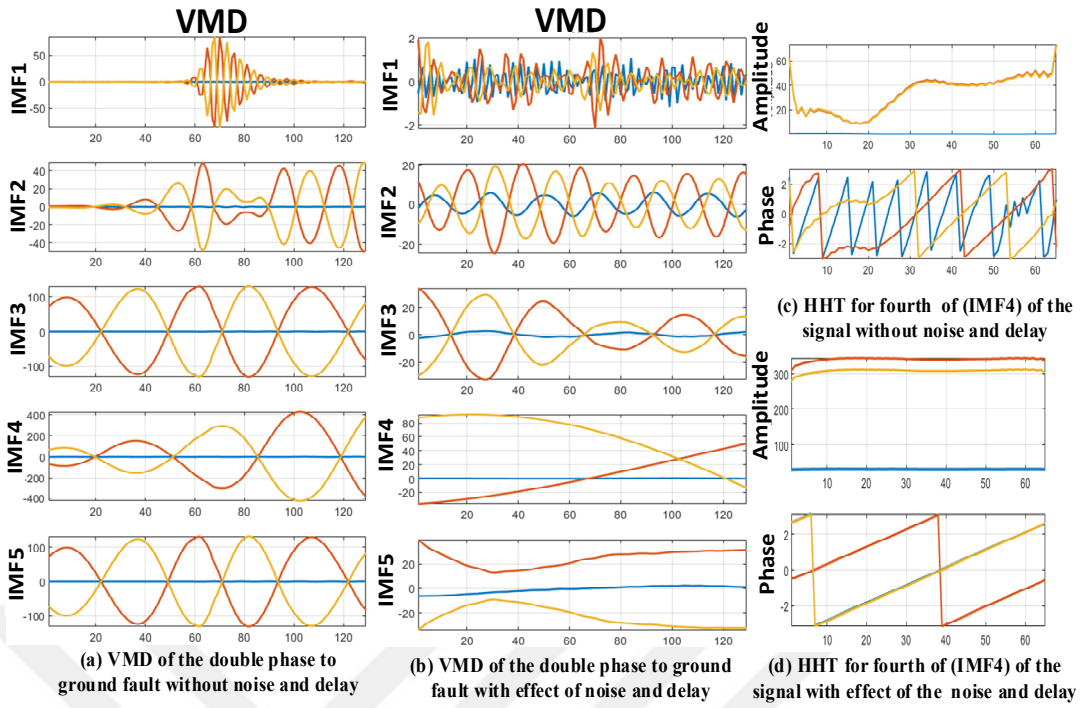

Figure 6.4 : Extracted IMFs of Variational Mode Decomposition (VMD) for Perfect Signal and Signal with Noise and Delay and HHT of the IMF4 for Both Condition.

6.2 Case Study 2: A Single Phase to Ground Fault in Line 4

In the following the results of the fault current level of the test microgrid in island mode with two different topologies is analyzed. The microgrid is operating at half load and in one scenario both switches S1 and S2 are open and in the other both are closed. The results of VMD and EMD are shown for both these conditions for signal without noise and delay and signal with SNR=20 and half cycle time delay. In Figure 6.5 results of the fault current level is depicted for this two types of topologies. It is seen when the fault current contribution is low due to inverter based DERs, there is a high risk of misclassification of sound phases as faulty phases. In additon the time delay make it difficult to detect one phase to ground fault (The fault resistance is 10 ohm).

In Figure 6.6 and Figure 6.7 the EMD and VMD for both swith close topology and for signal without noise and delay and signal with SNR=20 and half cycle time delay is depicted. As it is seen in EMD:

1- For EMD, the increase in the number of components in the faulty phase (Phase A) (5 in a noiseless and no-delay signal and 6 in signal with SNR=20 and half-cycle time) depends on the penetration level of delay and noise. This indicates the adaptability of the method of decomposing the signal.

2- When noise and delay are introduced into the signal, the intesity of some frequency components of the sound phases increase significantly. This leads to the risk of misclassification if the separation in the data area is not sufficient.

3- When the noise penetrated the in the EMD the components that detect fault are transferred to higher values (The lower components decompose the noise from other components).

4- When VMD results are compared with the EMD results the components of the faulty phase are more extensive. However some components for the sounds phase have larger amplitude compare to EMD for the sound phases.

5- The VMD left the high frequency components in the first three signal and compare to EMD it has less noisy component in the last low frequency components.

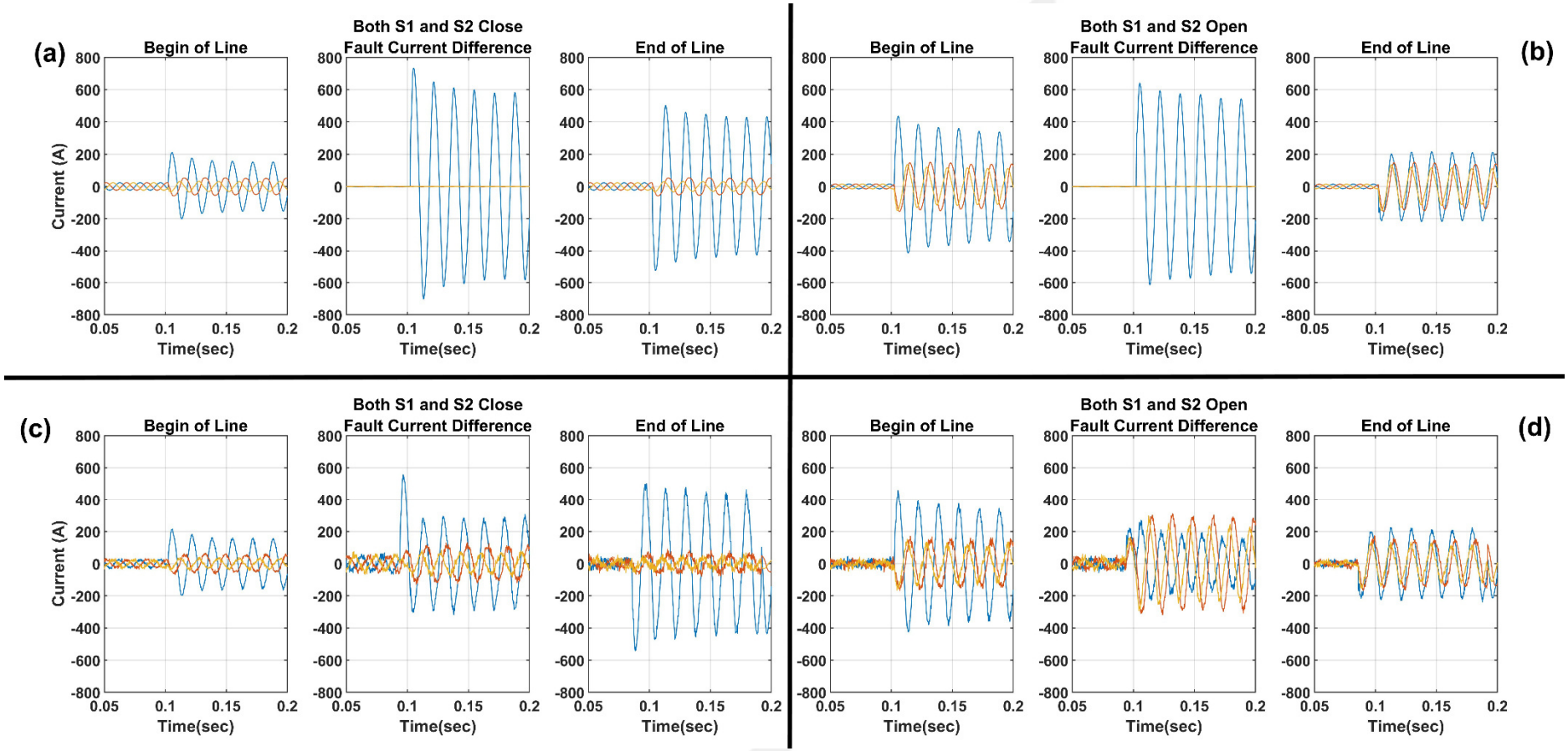

Figure 6.5 : Single Phase to Ground Fault on Line 4 (a) Both Swith Close and SNR=1, Delay = 0 (b) Both Switch Open and SNR = 1, Delay = 0 (c) Both Swith Close and SNR=20, Delay = ½ Cycle (d) Both Switch Open and SNR=20, Delay = ½ Cycle.

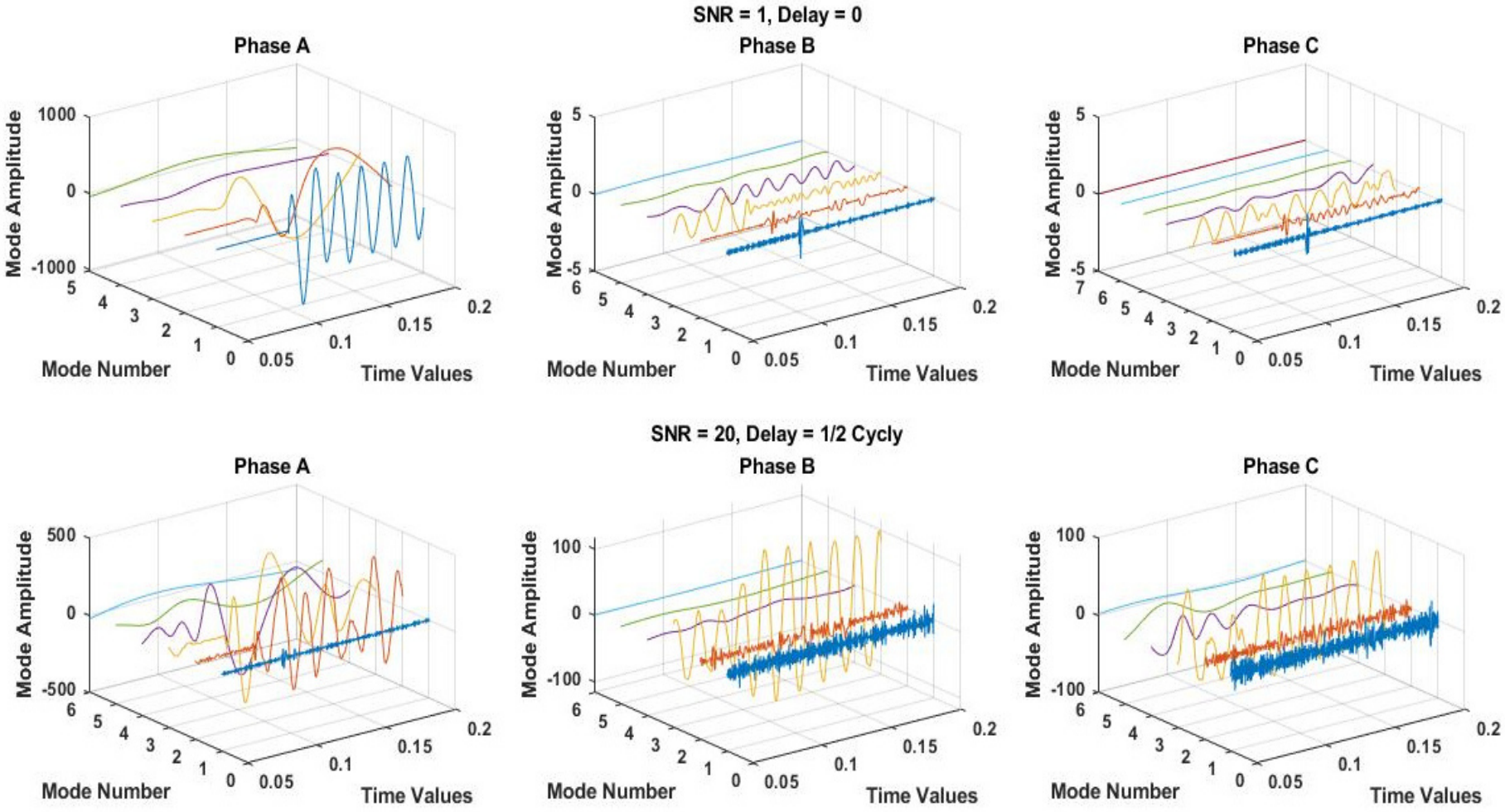

Figure 6.6 : EMD Decomposition for Both Switch Close Topology for Signal without Noise and Delay and Singal with SNR=20 and ½ Cycle Delay.

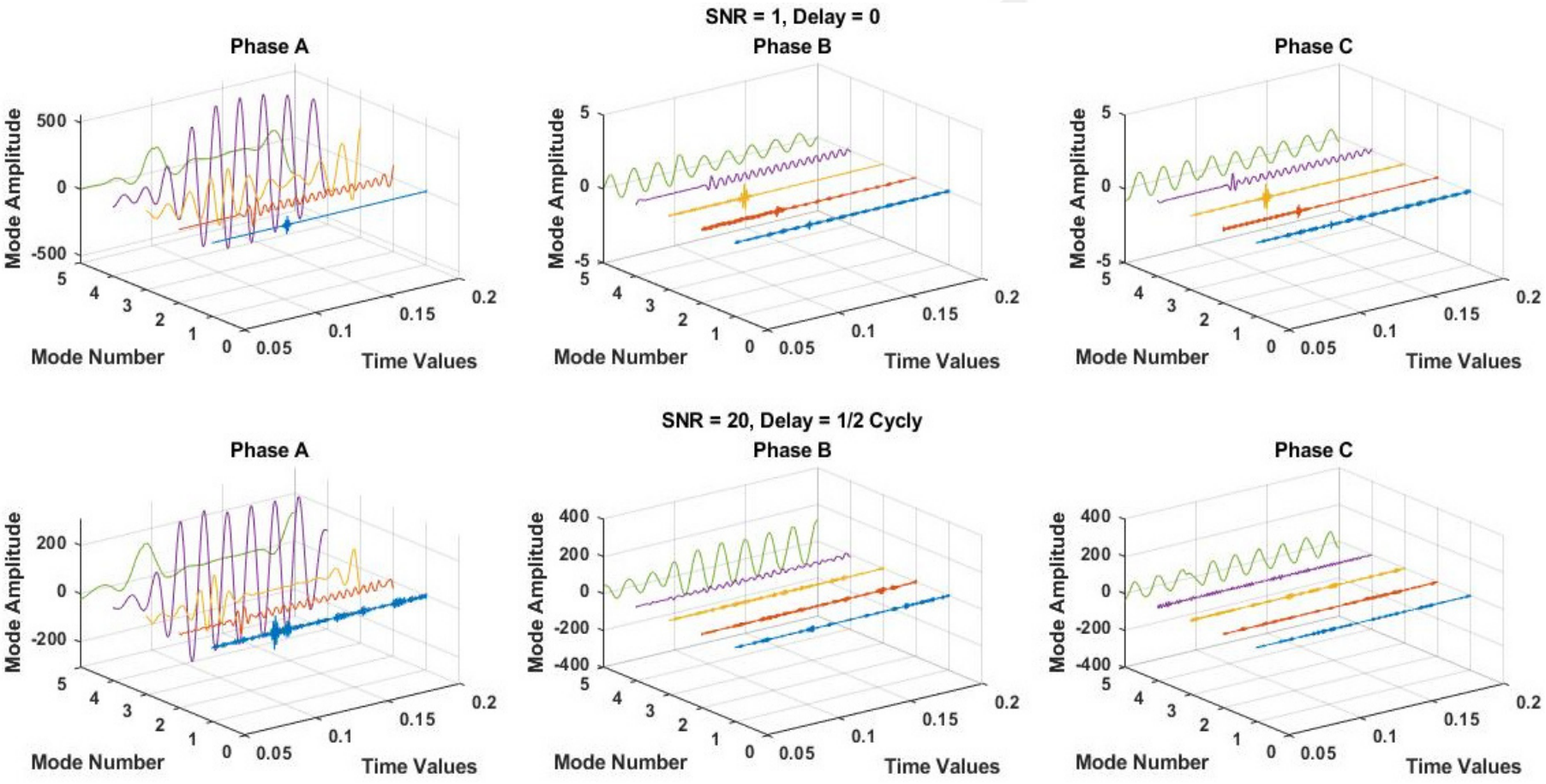

Figure 6.7 : VMD Decomposition for Both Switch Close Topology for Signal without Noise and Delay and Singal with SNR=20 and ½ Cycle Delay.

The EMD and VMD results of the both switch open topology are also shown in Figure 6.8 and Figure 6.9 respectively. The same can be argued for this topology. In addition, as can be seen from the differential current curve, it is difficult to distinguish between faulty and intact phases. However, when we examine the EMD curve, it is seen that the frequency components of the sound phases are lower than the faulty phase. When there is noise and delay in the VMD curve, the amplitude of the frequency components of the healthy phases is closer to the faulty phase. The only difference is that they have higher amplitude in various components.

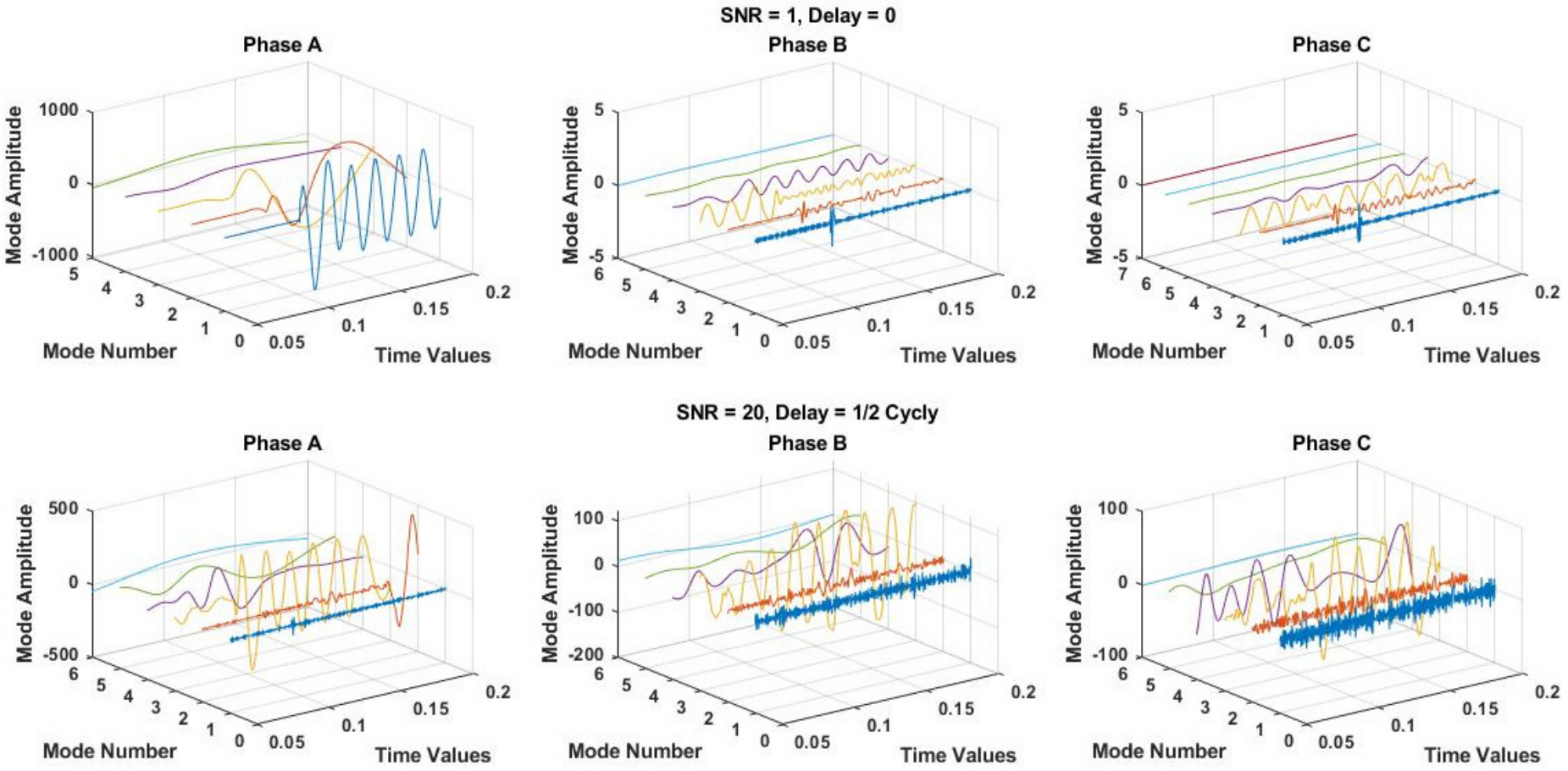

Figure 6.8 : EMD Decomposition for Both Switch Open Topology for Signal without Noise and Delay and Singal with SNR=20 and ½ Cycle Delay.

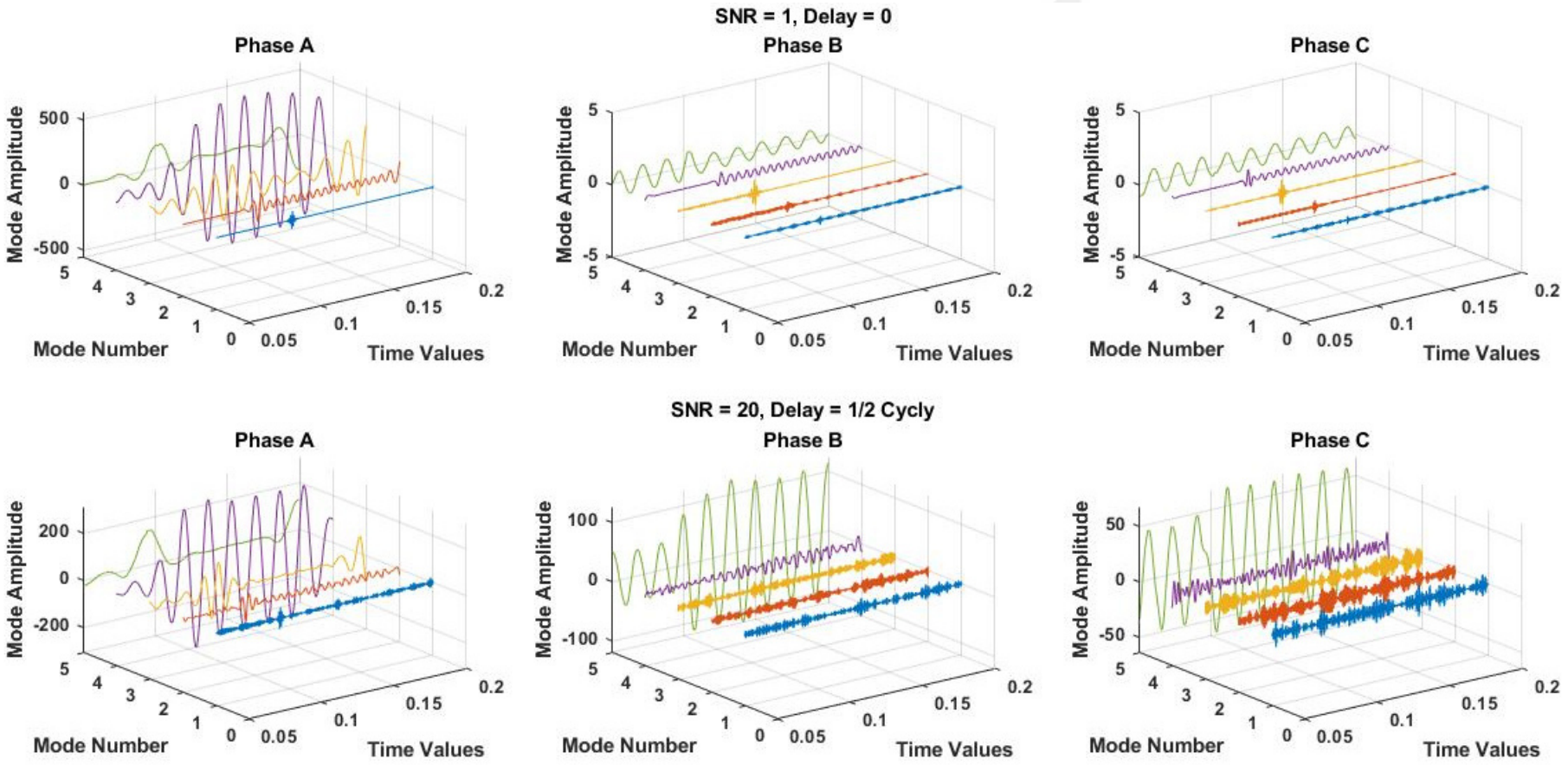

Figure 6.9 : VMD Decomposition for Both Switch Open Topology for Signal without Noise and Delay and Singal with SNR=20 and ½ Cycle Delay.

6.3 Case Study 3: A Three Phase to Ground Fault in Line 5

In this section the EWT results of a 3 phase to ground fault for system without delay and noise and sysyem with SNR = 30 and a quarter cycle delay is presented. The system is operating in min loading and the results belong to fault current level of the microgrid in islanded and grid connected mode. Here as it is seen with loading reduction the harmonic effects of inverters are more obvious in islanding mode.

The results of fault current level both these scenarios is presented in Figure 6.10. As it is seen the fault current level has increased significantly in grid connected mode compare to islanded mode. The EWT of islanded mode for perfect signal and signal with noise and delay is depicted in Figure 6.11. As it is seen the EWT is able to denoise the signal an attain the fault frequency components only after two level of the decomposition. However when the signal has noise and delay the IMFs amplitude is not zero. This amplitude can increase as the delay and noise increased. This in turn can lead misclassifaction of non-faulty signal as a fault. For grid-connected mode EWT according to Figure 6.12 the fault current level has larger components due to its higher contribution and thus the effect of the noise become negligible.

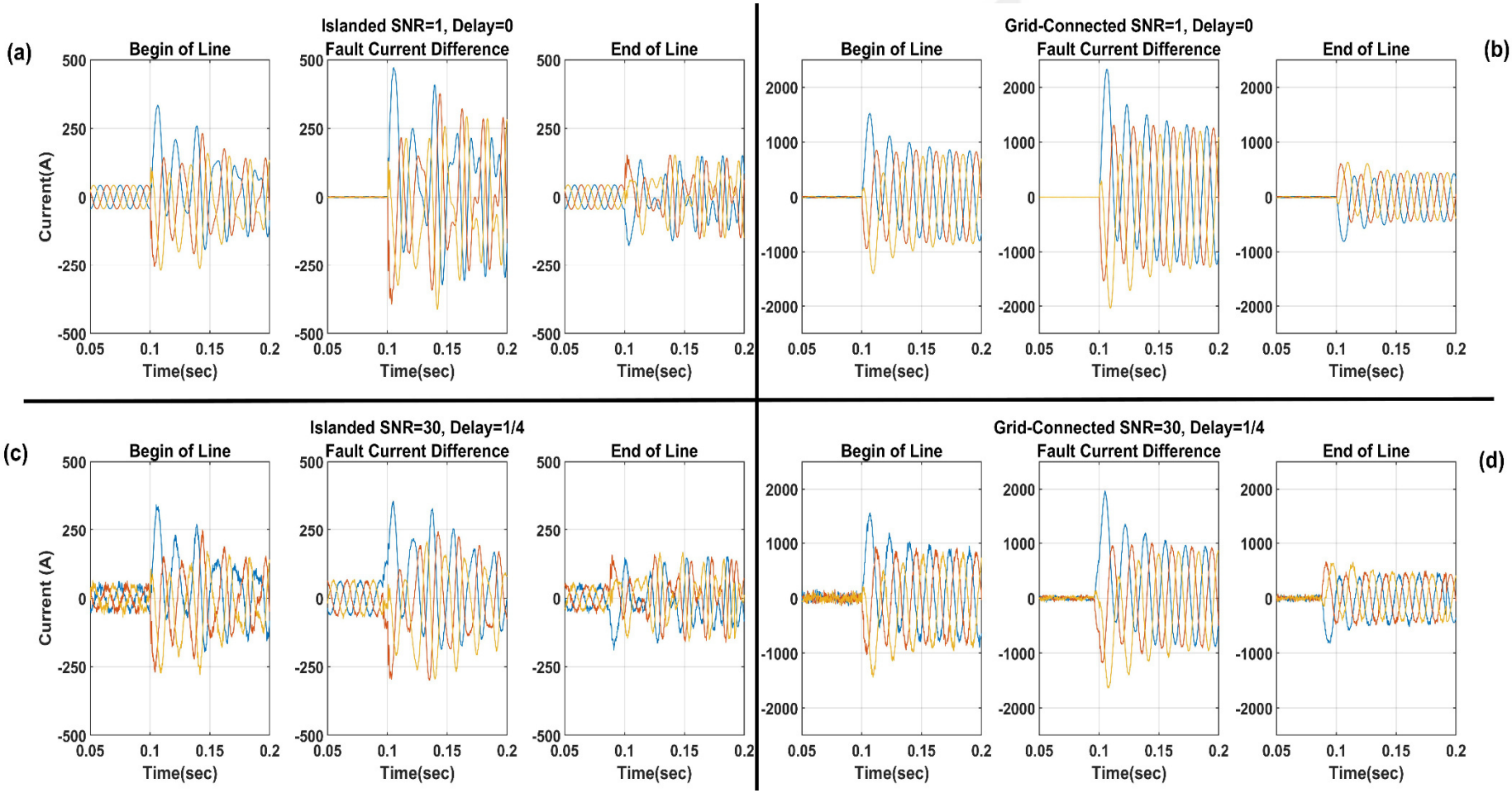

Figure 6.10 : 3 phase to Ground Fault on Line 5 (a) Islanded and SNR=1, Delay = 0 (b) Grid-Connected and SNR = 1, Delay = 0 (c) Islanded and SNR=30, Delay = ¼ Cycle (d) Grid-Connected and SNR=30, Delay = ¼ Cycle.

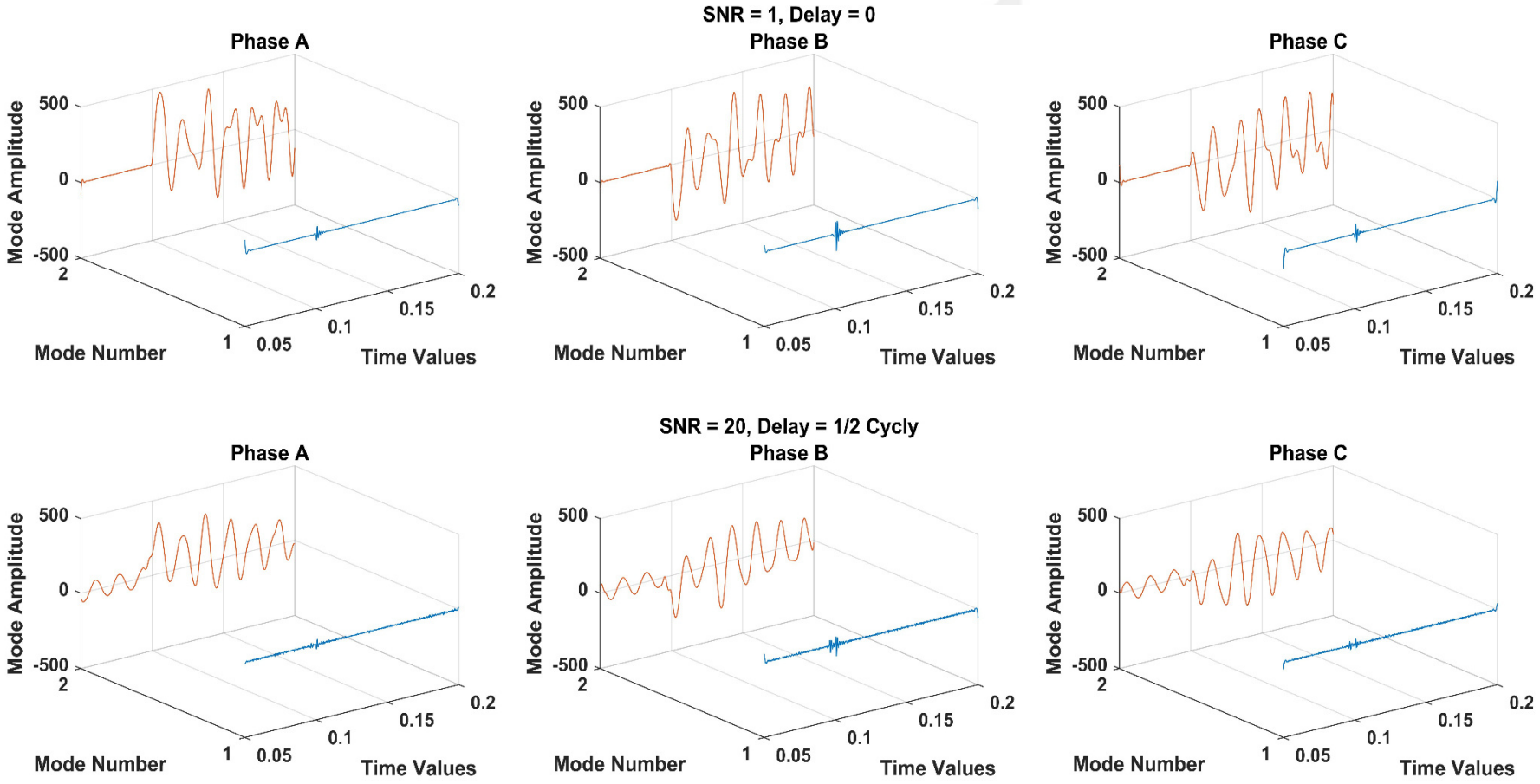

Figure 6.11 : EWT Decomposition for Islanded Mode Operation of the Microgrid for Signal with SNR=1 and Delay=0 and Signal with SNR =30 and ¼ Cycle Delay.

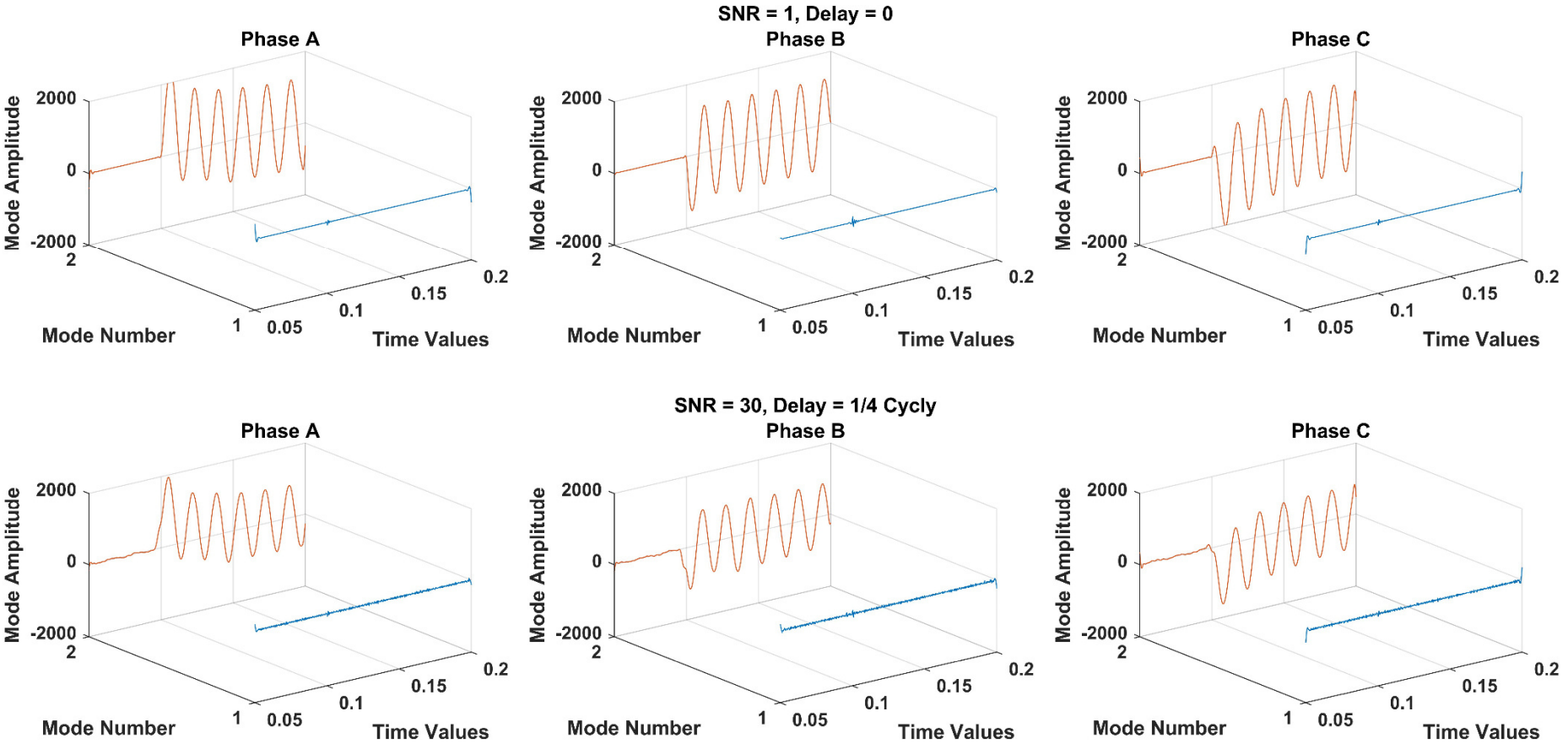

Figure 6.12 : EWT Decomposition for Grid-Connected Mode Operation of the Microgrid for Signal with SNR=1 and Delay=0 and Signal with SNR =30 and ¼ Cycle Delay.

Hilbert transform of the IMFs for islanded and grid-connected operation is presented in Figure 6.13 and Figure 6.14 respectively. It is seen the Hilbert transfrom have a better discrimination for detecting occurance of the fault even for the signal with noise and delay. The fault condition is also detectable for the first high frequency IMF amplitude in islanded mode. It is deduced that a HHT can have better discrimination even for a signal with noise and delay.

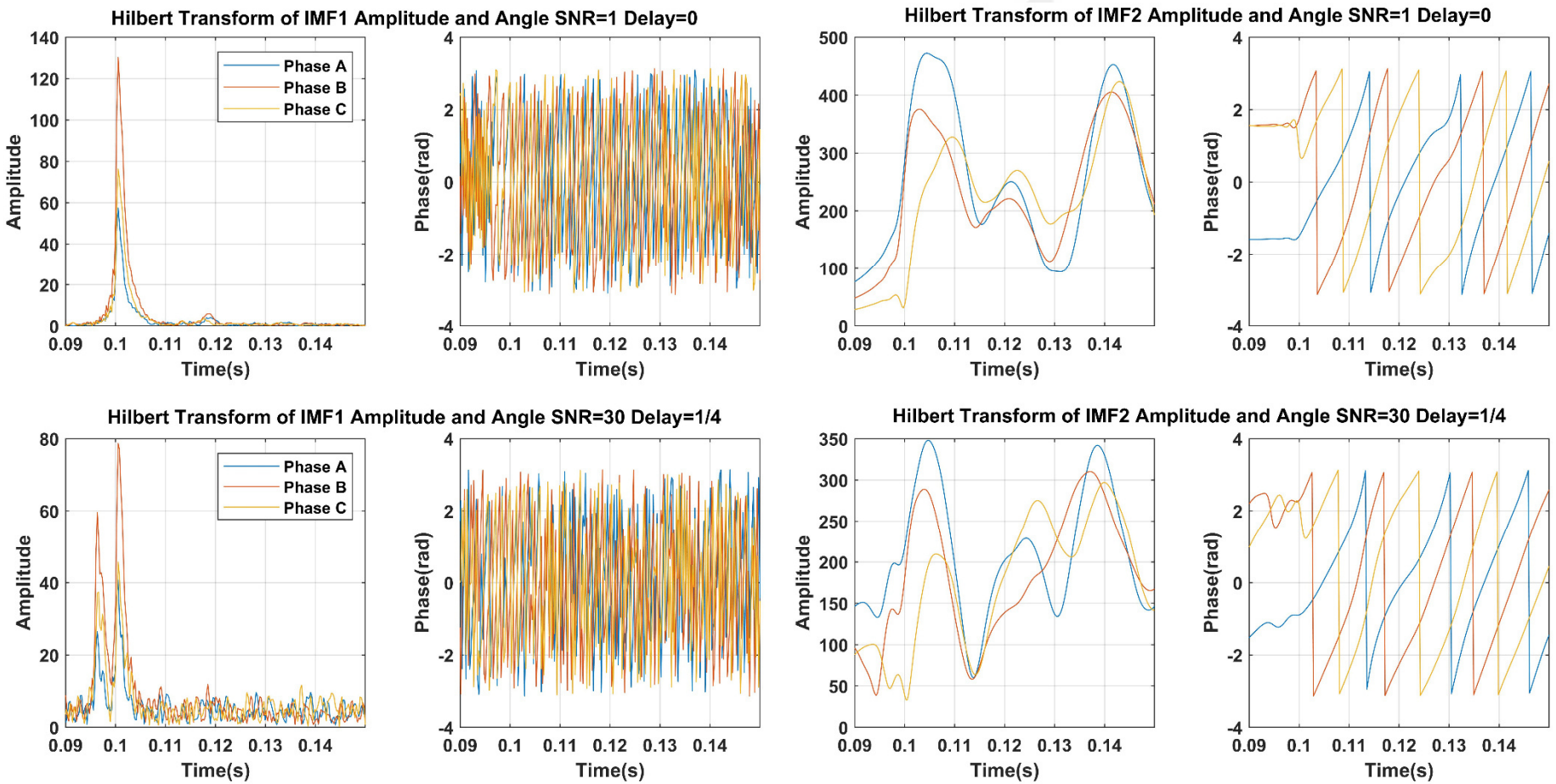

Figure 6.13 : Hilbert Transform of Islanding Mode Operation for EWT- Perfect Signal and Signal with SNR = 30 and Delay ¼ Cycle.

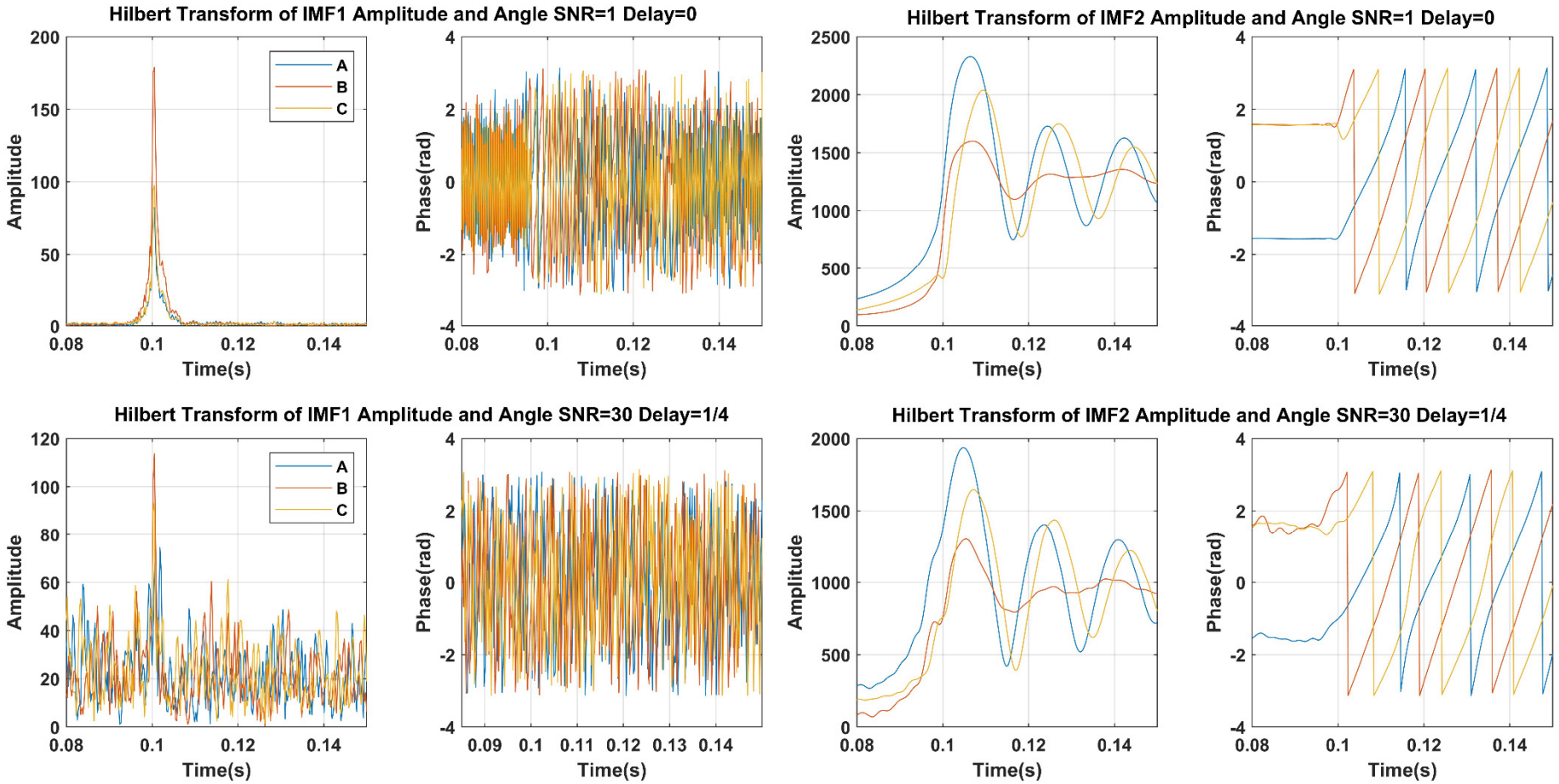

Figure 6.14 : Hilbert Transform of Grid-Connected Mode Operation for EWT- Perfect Signal and Signal with SNR = 30 and Delay ¼ Cycle.

7. CONCLUSIONS

A new intelligence-based method is used to deal with microgrid fault detection and classification. The proposed method is easy to program and tune. When trained on the data space, it's just a group decision tree with varying voting power. In this way, it has a very fast fault detection feature and it is easy to apply all kinds of protection relays. It is seen that it has a performance very close to the powerful classifier for synthetic perfect data as well as its simplicity. However, it has unique behavior against the real-world data challenge from measurement devices. There is usually a penetration level of noise in these data, and also there are always outliers in these data. Also, when the MGs operate in island mode and the loading of the network is low, harmonic distortion increases due to the switching frequencies of the inverters. When a traditional machine learning algorithm is trained with this data without removing these anomalies in the data, the risk of overfitting in training is high. There are tests that can detect and leave them out, but there is no guarantee of finding all of this violated data in the data space.

On the other hand, the proposed non-convex optimization-based Brownboost method is a margin-based adaptive method. Classifiers created in the data space not only have the minimum classification error, but also have the maximum discrimination between the data of each class. This feature allows the algorithm to make lower generalization errors to unseen new data. The adaptability feature of this classifier helps it to learn the data field step by step iteratively and try to correct its errors with each iteration. Finally, the non-convex optimization feature allows the algorithm to select or discard misclassified data in case of violation in another class domain or outliers due to malfunction of measuring devices. This unique feature makes it practical for real world purposes when compared to its predecessors or counterparts.

A collection of adaptive signal processing methods is used to transfer the raw data into three different data fields. They focused on the transient component of the signal rather than fault current level. Between these data spaces the one has less generalization error mean it is less sensitive to noise and outliers. This feature can be extracted an evaluated with the Brownboost margin criteria. A data space with a higher margin has higher

voting power. Therefore, the proposed method is more and applicable for real-world purposes. In order to have simulation results close to real world measurements the detail model with various control modes of the DERs and the frequency dependent line model is used.

When the performance of the proposed method is compared with other intelligence methods, it has close performance to them. Yet, some strong models outperms the model. This is because these models are strong and complex non-linear classifers. Ther are designed to deal with complex problems with huge amount of the data. On the other side our proposed model is the group of the linear model. This better performance seems natural for synthetic perfect data. Yet the proposed ensemble method has close performance to these strong models and classify the dataspace non-linearly and there is not a huge gap between accuracies.

One of the main disadvantages of the traditional differntial protection methods is their sensitivity to synchrnization dalay. The proposed traditional fault detection method is insufficient to have suitable performance as the delay increases. However, in the proposed method three type of the adaptive time-frequency method (EMD-HHT, EWT-HHT, VMD-HHT) are very effective to process data and helps the decsion making even during delays. Accordingly, when compare the results, the proposed method is also robust to synchronization delays and the accuray have not much deviation.

The other benefit of this method is ability the discriminate the external faults from the internal ones. Unlike the tradtional differential protection, this peculiarity helps to construct a backup protection of the same type for the system. In addition, the MGs are generally established in distribution system where the length of the line are shorter compare to transmission system. Thus, it is also possible to establish a proper backup communication links for the model. One other point is all processing and decision making is done locally and autonoumuosly by the devices protected the line or the area. There is no need to establish a central decision-making system. Therefore, is it possible to expand the result for large scale systems.

As a result, the porposed method is independent from fault current level, flexible enough for microgrids dynamic behaviour, fast, secure, easy to implement and robust to traditional machine learninig main concern overfitting.

7.1 Future Works

One of the reasons differential fault currents is used at both ends of the line helps to distinguish between external and internal faults in the system. This feature is applicable to create a backup protection for the proposed method, which will be examined in future studies. As shown in Figure 7.1, line 2 is selected for a backup protection on line 1 and the current difference between the beginning of line 2 and the end of line 1 is measured (R21-R12). Therefore, backup protection covers two lines 1 and line 2. If a fault F1 occurs on line 1, R11 and R12 are considered as main protection and for an internal fault that should trip in first priority. On the other hand, this fault is also considered an internal fault for R21 and R12. However, this is a backup protection and after a predefined delay time a trip signal must be issued if the fault is not cleared. In addition, if the fault occurred at point F3, at least one of R21-R12 or R11-R12 considers this fault as an external fault. Therefore, this combination should not give a trip signal. For a fault condition in F3, the main and backup protection must detect it.

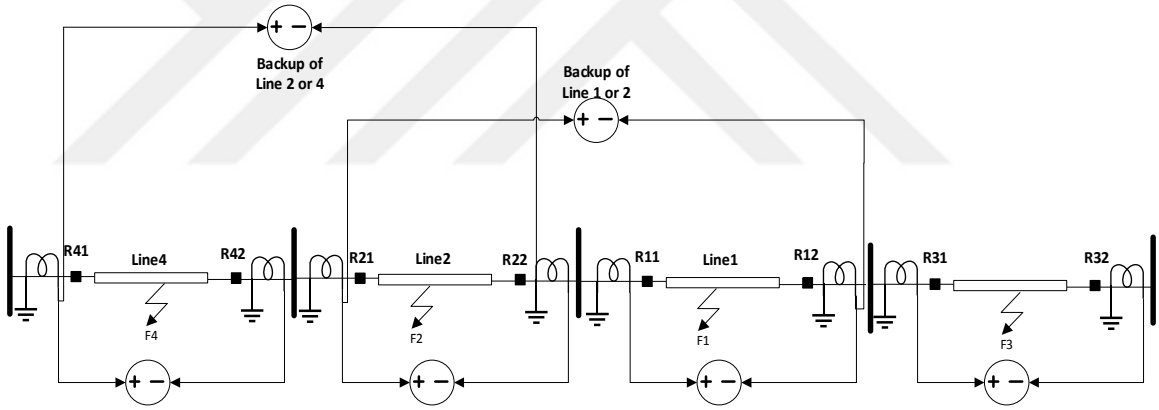

Figure 7.1 : Suggested Backup Protection Scheme.

Another point that is planned to be investigated in future studies is the applicability of the proposed method to high impedance faults. This is another type of fault that is a critical concern for distribution networks. They have the potential to be a serious challenge for MGs. It has completely different behavior in power system operation and it has different model. This study will also being evaluated for future studies.

REFERENCES

[1] **Casagrande, E., Woon, W. L., Zeineldin, H. H., Kan, N. H., apos, & an**. (2013). Data mining approach to fault detection for isolated inverter-based microgrids. *IET Generation, Transmission &Distribution, 7*(7), 745-754. https://digital-library.theiet.org/content/journals/10.1049/iet-gtd.2012.0518

[2] **Singh, J., Prakash Singh, S., Shanker Verma, K., Iqbal, A., & Kumar, B.** (2021). Recent control techniques and management of AC microgrids: A critical review on issues, strategies, and future trends. *International Transactions on Electrical Energy Systems, 31*(11), e13035. doi:https://doi.org/10.1002/2050-7038.13035

[3] **Bullich-Massagué, E., Díaz-González, F., Aragüés-Peñalba, M., Girbau-Llistuella, F., Olivella-Rosell, P., & Sumper, A.** (2018). Microgrid clustering architectures. *Applied Energy, 212*, 340-361. doi:https://doi.org/10.1016/j.apenergy.2017.12.048

[4] **Bandeiras, F., Pinheiro, E., Gomes, M., Coelho, P., & Fernandes, J.** (2020). Review of the cooperation and operation of microgrid clusters. *Renewable and Sustainable Energy Reviews, 133*, 110311. doi:https://doi.org/10.1016/j.rser.2020.110311

[5] **Mazidi, M., Rezaei, N., Ardakani, F. J., Mohiti, M., & Guerrero, J. M.** (2020). A hierarchical energy management system for islanded multi-microgrid clusters considering frequency security constraints. *International Journal of Electrical Power & Energy Systems, 121*, 106134. doi:https://doi.org/10.1016/j.ijepes.2020.106134

[6] **Liu, Y., Meliopoulos, A. P., Sun, L., & Choi, S.** (2018). Protection and control of microgrids using dynamic state estimation. *Protection and Control of Modern Power Systems, 3*(1), 31. doi:10.1186/s41601-018-0104-2

[7] **Palizban, O., & Kauhaniemi, K.** (2015). Hierarchical control structure in microgrids with distributed generation: Island and grid-connected mode. *Renewable and Sustainable Energy Reviews, 44*, 797-813. doi:https://doi.org/10.1016/j.rser.2015.01.008

[8] **Mohamed, A. A., Elsayed, A. T., Youssef, T. A., & Mohammed, O. A.** (2017). Hierarchical control for DC microgrid clusters with high penetration of distributed energy resources. *Electric Power Systems Research, 148*, 210-219. doi:https://doi.org/10.1016/j.epsr.2017.04.003

[9] **Zhou, X., Zhou, L., Chen, Y., Guerrero, J. M., Luo, A., Wu, W., & Yang, L.** (2018). A microgrid cluster structure and its autonomous coordination control strategy. *International Journal of Electrical Power & Energy Systems, 100*, 69-80. doi:https://doi.org/10.1016/j.ijepes.2018.02.031

[10] **Zheng, D., Zhang, W., Netsanet Alemu, S., Wang, P., Bitew, G. T., Wei, D., & Yue, J.** (2021). Chapter 6 - Protection of microgrids. In D. Zheng, W. Zhang, S. Netsanet Alemu, P. Wang, G. T. Bitew, D. Wei, & J. Yue (Eds.), *Microgrid Protection and Control* (pp. 121-168): Academic Press.

[11] **Beheshtaein, S., Cuzner, R. M., Forouzesh, M., Savaghebi, M., & Guerrero, J. M.** (2019). DC Microgrid Protection: A Comprehensive Review. *IEEE Journal of Emerging and Selected Topics in Power Electronics*, 1-1. doi:10.1109/JESTPE.2019.2904588

[12] **Manditereza, P. T., & Bansal, R. C.** (2020). Protection of microgrids using voltage-based power differential and sensitivity analysis. *International Journal of Electrical Power & Energy Systems, 118*, 105756-105756. doi:https://doi.org/10.1016/j.ijepes.2019.105756

[13] **Bukhari, S. B. A., Kim, C.-H., Mehmood, K. K., Haider, R., & Saeed Uz Zaman, M.** (2020). Convolutional Neural Network-Based Intelligent Protection Strategy for Microgrids. *14*(7), 1177-1185. doi:https://doi.org/10.1049/iet-gtd.2018.7049

[14] **Mishra, M., & Rout, P. K.** (2018). Detection and classification of micro-grid faults based on HHT and machine learning techniques. *12*(2), 388-397. doi:https://doi.org/10.1049/iet-gtd.2017.0502

[15] **Yu, J. J. Q., Hou, Y., Lam, A. Y. S., & Li, V. O. K.** (2019). Intelligent Fault Detection Scheme for Microgrids With Wavelet-Based Deep Neural Networks. *IEEE Transactions on Smart Grid, 10*(2), 1694-1703. doi:10.1109/TSG.2017.2776310

[16] Hardware Solutions for LVRT. (2011). In *Doubly Fed Induction Machine* (pp. 479-499).

[17] **Mumtaz, F., & Bayram, I. S.** (2017). Planning, Operation, and Protection of Microgrids: An Overview. *Energy Procedia, 107*, 94-100. doi:https://doi.org/10.1016/j.egypro.2016.12.137

[18] **Soleimanisardoo, A., Karegar, H. K., & Zeineldin, H. H.** (2019). Differential Frequency Protection Scheme Based on Off-Nominal Frequency Injections for Inverter-Based Islanded Microgrids. *IEEE Transactions on Smart Grid, 10*(2), 2107-2114. doi:10.1109/TSG.2017.2788851

[19] **Yılmaz, A., & Bayrak, G.** (2019). A real-time UWT-based intelligent fault detection method for PV-based microgrids. *Electric Power Systems Research, 177*, 105984-105984. doi:https://doi.org/10.1016/j.epsr.2019.105984

[20] **Liang, Z., Mu, L., Zhang, F., Zhou, H., & Zhang, X.** (2019). The fault detection method of islanded microgrid with the V/f controlled distributed generation. *International Journal of Electrical Power & Energy Systems, 112*, 28-35. doi:https://doi.org/10.1016/j.ijepes.2019.04.030

[21] **Mahfouz, M. M. A.** (2020). A protection scheme for multi-distributed smart microgrid based on auto-cosine similarity of feeders current patterns. *Electric Power Systems Research, 186*, 106405. doi:https://doi.org/10.1016/j.epsr.2020.106405

[22] **Singh, M., & Basak, P.** (2019). Adaptive protection methodology in microgrid for fault location and nature detection using q0 components of fault current. *IET Generation, Transmission & Distribution, 13*(6), 760-769. doi:10.1049/iet-gtd.2018.6347

[23] **Beheshtaein, S., Cuzner, R., Savaghebi, M., & Guerrero, J. M.** (2019). Review on microgrids protection. *IET Generation, Transmission & Distribution, 13*(6), 743-759. doi:10.1049/iet-gtd.2018.5212

[24] **Barra, P. H. A., Coury, D. V., & Fernandes, R. A. S.** (2020). A survey on adaptive protection of microgrids and distribution systems with distributed generators. *Renewable and Sustainable Energy Reviews, 118*, 109524-109524. doi:https://doi.org/10.1016/j.rser.2019.109524

[25] **Gush, T., Bukhari, S. B. A., Haider, R., Admasie, S., Oh, Y.-S., Cho, G.-J., & Kim, C.-H.** (2018). Fault detection and location in a microgrid using mathematical morphology and recursive least square methods. *International Journal of Electrical Power & Energy Systems, 102*, 324-331. doi:https://doi.org/10.1016/j.ijepes.2018.04.009

[26] **Dharmapandit, O., Patnaik, R. K., & Dash, P. K.** (2017). A fast time-frequency response based differential spectral energy protection of AC microgrids including fault location. *Protection and Control of Modern Power Systems, 2*(1), 30-30. doi:10.1186/s41601-017-0062-0

[27] **Maali Amiri, E., & Vahidi, B.** (2020). Integrated protection scheme for both operation modes of microgrid using S-Transform. *International Journal of Electrical Power & Energy Systems, 121*, 106051-106051. doi:https://doi.org/10.1016/j.ijepes.2020.106051

[28] **Kar, S., & Samantaray, S. R.** (2014). Time-frequency transform-based differential scheme for microgrid protection. *IET Generation, Transmission & Distribution, 8*(2), 310-320. doi:10.1049/iet-gtd.2013.0180

[29] **Gururani, A., Mohanty, S. R., & Mohanta, J. C.** (2016). Microgrid protection using Hilbert–Huang transform based-differential scheme. *IET Generation, Transmission & Distribution, 10*(15), 3707-3716. doi:10.1049/iet-gtd.2015.1563

[30] **Escudero, R., Noel, J., Elizondo, J., & Kirtley, J.** (2017). Microgrid fault detection based on wavelet transformation and Park's vector approach. *Electric Power Systems Research, 152*, 401-410. doi:https://doi.org/10.1016/j.epsr.2017.07.028

[31] **Guillen, D., Paternina, M. R. A., Zamora, A., Ramirez, J. M., & Idarraga, G.** (2015). Detection and classification of faults in transmission lines using the maximum wavelet singular value and Euclidean norm. *IET Generation, Transmission & Distribution, 9*(15), 2294-2302. doi:10.1049/iet-gtd.2014.1064

[32] **Gashteroodkhani, O. A., Majidi, M., Fadali, M. S., Etezadi-Amoli, M., & Maali-Amiri, E.** (2019). A protection scheme for microgrids using time-time matrix z-score vector. *International Journal of Electrical Power & Energy Systems, 110*, 400-410. doi:https://doi.org/10.1016/j.ijepes.2019.03.040

[33] **Kar, S., & Samantaray, S. R.** (2014, 28-30 May 2014). *Combined S-transform and data-mining based intelligent micro-grid protection scheme.* Paper presented at the 2014 Students Conference on Engineering and Systems.

[34] **Hooshyar, A., El-Saadany, E. F., & Sanaye-Pasand, M.** (2016). Fault Type Classification in Microgrids Including Photovoltaic DGs. *IEEE Transactions on Smart Grid, 7*(5), 2218-2229. doi:10.1109/TSG.2015.2451675

[35] **Mishra, D. P., Samantaray, S. R., & Joos, G.** (2016). A Combined Wavelet and Data-Mining Based Intelligent Protection Scheme for Microgrid. *IEEE Transactions on Smart Grid, 7*(5), 2295-2304. doi:10.1109/TSG.2015.2487501

[36] **Abdelgayed, T., Morsi, W., & Sidhu, T.** (2017). A New Approach for Fault Classification in Microgrids Using Optimal Wavelet Functions Matching Pursuit. *IEEE Transactions on Smart Grid*, 1-1. doi:10.1109/TSG.2017.2672881

[37] **Lin, H., Sun, K., Tan, Z., Liu, C., Guerrero, J. M., & Vasquez, J. C.** (2019). Adaptive protection combined with machine learning for microgrids. *IET Generation, Transmission Distribution, 13*(6), 770-779. doi:10.1049/iet-gtd.2018.6230

[38] **Netsanet, S., Zhang, J., & Zheng, D.** (2018). Bagged Decision Trees Based Scheme of Microgrid Protection Using Windowed Fast Fourier and Wavelet Transforms. *Electronics, 7*(5), 61-61. doi:10.3390/electronics7050061

[39] **Mishra, M., & Rout, P. K.** (2018). Detection and classification of micro-grid faults based on HHT and machine learning techniques. *IET Generation, Transmission & Distribution, 12*(2), 388-397. doi:10.1049/iet-gtd.2017.0502

[40] **Abdelgayed, T. S., Morsi, W. G., & Sidhu, T. S.** (2018). A New Approach for Fault Classification in Microgrids Using Optimal Wavelet Functions Matching Pursuit. *IEEE Transactions on Smart Grid, 9*(5), 4838-4846. doi:10.1109/TSG.2017.2672881

[41] **Gashteroodkhani, O. A., Majidi, M., & Etezadi-Amoli, M.** (2020). A combined deep belief network and time-time transform based intelligent protection Scheme for microgrids. *Electric Power Systems Research, 182*, 106239-106239. doi:https://doi.org/10.1016/j.epsr.2020.106239

[42] **Bukhari, S. B. A., Kim, C., Mehmood, K. K., Haider, R., & Saeed Uz Zaman, M.** (2020). Convolutional Neural Network-Based Intelligent Protection Strategy for Microgrids. *IET Generation, Transmission Distribution, 14*(7), 1177-1185. doi:10.1049/iet-gtd.2018.7049

[43] **Schapire, R., & Freund, Y.** (2012). *Boosting: Foundations and Algorithms*: The MIT Press.

[44] **Freund, Y.** (2001). An Adaptive Version of the Boost by Majority Algorithm. *Machine Learning, 43*(3), 293-318. doi:10.1023/A:1010852229904

[45] **Debnath, L., & Shah, F. A.** (2015). The Wavelet Transforms and Their Basic Properties. In L. Debnath & F. A. Shah (Eds.), *Wavelet Transforms and Their Applications* (pp. 337-373). Boston, MA: Birkhäuser Boston.

[46] **Gush, T., Bukhari, S. B. A., Mehmood, K. K., Admasie, S., Kim, J.-S., & Kim, C.-H.** (2019). Intelligent Fault Classification and Location Identification Method for Microgrids Using Discrete Orthonormal Stockwell Transform-Based Optimized Multi-Kernel Extreme Learning Machine. *12*(23), 4504.

[47] **Dragomiretskiy, K., & Zosso, D.** (2014). Variational Mode Decomposition. *IEEE Transactions on Signal Processing, 62*(3), 531-544. doi:10.1109/TSP.2013.2288675

[48] **Gilles, J.** (2013). Empirical Wavelet Transform. *IEEE Transactions on Signal Processing, 61*(16), 3999-4010. doi:10.1109/TSP.2013.2265222

[49] **Freund, Y., & Schapire, R. E.** (1997). A Decision-Theoretic Generalization of On-Line Learning and an Application to Boosting. *Journal of Computer and System Sciences, 55*(1), 119-139. doi:https://doi.org/10.1006/jcss.1997.1504

[50] **Schapire, R. E., & Singer, Y.** (1999). Improved Boosting Algorithms Using Confidence-rated Predictions. *Machine Learning, 37*(3), 297-336. doi:10.1023/a:1007614523901

[51] **Friedman, J. J. A. o. S.** (2001). Greedy function approximation: A gradient boosting machine. *29*, 1189-1232.

[52] **Azizi, R., & Noroozian, R.** (2021). Islanding detection in distributed energy resources based on gradient boosting algorithm. *15*(2), 436-451. doi:https://doi.org/10.1049/rpg2.12040

[53] **Breiman, L.** (1996). Bagging Predictors. *Machine Learning, 24*(2), 123-140. doi:10.1023/A:1018054314350

[54] **Du, W., Tuffner, F. K., Schneider, K. P., Lasseter, R. H., Xie, J., Chen, Z., & Bhattarai, B.** (2021). Modeling of Grid-Forming and Grid-Following Inverters for Dynamic Simulation of Large-Scale Distribution Systems. *IEEE Transactions on Power Delivery, 36*(4), 2035-2045. doi:10.1109/TPWRD.2020.3018647

[55] **Han, J., Bieber, L., Zhang, Y., Wang, L., Li, W., & Belanger, J.** (2020). Detailed Equivalent and Average Value Models of Hybrid Cascaded Multilevel Converters for Efficient and Accurate EMT-Type Simulation. *IEEE Transactions on Power Delivery, 35*(6), 2951-2962. doi:10.1109/TPWRD.2020.3002237

[56] **Biain, G., & Arocena, A. d. M.** (2019). *Mathematical Model Equations in Stationary Reference Frame of Current Controls for Grid-Connected Converters*.

[57] **Hlaili, M., & Mechergui, H.** (2016). Comparison of Different MPPT Algorithms with a Proposed One Using a Power Estimator for Grid Connected PV Systems. *International Journal of Photoenergy, 2016*, 1728398. doi:10.1155/2016/1728398

[58] **Podder, A. K., Roy, N. K., & Pota, H. R.** (2019). MPPT methods for solar PV systems: a critical review based on tracking nature. *13*(10), 1615-1632. doi:https://doi.org/10.1049/iet-rpg.2018.5946

[59] **Qoria, T., Gruson, F., Colas, F., Kestelyn, X., & Guillaud, X.** (2020). Current limiting algorithms and transient stability analysis of grid-forming VSCs. *Electric Power Systems Research, 189*, 106726. doi:https://doi.org/10.1016/j.epsr.2020.106726

[60] **Rathnayake, D. B., Akrami, M., Phurailatpam, C., Me, S. P., Hadavi, S., Jayasinghe, G., . . . Bahrani, B.** (2021). Grid Forming Inverter Modeling, Control, and Applications. *IEEE Access, 9*, 114781-114807. doi:10.1109/ACCESS.2021.3104617

[61] **Wang, J., Pratt, A., & Baggu, M.** (2019, 4-8 Aug. 2019). *Integrated Synchronization Control of Grid-Forming Inverters for Smooth Microgrid Transition.* Paper presented at the 2019 IEEE Power & Energy Society General Meeting (PESGM).

[62] **Milicua, A., & Abad, G.** (2016). Control of grid-connected converters. In *Power Electronics and Electric Drives for Traction Applications* (pp. 148-220).

[63] Basics of Wind Energy Conversion Systems (Wecs). (2017). In *Model Predictive Control of Wind Energy Conversion Systems* (pp. 1-60).

[64] Introduction to A Wind Energy Generation System. (2011). In *Doubly Fed Induction Machine* (pp. 1-85).

[65] **Abad, G., & Iwanski, G.** (2014). Properties and Control of a Doubly Fed Induction Machine. In *Power Electronics for Renewable Energy Systems, Transportation and Industrial Applications* (pp. 270-318).

[66] Modeling of DFIG Wind Power Systems. (2018). In *Advanced Control of Doubly Fed Induction Generator for Wind Power Systems* (pp. 65-97).

[67] Control of DFIG Power Converters. (2018). In *Advanced Control of Doubly Fed Induction Generator for Wind Power Systems* (pp. 99-138).

[68] **Wang, C.-N., Lin, W.-C., & Le, X.-K.** (2014). Modelling of a PMSG Wind Turbine with Autonomous Control. *Mathematical Problems in Engineering, 2014*, 856173. doi:10.1155/2014/856173

[69] **Tohidi, S., & Behnam, M.-i.** (2016). A comprehensive review of low voltage ride through of doubly fed induction wind generators. *Renewable and Sustainable Energy Reviews, 57*, 412-419. doi:https://doi.org/10.1016/j.rser.2015.12.155

[70] Grid Fault Ride-Through Of DFIG. (2018). In *Advanced Control of Doubly Fed Induction Generator for Wind Power Systems* (pp. 341-386).

[71] **Chavoshi, S. A., Noroozian, R., & Amiri, A.** (2016). Islanding detection of synchronous distributed generation resources using AdaBoost algorithm. *International Transactions on Electrical Energy Systems, 26*(8), 1604-1624. doi:10.1002/etep.2161

[72] **Jarrahi, M. A., Samet, H., & Ghanbari, T.** (2020). Novel Change Detection and Fault Classification Scheme for AC Microgrids. *IEEE Systems Journal, 14*(3), 3987-3998. doi:10.1109/JSYST.2020.2966686

CURRICULUM VITAE

Name Surname **:** Resul AZİZİ

EDUCATION **:**

- **B.Sc.** **:** 2012, University of Zanjan, Faculty of Engineering, Department of Electrical Engineering, Power System Engineering
- **M.Sc.** **:** 2014, University of Zanjan, Faculty of Engineering, Department of Electrical Engineering, Power System Engineering

PROFESSIONAL EXPERIENCE AND REWARDS:

- 2019 Scientific and Technological Research Council of Turkey(TÜBİTAK), Marmara Research Centre, Energy Enstitute

PUBLICATIONS, PRESENTATIONS AND PATENTS ON THE THESIS:

- **Azizi, R.**, Şeker, S., 2021. Microgrid Fault Detection and Classification Based on the Boosting Ensemble Method with Hilbert-Huang Transform, *IEEE Transaction on Power Delivery*, DOI: 10.1109/TPWRD.2021.3109023
- **Azizi, R.**, Noroozian, R. 2021. Islanding Detection in Distributed Energy Resources Based on Gradient Boosting Algorithm, *IET Renewable Power Generation*, V.15, Issue 2, p. 436-451
- **Azizi, R.**, Gürsanlı, Ö., Karacasu, Ö., Güzel, S., Hocaoğlu, M. H., 2020. The importance of Multi Layer Soil Model in Substation Grounding System Design, *12th International Conference on Electrical and Electronics Engineering*, Bursa, Turkey